The Behaviour and Control of Impurities During the Solvent Extraction of Platinum Metals with an Alkylated 8-Hydroxyquinoline

by

Vicken Haroutiun Aprahamian

A Thesis submitted to the Faculty of Graduate Studies and Research in partial fulfillment of the requirements for the degree of Master of Engineering in Metallurgical Engineering

Department of Mining and Metallurgical Engineering McGill University, Montreal, Canada, October 1991

THE BEHAVIOUR AND CONTROL OF IMPURITIES DURING THE SOLVENT EXTRACTION OF PLATINUM METALS WITH AN ALKYLATED 8-HYDROXYQUINOLINE

By

Vicken Haroutiun Aprahamian

ABSTRACT

In order to understand and control the deportment of common impurity elements in the Pt(IV)-Pd(II)-HCl-8-hydroxyquinoline (TN 1911) system, their solvent extraction chemistry in chloride solution has been studied. The investigated elements were Fe(III), Cu(II), Ni(II), Zn(II), Pb(II), Sn(IV), Ag(I), As(V), Sb(V), Bi(III), Se(IV) and Te(IV). Extraction experiments carried out using multi-element and single element feed solutions helped to elucidate the extraction behaviour of the elements with the extractant TN 1911 From the collected data it was deduced that the majority formed anionic chlorocomplexes and extracted via the ion-pair mechanism involving the protonated extractant Consequently, scrubbing procedures were developed to control the deportment of these elements. These scrubbing steps were then incorporated into a tentative flowsheet which was simulated in a batch-wise fashion in the laboratory. The most contaminating elements were found to be Zn(II), Pb(II), Ag(I), Te(IV), Se(IV) and Bi(III). The first five were effectively scrubbed with 2.0M HCl whereas Bi(III) could only be scrubbed with 2.0M H_2SO_4 at A/O ratios of >3:1. The element Sn(IV) which was found to build-up in the organic, could only be scrubbed with a 1.0M NaOH solution for long contact times (60 minutes).

^{*} A proprietary alkylated derivative of 8-hydroxyquinoline (Schering Berlin AG).

RÉSUMÉ

Afin de mieux connaître et contrôler la répartition d'éléments impurs communs dans le système Pt(IV)-Pd(II)-HCl-8-hydroxyquinoline (TN 1911)^b, leur chimie d'extraction en milieu chlorure fut révisé. Les éléments étudiés furent le Fe(III), Cu(II), $N_1(II)$, $Z_1(II)$, $P_2(II)$, $S_1(IV)$, $S_2(I)$, $S_2(IV)$, expériences d'extractions à partir de solutions d'éléments simples ou multiples aidèrent à élucider les comportements d'extractions des éléments avec le réactif TN 1911. A partir des données récupérées, il fut déduit que la majorité forment des composés de complexes chlorures anioniques et sont extraits par le méchanisme de paire d'ions avec le réactif protoné. Par conséquent, des procédures de ré-extraction furent développées pour contrôler la répartition des éléments. Ces étapes de ré-extraction furent ensuite incorporées dans un schéma provisoire qui fut simulé par une technique batch en laboratoire. Les éléments les plus contaminants furent le Zn(II), Pb(II), Ag(I), Te(IV), Se(IV) et le Bi(III). Les cinq premiers éléments furent ré-extrait avec de l'HCl, 2,0M et le Bi(III) avec de l'H₂SO₄, 2,0M avec proportion A/O de >3:1. Le Sn(IV) qui s'accumulait en phase organique put seulement être ré-extrait par le NaOH, 1,0M après une longue durée de contact (60 minutes).

^b Un dérivé alkylé d'un 8-hydroxyquinoline de marque déposé (Schering Berlin AG).

ACKNOWLEDGEMENTS

I would like to extend my great appreciation and thanks to my supervisor, Prof. George P. Demopoulos, for having supported and encouraged me throughout the course of my graduate work, and especially during some difficult moments for me

I am grateful to Schering Berlin AG for having funded the project and the Quebec Government for having provided me with a grant from the Fond pour la Formation de Chercheurs et l'Aide à la Recherche (FCAR). Also, I would like to thank the kind support of the Copper Research Group at the Noranda Technology Centre, Pointe-Claire, Quebec.

Lastly, I would like to acknowledge the keen laboratory assistance of Miss Maral Backmazjian as well as the sound advice of Dimitris Filippou, fellow student and friend Special thanks also go to Elyse Benguerel, fellow student and friend, for her suggestions, charm and humour.

CONTENTS

Page	
1	ABSTRACT
ii	RÉSUMÉ
111	ACKNOWLEDGEMENTS
IV	CONTENTS
VI	LIST OF FIGURES
xi	LIST OF TABLES
i	CHAPTER I: INTRODUCTION
5	CHAPTER II: LITERATURE SURVEY
5	II.1 PGM Refining Practice
13	II.2 Oxidation States of the Impurity Elements
18	II.3 Impurity Speciation in HCl-MeCl _x Media
27	II.4 Solvent Extraction of the Impurity Elements
39	CHAPTER III: EXPERIMENTAL
39	III.1 Apparatus and Reagents
42	III.2 Experimental Procedures
46	III.3 Chemical Analysis
49	CHAPTER IV: RESULTS AND DISCUSSION
49	IV.1 Introduction
50	IV.2 Preliminary Tests
57	IV.3 Single Element Distribution Behaviour during Extraction

70	IV.4 Single Element Distribution Behaviour during Stripping/Scrubbing
81	IV.5 Flowsheet Design Considerations
92	IV.6 Bench-Scale Simulation of the Tentative Flowsheet
101	CHAPTER V: CONCLUSIONS
101	V.1 Conclusions
103	V.2 Further Investigations
104	APPENDIX A. FREE ACID DETERMINATION
106	APPENDIX B. THE SUPPRESSING EFFECT OF Sn(II) ON Pt(IV) EXTRACTION
110	APPENDIX C. CALCULATIONS BASED ON THE DISTRIBUTION COEFFICIENT
118	APPENDIX D: AQUEOUS AND ORGANIC ASSAYS FOR SIMULATION TEST
120	REFERENCES

LIST OF FIGURES

	Page
Figure 1.1 The structure of an alkylated 8-hydroxyquinoline.	2
Figure 1.2 The basic coextraction route ⁽⁴⁾ for TN 1911.	3
Figure II.1 Recovery of PGMs from Matte ⁽⁹⁾ .	5
Figure II.2 Copper Refinery Slimes Processing.	6
Figure II.3 Classical flowsheet for PGM recovery(11).	8
Figure II.4 Inco (U K) PGM flowsheet incorporating solvent extraction ⁽¹³⁾ .	11
Figure II.5 Matthey Rustenburg's latest PGM flowsheet(14).	12
Figure II.6 Distribution of cupric chloride complexes as a function of chloride ion concentration. Conditions: @25°C, $[Cu(II)] = 6 \times 10^4 - 6 \times 10^3 M$, (non-corrected for ionic strength).	21
Figure II.7 Distribution of ferric chloride complexes ⁽³⁶⁾ as a function of HCl concentration. Condition: @20°C, [Fe(III)] = 10 ³ M, (non-corrected for ionic 'crength).	22
Figure II.8 Distribution of zinc chloride complexes ⁽²⁹⁾ as a function of chloride ion concentration. Conditions: @25°C, [Zn(II)]=0.05M (diagram computed from stability constant data and corrected for ionic strength).	22
Figure II.9 Distribution of lead chloride complexes ⁽²⁹⁾ as a function of chloride ion concentration. Conditions: @25°C, [Pb(II)]=0.05M (diagram computed from stability constant data and corrected for ionic strength).	23
Figure II.10 Distribution of stannic chloride complexes ⁽²⁷⁾ as a function of chloride ion concentration. Conditions: @25°C, I=5.0M HClO_[Sp(IV)]=0.003-0.01M	23

Figure II.11 Distribution of silver chloride complexes ⁽³⁷⁾ as a function of chloride ion concentration. Conditions: @25°C, (diagram computed from stability constant data and non-corrected for ionic strength).	24
Figure II.12 Distribution of antimonic chloride complexes as a function of HCl concentration. Conditions @25°C, $[Sb(V)]=2\times10^{-4}M$, (non-corrected for ionic strength).	24
Figure II.13 Distribution of bismuth chloride complexes ⁽²⁵⁾ as a function of chloride ion concentration Conditions: $@25^{\circ}C$, I=2.5M NaClO ₄ , [Bi(III)]= 10^{4} M.	25
Figure II.14 Distribution of selenous complexes ⁽³⁵⁾ as a function of hydrogen ion concentration. Conditions: @25°C, I=1M NaClO ₄ , L=SeO ₃ ²⁻ =0.1M.	25
Figure II.15 Distribution of tellurous chloride complexes ⁽³⁹⁾ as a function of chloride ion concentration Conditions @25°C, $[H^+]$ = const = 0.5M, $[Te(IV)]$ = 10^4 – 10^3 M.	26
Figure II.16 Distribution of metal species in Alamine $336^{(51)}$ as a function of HCl concentration. Conditions 25% Alamine 336, 15% dodecanol in Kerosene, $M^{n+} = 1,000 \text{ mg/L}$.	30
Figure II.17 Distribution of metal species ⁽⁵⁵⁾ in TIOA as a function of HCl concentration a) Sn, As, Sb, Bi, Pb and b) Fe, Ag, Cu, Co, Mn. Conditions. 20v% TIOA in CCl ₄ , aqueous phase=[Mn]=0.1M.	32
Figure II.18 Distribution of metal species ⁽⁶⁰⁾ as a function of HCl in TBP. Conditions: $40v\%$ TBP in white spirit, Aqueous phase=Cu(II) = 1000 mg/L, Sb(III) = $80,000$ mg/L, Bi(III)=As(III)=Fe(II)+Fe(III)= $1750-3000$ mg/L	37
Figure III.1 pH control set-up for agitation tests.	39
Figure III.2 Treybal's batch-wise simulation of continuous counter-current contacting. F= aqueous feed, S= fresh organic, E= loaded organic and R= aqueous raffinate.	45
Figure III.3 The method of standard additions.	48

Figure IV.1 Distribution of impurity elements in 5v% TN 1911 as a function of HCl concentration (<i>Experiment 1</i>), conditions: 3 min., $A/O=1$, 25°C, $M_{aq}=1,000\pm200$ mg/L.		
Figure IV.2 Distribution of impurity elements in 5v% TN 1911 as a function of contact time (<i>Experiment 1</i>), conditions: 0.7M HCl, A/O=1, 25°C, $M_{eq} = 1,000 \pm 200 \text{ mg/L}$.	53	
Figure IV.3 Distribution of impurity elements in 5v% TN 1911 as a function of HCl concentration (<i>Experiment 2</i>), conditions: 3 min., $A/O=1$, 25°C, $M_{eq}=1,000\pm200$ mg/L, with the exception of $[Ag(I)]=30$ mg/L.	54	
Figure IV.4 Extraction behaviour of Sb(III), As(III), Sb(V) and As(V) in 5v% TN 1911 as a function of HCl concentration (<i>Experiment 1 & 2</i>), dash/number refer to experiment. Conditions: 3 min , A/O=1, 25°C , $M_{\text{aq}} = 1,000 \pm 200 \text{ mg/L}$.	55	
Figure IV.5 Distribution of impurity elements in 5v% TN 1911 as a function of contact time (<i>Experiment 2</i>), conditions: 0.7M HCl, A/O=1, 25°C, $M_{sq} = 1,000 \pm 200 \text{ mg/L}$.	56	
Figure IV.6 Single metal plot for Pt(IV) and Pd(II), 5v% TN 1911, A/O=1, 3 min	57	
Figure IV.7 Single metal plot of Bi(III), 5v% TN 1911, A/O=1, 3 min.	58	
Figure IV.8 Single metal plot of Sn(IV), 5v% TN 1911, A/O=1, 3 min	5 9	
Figure IV.9 Single metal plot of Te(IV), 5v% TN 1911, A/O=1, 3 min.	60	
Figure IV.10 Single metal plot of Fe(III), 5v% TN 1911, A/O=1, 3 min.	61	
Figure IV.11 Single metal plot of Zn(II), 5v% TN 1911, A/O=1, 3 min.	62	
Figure IV.12 Single metal plot of Ag(I), 5v% TN 1911, A/O=1, 3 min.	63	

Figure IV.13 Single metal plot of Sb(V), 5v% TN 1911, A/O=1, 3 min.	64
Figure IV.14 Single metal plot of Pb(II), 5v% TN 1911, A/O=1, 3 min.	65
Figure IV.15 Single metal plot of Cu(II), 5v% TN 1911, A/O=1, 3 min.	66
Figure IV.16 Single metal plot of As(V), 5v% TN 1911, A/O=1, 3 min.	67
Figure IV.17 Single metal plot of Se(IV), 5v% TN 1911, A/O=1, 3 min.	68
Figure IV.18 Deportment of impurity elements in four scrub/strip solutions with 5v% TN 1911 @ 25°C, A/O=1, 3 min. (Metal concentrations refer to loaded organic phase. Organic loaded with HCl, $CM_{aq} = 1.000 \pm 200 \text{mg/L}$).	71 h 2.7M
Figure IV.19 Scrubbing Sn(IV) from loaded 5v% TN1911 single metal tests, A/O=1, 3 min., 25°C.	76
Figure IV.20 Sn(IV) six-stage scrubbing using 1.0M NaOH solution, $5v\%$ TN 1911, A/O=1, 3 min, 25°C, [Sn(IV)] _(o) = 455 mg/L.	76
Figure IV.21 The effect of contact time on the removal of $Sn(IV)$ using 1.0M NaOH, 5v% TN 1911, A/O=1, 25°C, $[Sn(IV)]_{(0)} = 455 \text{ mg/L}$.	77
Figure IV.22 4-Stage loading of 5v% TN 1911. Conditions: A/O=1, 3 min., 2.7M HCl feed, impurity element concentrations appear in legends.	83
Figure IV.23 Tentative flowsheet designed for testing in the laboratory the effectiveness of the incorporated scrubbing steps.	91
Figure IV.24 Adapting the Treybal cascade to the tentative flowsheet. Analysed streams appear in <i>italics</i> , flow of organic is denoted by an asterisk and SCRUB I= 2.0M HCl, SCRUB II= 2.0M H ₂ SO ₄ , SCRUB III= 0.1M HCl + 2.0M MgCl ₂ , SCRUB IV= 1.0M NaOH AF/OF refer to aqueous and organic feeds respectively and	93

Figure IV.25 Effectiveness diagram for the strongly extracted impurities Zn(II), Te(IV), Pb(II) and Bi(III). (SCR I = 2.0M HCl/1 contact,	95
SCR II = $2.0M H_2SO_4/2$ contacts, SCR III = $0.1M HC1+2.0M MgCl_2$, SCR IV = $1.0M NaOH/1$ contact).	
Figure IV.26 Effectiveness diagram for the minor impurities Se(IV), As(V), Ag(I), Ni(II).	95
Figure IV.27 Effectiveness diagram for the other elements Sn(IV), Sb(V), Fe(III), Cu(II).	96
Figure IV.28 Treybal extraction for Pd(II) and Zn(II). (numbers shown are concentrations in mg/L). Conditions: A/O=1, 3 min.	97
Figure IV.29 Treybal diagram assays: H_2SO_4 scrubbing for $Zn(II)$ and $Bi(III)$. (numbers shown are concentrations in mg/L). Conditions: $A/O=3$,	97 3 min.
Figure IV.30 Treybal diagram assays: Pd stripping with 6.0M HCl $PS = I-VI$ indicate final 6 contacts in 6×6 array (numbers shown are concentrations in mg/L). Conditions: $A/O = 1$, 3 min.	98
Figure IV.31 Revised flowsheet designed for the refining of Pt and Pd using TN 1911.	100
Figure B-1 The extraction of Pt(IV) in the presence of Sn(II) in single metal solution, 0.7M HCl, 5v% TN 1911, A/O=1, 3 min.	108
Figure B-2 The extraction of Pt(IV) in the presence of Sn(IV) in single metal solution, 0.7M HCl, 5v% TN 1911, A/O=1, 3 min.	109
Figure B-3 The effect of Sn(II) on Pt(IV) in RC Mint solution and extraction with TN 1911. Conditions: 0.7M HCl, 5v% TN 1911, A/O=1, 3 min.	109

LIST OF TABLES

	Page
Table II.1 Standard reduction potentials of impurity elements in solution at 25°C.	16
Table II.2 Strength of chloride complexes according to periodicity ⁽²⁴⁾ .	18
Table II.3 Stability constant data for chlorocomplexes of some elements at 25°C. Data for N _I (II), A _S (V) and Se(IV) was not available.	19
Table II.4 Summary of most relevant impurity element SX systems: extraction of base metals and silver from chloride liquors. Legend: CF= compound formation, IP= ion-pair formation and S= solvation.	37
Table II.5 Summary of most relevant impurity element SX systems: extraction of metalloids from chloride liquor. Legend: IP= ion-pair formation, S= solvation.	38
Table III.1 The chemical identity of the organic phase components.	40
Table III.2 List of the reagents used in the experiments.	41
Table III.3 Full assay of as-received Royal Canadian Mint solution (RCMint-12-II).	42
Table III.4 Atomic absorption settings used for the elements on the IL 357 instrument. BKG= Background correction with deuterium lamp. Pt analysis from mixed-metal solutions was followed by spiking with 2,000 mg/L La ³⁺ . Reproducibility: excellent $(\pm 1\%)$ to poor $(\pm 10\%)$.	47
Table IV.1 Summary of single metal extraction observations and postulated mechanisms. CF=compound formation, IP=10n-pair formation, S=solvation.	69

Table IV.2 Comparison of distribution coefficients at 2.7M HCl obtained from extraction and scrubbing tests. For $D_{\rm EXTRACTION}$, $M_{\rm aq,inital} = -1,000 {\rm mg/L}$, except for Ag(I) ($\sim 100 {\rm mg/L}$), and for $D_{\rm 5CRIJBBING}$, $M_{\rm org,inital} < 1,000 {\rm mg/L}$, except for Bi(III) and Zn(II) (see Figure IV.18).	74
Table IV.3 Scrubbing results for Ag(I) using strong chloride ion in solution. 5v% TN 1911, A/O=1, 3 min., 25°C. Mixed metal organic phase: Pd 400, Cu 60, Ag 30, Bi 1730 (in mg/L).	78
Table IV.4 Sb(V) scrubbing with KNa tartrate solutions from 5v% TN 1911. Conditions: A/O=1, 3 min., 25°C, [Sb(V)]=109 mg/L loaded from single metal solution at 2.7M HCl.	78
Table IV.5 Pt-Pd single metal scrubbing tests in HCl and H ₂ SO ₄ solution.	80
Table IV.6 Typical refinery feeds vs McGill synthetic feed.	82
Table IV.7 Classification of impurity elements according to their potential to contaminate PGM strip liquors. Conditions: 5v% TN 1911 with feed [HCl]=2.7M, 1000 mg/L M ⁿ⁺ .	84
Table IV.8 Predicted scrubbing data for 1.5M HCl solution. Conditions: single 3 min. contact on 5v% TN 1911. Last four columns depict removal efficiency (levels of loading were taken from single element extraction tests at 2.7M HCl; Section IV.3).	86
Table IV.9 Predicted scrubbing data for 2.5M HCl scrubbing solution. Conditions: single 3 min. contact on 5v% TN 1911. Last four columns depict removal efficiency For Fe, Zn, Pb, Ag, Te cummulative % data for two stage contact is shown as well (levels of loading were taken from single element extraction tests at 2.7M HCl; Section IV.3)	87
Table IV.10 Multi-element scrubbing test with 2.0M H ₂ SO ₄ . Conditions: 5v% TN 1911, 3 min. contact.	89
Table A-1 Free acid determination experimental results.	105
Table B-1 Effect of Sb(III), Bi(III) and Sn(II/IV) spiking on Pt(IV) extraction from RC Mint solution (0.7M HCl) with 5v% TN 1911, A/O=1, 3 min.	106

Table C-1 Expected Pt and Pd concentrations in HCl scrubbing solutions as a function of their extraction distribution coefficients (organic feed: 990 mg/L Pt and 923 mg/L Pd).	112
Table C-2 Expected Pt and Ag concentrations in the HCl scrubbing solutions as a function of their extraction distribution coefficients (organic feed: 990 mg/L Pt and 80 mg/L Ag).	112
Table C-3 Expected Pt and Cu concentrations in HCl scrubbing solutions as a function of their extraction distribution coefficients (organic feed: 990 mg/L Pt and 105 mg/L Cu).	113
Table C-4 Expected Pt and Fe concentrations in HCl scrubbing solutions as a function of extraction distribution coefficients (organic feed: 990 mg/L Pt and 231 mg/L Fe).	113
Table C-5 Expected Pt and Zn concentrations in HCl scrubbing solutions as a function of extraction distribution coefficients (organic feed: 990 mg/L Pt and 697 mg/L Zn).	114
Table C-6 Expected Pt and Sn concentrations in HCl scrubbing solutions as a function of extraction distribution coefficients (organic feed: 990 mg/L Ft and 972 mg/L Sn).	114
Table C-7 Expected Pt and Pb concentrations in HCl scrubbing solutions as a function of extraction distribution coefficients (organic feed: 990 mg/L Pt and 565 mg/L Pb).	115
Table C-8 Expected Pt and As concentrations in HCl scrubbing solutions as a function of extraction distribution coefficients (organic feed: 990 mg/L Pt and 83 mg/L As).	115
Table C-9 Expected Pt and Sb concentrations in HCl scrubbing solutions as a function of extraction distribution coefficients (organic feed: 990 mg/L Pt and 286 mg/L Sb).	116
Table C-10 Expected Pt and Bi concentrations in HCl scrubbing solutions as a function of extraction distribution coefficients (organic feed: 990 mg/L Pt and 980 mg/L Bi).	116
Table C-11 Expected Pt and Se concentrations in HCl scrubbing solutions as a function of extraction distribution coefficients (organic feed: 990 mg/L Pt and 60 mg/L Se).	117

Table C-12 Expected Pt and Te concentrations in HCl scrubbing solutions as a function of extraction distribution coefficients (organic feed: 990 mg/L and 714 mg/L Te).	117
Table D-1 Aqueous stream assays for simulation test (units in mg/L). R/r = extraction raffinates, $S/s = scrubbing raffinates$, SPt = Pt strip liquor, $PS = Pd strip liquors$.	118
Table D-2 Further aqueous stream assays and organic assays for simulation test (units in mg/L). Numbers = Pd strip liquor streams, O = organic streams in Pd stripping.	119

CHAPTER I: INTRODUCTION

Platinum group metals, also known as PGMs, are gradually finding new applications outside the jewelry industry due to their outstanding physical, chemical and mechanical properties. New uses have been found in autocatalysts as well as in electronics, and with the advent of fuel cells for the production of electricity, the future looks even more promising. They are classed in two groups, namely the Primary PGMs comprised of Pt, Pd and the Secondary PGMs which occur in lesser amounts in nature and are more difficult to treat, consisting of Rh, Ir, Ru, Os. It is customary to include within this group the other precious metals, namely Ag and Au. The recovery of Pt-Pd from contaminated chloride solutions originating from leaching of various primary and secondary materials is a challenging problem in precious metal refining. Classical refining techniques have been made up of precipitation-dissolution steps which are no longer considered to be efficient.

Currently, the bigger refineries are using solvent extraction in their flowsheets. Although more efficient than the older techniques, solvent extraction has not been without drawbacks. Novel reagents have been studied to improve performance and reduce any inefficiencies. Among them are the 8-hydroxyquinoline reagents, which have been advocated for the recovery and separation of Pt and Pd from chloride leach liquors^(1/2). The reagents Kelex 100° and Lix 26° under study in previous years⁽³⁾ have been surpassed recently by TN 1911, a high-performance 7-alkylated 8-hydroxyquinoline made available from Schering AG⁽⁴⁾. Figure I.1 depicts the structure of TN 1911. The R group is a long chain alkenyl group.

^{*} Proprietary product of Sherex Chemical Co. (Dublin, OH, USA)

^b Proprietary product of Henkel Chemical Co. (Tucson, AZ, USA).

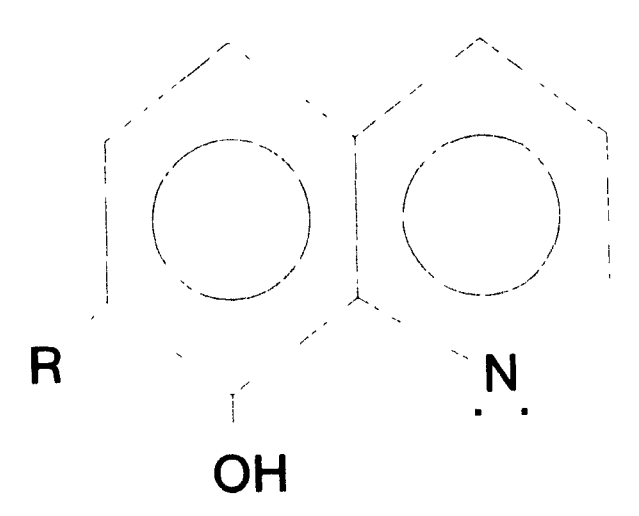


Figure I.1 The structure of an alkylated 8-hydroxyquinoline⁽⁴⁾.

The unique property of 8-hydroxyquinoline derivatives to extract metal species both by chelation and/or ion-pair formation is exploited in this system. Platinum (IV) and palladium (II) are coextracted according to the following equations:

1) Extractant protonation:

$$HL_{(0)} + HCl \rightleftharpoons H_2L^+Cl^-_{(0)}$$
 (I.1)

2) Extraction of Pt(IV) by anion-exchange:

$$PtCl_6^{2-} + 2H_2L^+Cl_{(0)}^- \rightleftharpoons PtCl_6^{2-}(H_2L^+)_{2(0)} + 2Cl^-$$
 (I.2)

3) Extraction of Pd(II) by chelation:

$$PdCl_4^{2-} + 2H_2L^+Cl_{(0)}^- \rightleftharpoons PdL_{2(0)} + 4H^+ + 6Cl^-$$
 (I.3)

After coextraction, the metals would be separated first by stripping the loaded organic with water for Pt, followed by stripping with 6M HCl for Pd. Recovery from

the strip liquors would typically be achieved by ammoniacal salt precipitation or solution reduction. Patents have been issued recently for the use of 8-hydroxyquinoline reagents in the PGM industry⁽⁵⁻⁶⁾. The simplified coextraction flowsheet employing TN 1911 is shown in Figure 1.2.

One of the difficulties in applying a solvent extraction system for the refining of PGMs is the presence of the great variety of impurity elements in industrial feedstocks, which depending on their concentrations would create problems in a circuit. Contamination of the Pt and Pd strip liquors would be the evident conclusion, however, third phase formation and possibly PGM suppression could also result.

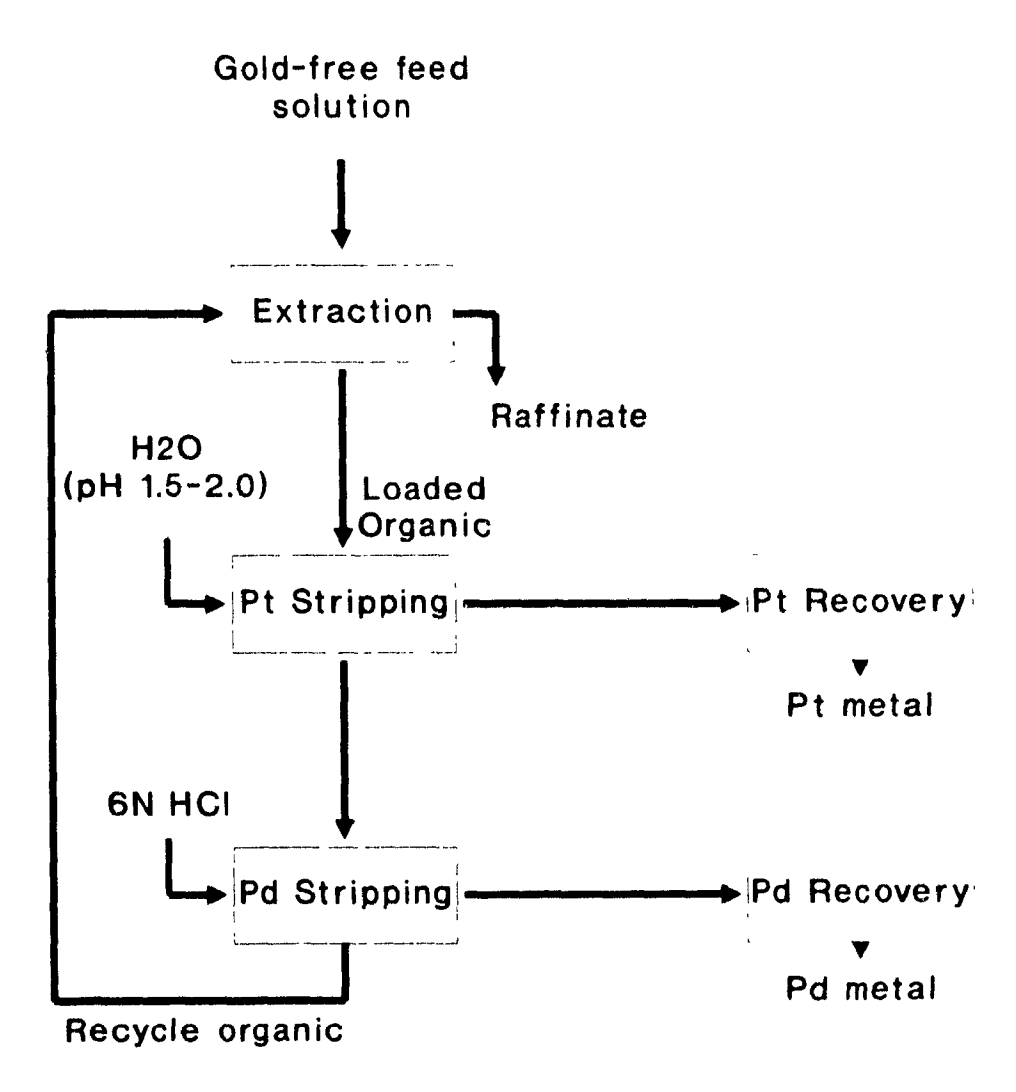


Figure I.2 The basic coextraction route⁽⁴⁾ for TN 1911.

The <u>objective</u> of this study was to study the behaviour of the common impurity elements Fe, Cu, Ni, Zn, Sn, Pb, Ag, As, Sb, Bi, Se and Te in the Pt(IV)-Pd(II)-HCl-TN 1911 system and devise means for their control. To this end it was essential to review first the literature on the behaviour of the impurity elements in various solvent extraction systems as well as the relevant aqueous chloride chemistry. Following that, preliminary loading tests using a composite semi-synthetic chloride feed revealed the major trends of impurity coextraction. The next step in the experimental program involved conducting single metal tests to establish the distribution of each impurity as a function of HCl concentration. This work provided information as to possible loading mechanisms for each metal and permitted the selection of scrubbing solutions for the next step of the work. After testing the scrub solutions, control strategies were formulated and a tentative flowsheet was designed.

The flowsheet was tested in the laboratory by a batch-wise technique simulating counter-current contacting. The final outcome of the investigation was the establishment of scrubbing regimes for dealing with impurities in a generic rather than a feed-specific manner. This, hopefully, makes much easier the implementation and operation of 8-hydroxyquinoline based-solvent extraction circuits in the PGM industry.

CHAPTER II: LITERATURE SURVEY

II.1 PGM Refining Practice

PGM Sources and Extraction: Nowadays, there is much interest in a new source of PGMs, namely the secondary source comprised of recycled automotive catalysts and electronic scrap⁽⁷⁾. However, the bulk of the production still originates from ores, as PGMs often occur in sulphide mineralization such as in the Merensky Reet in the Transvaal region of South Africa⁽⁸⁾. Figure II.1 shows that in the latter case, PGM-rich matte reports to a PGM liberation step after flotation and smelting of sulphide ore. In the next step, the matte is subjected to an acid leach process where base metals Cu, Ni and Fe may either be removed or recovered as saleable by-products. The acid leach residues are then subjected to chloride leaching for solubilisation of PGMs which are eventually separated.

SULPHIDE ORE

#
FLOTATION

SMELTING PRODUCING MATTE

#
H₂SO₄ LEACH FOR Cu/N₁/Fe

#
CHLORIDE LEACH FOR PGMs

#
PGMS TO RECOVERY

Figure II.1 Recovery of PGMs from Matte⁽⁹⁾.

A second source of industrial PGM production is in the Cu and Ni electrorefinery anode slimes (10). Copper refinery anode slimes may have a PGM content as high as 20 wt% with 90% of this value being made up of Au and Ag. The flowsheet in Figure II.2 illustrates the common route followed in the processing of Cu refinery slimes. Here, Au and Ag are rich enough to be electrorefined from Doré anode after smelting. The Au anode slimes are then subjected to wet chlorination for PGM recovery. In some cases the Ag slimes may directly report to leaching.

ANODE SLIMES

U
DECOPPERIZING WITH H₂SO₄

U
Doré SMELTING AND REFINING

U
SILVER REFINING

U
GOLD REFINING

U
PGMs TO WET CHLORINATION
AND SEPARATION

Figure II.2 Copper Refinery Slimes Processing.

Classical Refining of Platinum Group Metals: Irrespective of their source, PGMs are eventually solubilized with a wet chlorination step which consists in bubbling Cl₂ gas in an HCl medium. Aqua-regia is another oxidizing chloride medium which is still commonly used and other chloride based media in which HNO₃ has been replaced by H₂O₂ have also been adopted. Secondary PGMs, Ir, Rh, Ru and Os are inert in leaching⁽¹⁰⁾. The result is that PGMs are split into two streams, the first holding the Primary PGMs Pt, Pd, as well as Au, and the second consisting of Ir, Rh, Os and Ru and representing the Secondary PGMs. This is the partial leach route which makes use of aqua-regia and is associated with complications, thus the trend for the adoption of a

after an initial chloride leach to render the secondary PGMs into a soluble form for a subsequent second chloride leach which dissolves all the PGMs⁽¹¹⁾. A typical complex conventional flowsheet involving *aqua-regia* leaching is shown in Figure II 3⁽¹²⁾. The solubilized primary PGMs report first to Au precipitation by the introduction of either SO₂ or ferrous sulphate. Ammonium hexachloroplatinate is then precipitated by the addition of ammonium chloride. An ammoniacal precipitate of Pd immediately follows in the next stage upon addition of ammonia and hydrochloric acid. Zinc dust cements out any remaining PGMs which report to Pb smelting for removal of any impurities. Ph is removed by parting with nitric acid. Addition of *aqua-regia* re-leaches Pt Pd Au leaving behind a residue of Ir-Rh-Ru-Os which reports to peroxide fusion. The addition of HCl solubilizes the PGMs and ruthenium and osmium are removed first on the basis of their volatile tetravalent oxides which undergo distillation. Iridium is then precipitated with ammonium chloride under oxidizing conditions. Finally, Rh is purified with a mixture of ammonium chloride and sodium nitrite.

Each of the impure salts of Pt, Pd, Ir and Rh are usually redissolved and reprecipitated making the classical technique extremely lengthy and quite mefficient. In fact, the rhodium which appears at the tail-end of the process may take up to six months to be recovered. In the last 25 years, the industry has taken steps to accelerate and modernize the recovery and purification of PGMs and they have looked at new technologies and in particular the use of solvent extraction⁽¹³⁾.

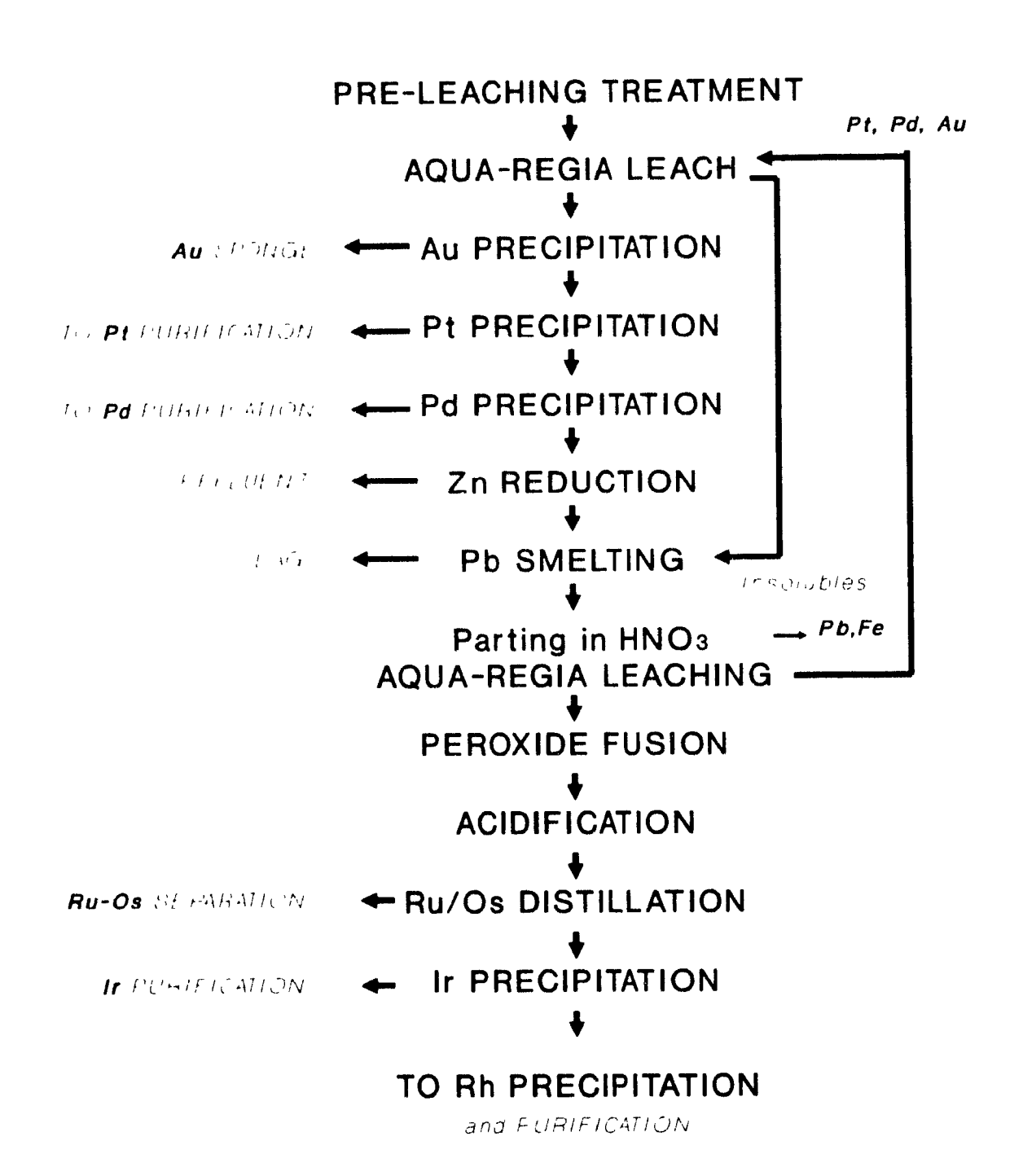


Figure II.3 Classical flowsheet for PGM recovery⁽¹²⁾.

Modern Refining Involving Solvent Extraction:

a) Selective extraction with different reagents: After the successful introduction of a solvent extraction process for gold using dibutyl carbitol (DBC) in 1971. Inco began developing a flowsheet which was to adopt this advanced technology for refining PGMs⁽¹³⁾. Figure II.4 shows a simplified version of today's flowsheet. They opted to first distill off Ru and Os prior to the recovery of the remaining PGMs. Gold is first removed using DBC by contacting with 3-4M HCl aqueous phase. 1.5M HCl is then used as a scrub medium at 1:1 phase ratio. Loaded gold is then directly reduced with oxalic acid. The raffinate then goes to a batch stage where Pd(II) is loaded onto di-n-octyl sulphide (DOS), which is very selective over other PGMs except Au(III) Due to slow extraction kinetics the palladium separation process is a batch process and is interfaced with continuous (up and down-stream) counter-current operation. HCl scrubbing is used once more, and although the conditions are not specified, the main effect is to remove any entrained raffinate from the organic phase⁽¹³⁾. Palladium is then stripped with aqueous ammonia and recovered from the strip liquor as the ammoniacal salt by neutralization with HCl. The next solvent extraction circuit is with tributyl phosphate (TBP), which is contacted with an acidified feed liquor (5-6M HCl) for loading Pt(IV) Ir(IV) is reduced to the III state with SO₂ gas prior to loading as it coextracts with Pt(IV). Scrubbing is conducted on the loaded TBP at 5M HCl with high O/A ratios to recycle any entrained PGMs. After stripping with water at 1:1 phase ratio, the raffinate from the TBP circuit ends up as the feed liquor to Rh/Ir recovery. The latter metals are refined with classical techniques.

The selective solvent extraction approach is also adopted at Matthey Rustenburg Refiners in South Africa⁽¹⁴⁾. There Pd(II) is extracted with an oxime instead of an alkyl sulphide. Originally, hydroxyoximes assisted by accelerator additives were employed. But more recently, a new oxime reagent (alkoxyoxime) marketed as MOC·15^a, is believed to be used instead. The latter oxime type offers better selectivity and kinetics but requires rather stringent stripping conditions (NH₄OH/NH₄Cl at pH 9.5)⁽¹⁵⁾. In the case of Pt(IV) extraction, which follows the Ru/Os distillation step, a tertiary amine has been known to have been used. This reagent is known to suffer from various drawbacks like metal lock-up and the necessity of operating the strip circuit at 10-12M HCl. As at Inco, reduction of Ir(IV) to Ir(III) is practiced prior to Pt(IV) extraction. Reoxidation of iridium to the IV state permits extraction with a proprietary amide which was reported recently to have replaced the amine extractant⁽¹⁶⁾.

b) Coextraction followed by selective stripping: Lonrho, based in South Africa, have opted for Pt-Pd coextraction using an acetic acid derivative of a secondary amine instead of a selective extractant. It is not documented whether they achieved success in separation during stripping. The PGP group of USA have also followed the coextraction route, and it is highly likely that amines are employed in their circuit with selective stripping effected with hydrazine for Pt and sodium bicarbonate for Pd⁽¹⁵⁾.

^{*} Proprietary product of Allied Chemicals.

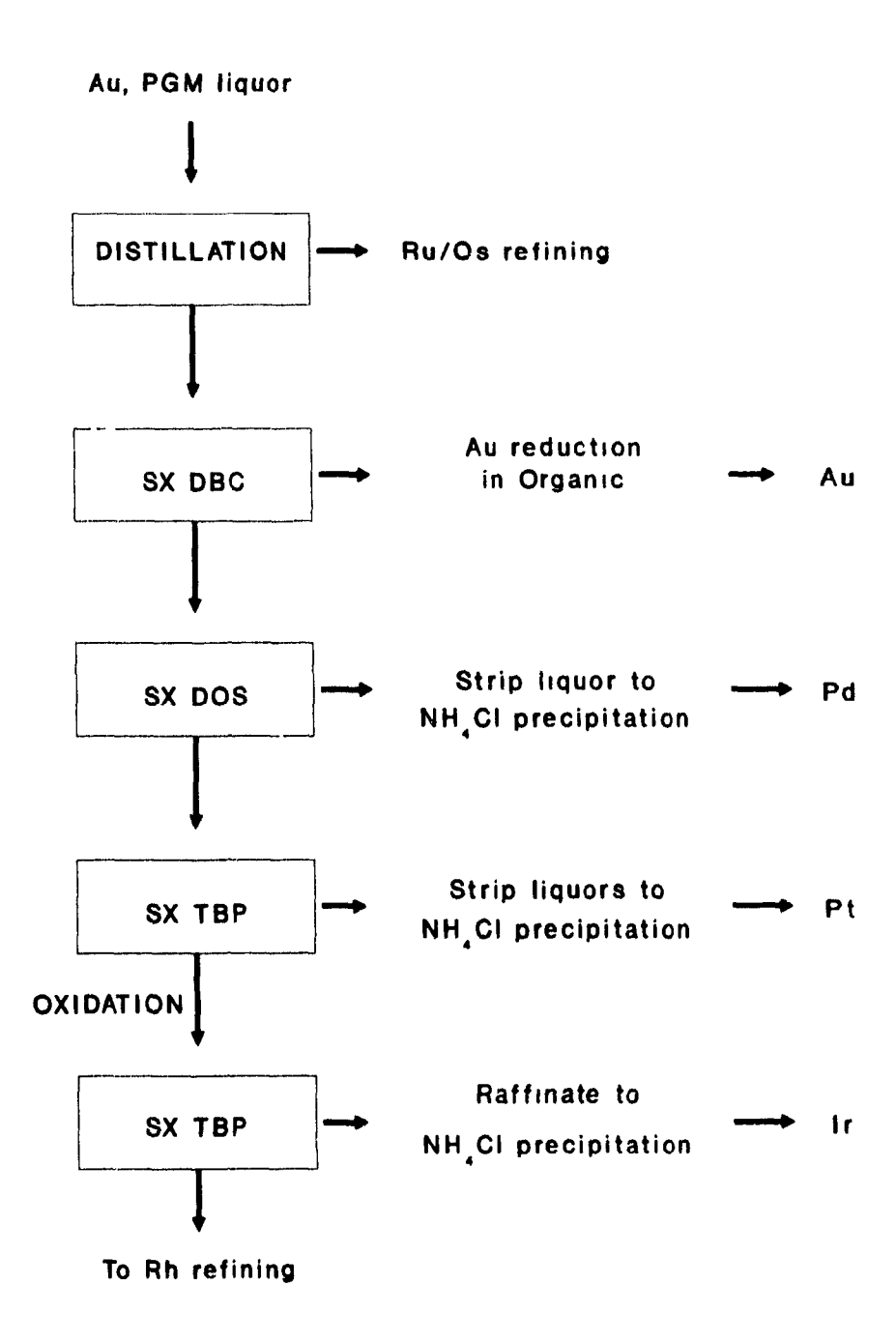


Figure II.4 Inco (U.K.) PGM flowsheet incorporating solvent extraction (13).

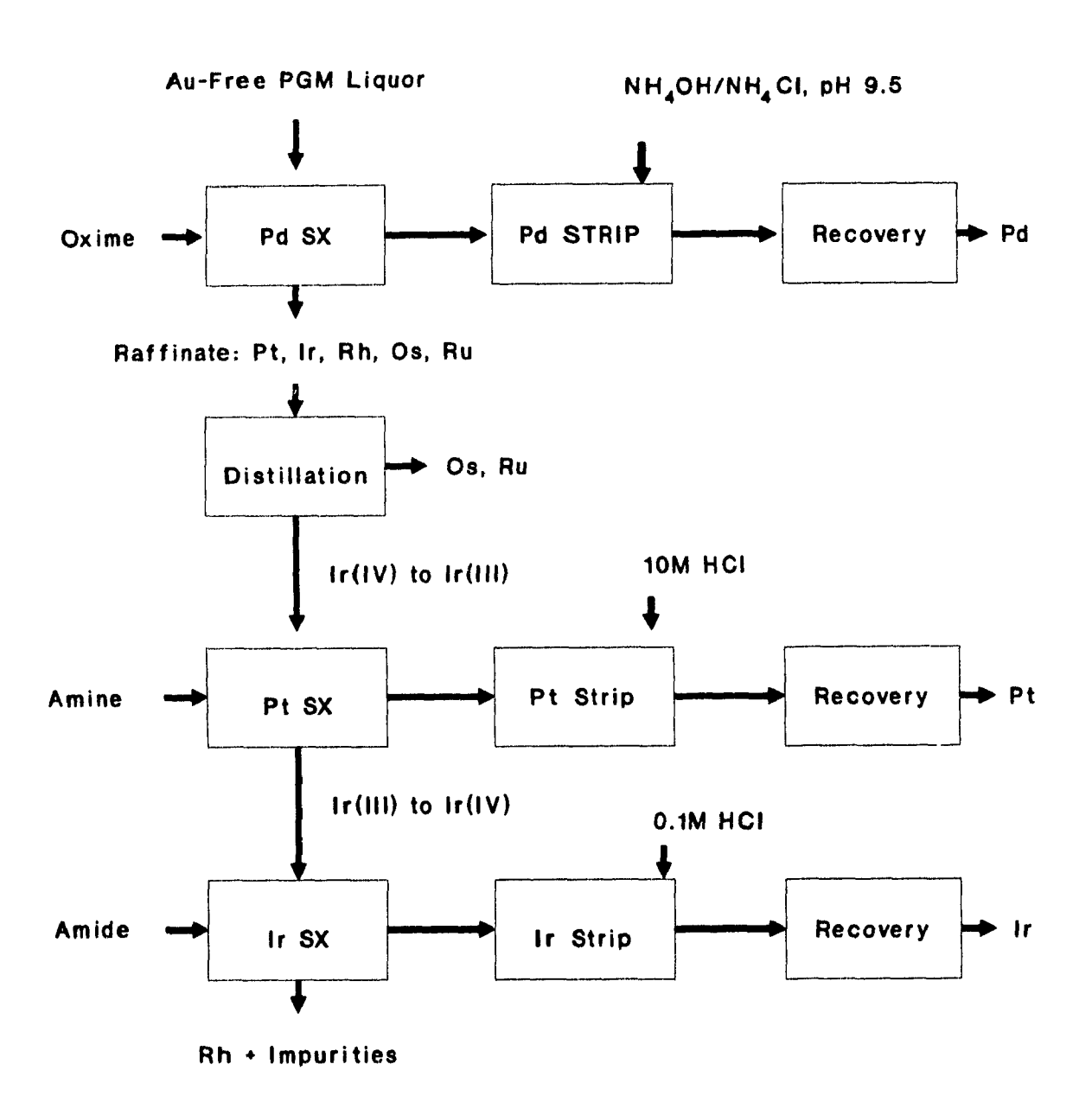


Figure II.5 Matthey Rustenburg's latest PGM flowsheet(14).

II.2 Oxidation States of the Impurity Elements

Strong oxidising conditions are used in the industry to solubilize the primary or secondary feedstocks reporting to leaching prior to solvent extraction purification/separation steps. Aqua-regia treatment used in the classical processes, although still useful, has been surpassed by the more efficient wet chlorination technique, due to better overall performance in the leaching of primary and secondary PGMs. The absence of nitrate is also quite appreciated as it could combine with the organic extractant to produce potentially explosive mixtures. Wet chlorination is essentially composed of Cl_2 fed in an HCl medium. Alternatively, other strong oxidising agents such as H_2O_2 can be used in lieu of Cl_2 . Wet chlorination is used at Inco, Matthey Rustenburg and in the Lonrho flowsheet whereas HCl/H_2O_2 leaching is used at CCR-Noranda.

The Oxidation Power of Wet Chlorination: Latimer⁽¹⁷⁾ states that chlorine is stable in acid solution with respect to disproportionation, but the reaction does go to a measurable equilibrium:

$$Cl_{2(g)} + H_2O \rightleftharpoons H^+ + Cl^- + HClO$$
 $K = 4.66 \times 10^4$ (II.1)

The HClO species is rather unstable as $\Delta G^{\circ}_{f,HClO} = 25.9 \text{ kJ/mol}$. Both $Cl_2(aq)$ and HClO, as well as other intermediate species which are neglected in this account, might be present. Thus, the half reactions and standard potentials for $Cl_{2(g)}$ and HClO are⁽¹⁷⁾:

$$Cl_{2(e)} + 2e^{-} \rightleftharpoons 2Cl^{-}$$
 (II.2)

$$HCIO + H^+ + 2e^- \rightleftharpoons Cl^- + H_2O$$
 $E^0 = +1.482 \text{ V}$ (II.3)

The actual potentials though, are a function of the pertinent solution composition, as the Nernst equation suggests:

oxidised form + ne⁻ ≠ reduced form

$$E = E^{o} - \frac{RT}{nF} \ln \frac{[reduced \ form]}{[oxidised \ form]}$$
 (II.4)

and the respective half reaction potentials become for T = 298K,

$$E_{CL_jCI^-} = 1.359 - \frac{0.059}{2} \log \frac{\alpha_{Cl^-}^2}{P_{CL_j}}$$
 (II.5)

$$E_{HClO/Cl^{-}}=1.482-\frac{0.059}{2}\log\frac{\alpha_{Cl}-\alpha_{H_2O}}{\alpha_{H^*}\alpha_{HClO}}$$
(II.6)

Assuming 1 atm Cl_2 and 1M HCl solution, then from eqn. II.1 we obtain $C_{HClO} = 4.7 \text{ x}$ 10^4 M^c . For this set of assumptions eqns. II.5 and II.6 produce practically the same results as E = 1.36 V. Considering in actual refining practice that the partial pressure of Cl_2 is actually lower than 1 atm and $[Cl^2] > 1.0 \text{M}$, a somewhat lower potential is expected.

The Oxidation Power of Aqua-regia:

Aqua-regia is traditionally formulated by using 12M HCl and 14M HNO₃ at a 3:1 volume ratio. The same formulation was used in this study (see Chapter III). The dissolution power of aqua-regia arises from the oxidizing power of nitric acid and the complexing properties of Cl⁻. The oxidising power of nitric acid can be explained through its main half-reaction⁽¹⁷⁾:

$$NO_1 + 4H^+ + 3e^- \rightleftharpoons NO + 2H_2O$$
 $E^0 = +0.96V$ (II.7)

Via complexation the Cl iHx lowers the reduction potential of the dissolved species

^c It is also assumed that activities are equal to concentrations.

making oxidation easier for the latter. By applying the Nernst equation:

$$E_{aqua-regua} = E^{o} - \frac{0.059}{3} \times \log \left(\frac{[NO]}{[H^{+}]_{HCl+HNO_{3}}^{4} \times [NO_{3}^{-}]} \right)$$
(11.8)

and by making certain assumptions for a 3:1 HCl:HNO₃ mixture, we see that the potential may not increase significantly unless unknown intermediate species are favoured:

For [HNO₃] = 14M and [HCl] = 12M, [H⁺]_{HNO3} = 3.5M, [H⁺]_{HCl} = 9.0M, [NO₃] ≈ 3.5 M assuming trace reduction, and [NO] = 1.78 x 10⁻³ M (solubility in water at 25°C)⁽¹⁸⁾

$$E_{aqua-regua} = 0.96 - \frac{0.059}{3} \times \log \left(\frac{[1.78 \times 10^{-3}]}{[12.5] \times [3.5]} \right) = +1.05V$$
 (II.9)

Reduction Potentials and the Impurity Elements: In Table II.1, the standard reduction potentials of the impurity elements present in aqueous chloride solutions are presented.

Element	Most Probable State	Couple	E⁰, V	Medium	Ref.
Cu	11	Cu(II)/(0)	+0.178	1M HCl	19
Fe	III	Fe(III)/(II)	+0.771	0.5M HCl	19
Zn	II	Zn(II)/(0)	-0.763	calculated	20
Ni	II	Ni(II)/(0)	-0.250	thermodyna- mically	20
Pb	II	Pb(IV)/(II)	+1.690	5.8M HClO₄	19
Sn	IV	Sn(IV)/(II)	+0.140	1M HCl	20
Ag	I	Ag(II)/(I)	+2.000	4M HClO ₄	19
As	V	As(V)/(III)	+0.597	IM HCI	19
Sb	v	Sb(V)/(III)	+0.746	3.5M HCl	21
Bi	III	Bi(V)/(III)	+2.000	0.5M H ⁺ ,	20
Se	IV	Se(VI)/(IV)	+1.150	I=2.0 calculated	18
Те	IV	Te(VI)/(IV)	+0.926	thermodyna- mically	18
Pt	IV	Pt(IV)/(II)	+0.680	3м нсі	20
Pd	II	Pd(IV)/(II)	+1.290	1M HCl	20

Table II.1 Standard reduction potentials of impurity elements in aqueous solution at 25°C.

According to these potentials, the most likely oxidation states to be found in aquaregia or HCl/Cl₂ are listed on the Table. The Pt(IV)-Pt(II) and Pd(IV)-Pd(II) couples are

also included in the Table for completeness and Pt(IV) and Pd(II) are reported to be the stable states. This is in agreement with all other reports on PGM chloride chemistry and refining practice⁽¹¹⁻¹²⁾. It is important to note also that in the cases of Se and Te, Se(IV) and Te(IV) instead of Se(VI) and Te(VI) are reported as the stable species^(1/22/24).

II.3 Impurity Speciation in HCl-MeCl, Media

To better understand and ultimately control the distribution of the impurity elements in solvent extraction-based PGM refining circuits, information pertaining to the stability and abundance of their complexes in chloride media is needed. The formation of chloro-complexes is described by the following general reaction:

$$M^{z+} + nCl^{-} \rightleftarrows MCl_n^{(a-z)-}$$
 (II.10)

$$\beta_{n} = \frac{[MCl_{n}^{(n-z)^{-}}]}{[M^{z^{+}}][Cl^{-}]^{n}}$$
 (II.11)

 β_n represents the overall stability constant of a particular complex. The larger the magnitude of β_n , the stronger the complex will be. According to Muir and Senanayake⁽²⁴⁾, stronger chlorocomplexes are formed by second row transition metals compared with first row ones, and also by higher valence ions. Table II.2 illustrates the strength of chlorocomplexes according to periodicity.

Weak $(\log \beta < 1)$ $(Ni^{2+} < Fe^{2+} < Co^{2+} < Cu^{2+})$ Moderate $(\log \beta = 1-3)$ $(Sn^{2+} < Pb^{2+})$ (Fe^{3+})	Transition Metals Lanthanides, Actinides Group IV Group VIII		
Moderate-Strong (log β =3-15) (Cu ²⁺ < Ag ⁺ < Au ³⁺) (Zn ²⁺ < Cd ²⁺ < Hg ²⁺) (Os ³⁺ < < Ir ³⁺ < < Pt ²⁺ , Pd ²⁺ , Pt ⁴⁺ (As ³⁺ < Sb ³⁺ < Bi ³⁺	Coinage Metals Volatile Metals Precious Metals Group V		

Table II.2 Strength of chloro species according to periodicity⁽²⁴⁾.

Chlorocomplexes are formed in step-wise fashion. Thus a cation (M'^+) can have n constants, from n=0 to n=6. The relative abundance of each of these complexes on the same element will depend on the magnitude of the respective β_n and the activity of the chloride ion (see eqn. II.11). Table II.3 summarizes the stability constants for several chlorocomplexes of the various impurity elements. Some values at ionic strength greater than zero are included.

Equilibrium data	$\log \beta_1$	$\log \beta_2$	$\log \beta_3$	$\log eta_4$	Ref.
At $I=0$ FeCl _n ^{3 n}	1.48	2.13	-0.01		25
CuCl _n ^{2 n}	0.21	-0.40			94
AgCl _n ⁴⁻ⁿ	3.22	5.48	4.80	10.30	"
PbCl _n ²⁻ⁿ	1.60	1.78	1.68	1.38	"
ZnCl _n ^{2 n}	0.43	0.61	0.53	0.20	11
BıCl _n ³-n	2.09	3.90	5.40	6.87	"
SbCl _n ³⁻ⁿ	2.26	3.49	4.18	4.72	11
As(OH) _{3-n} Cl _n	-1.07	-4.54	-8.74		#
At I=5 CuCl _n ²⁻ⁿ	0.60	0.70	0.20	-0.79	26
SnCl _n ⁴⁻ⁿ	3.70	6.46	8.77	9.48	27
At I=7 TeCl _n ⁴⁻ⁿ	3.24	6.28	8.34	10.18	28

Table II.3 Stability constant data for chlorocomplexes of some elements at 25°C. Data for Ni(II),As(V) and Se(IV) was not available

In solvent extraction, in addition to knowing the relative abundance of each chlorospecies it is equally important to know the ligand exchange kinetics of the complex ion in question. The latter refers to the speed by which the Cl is exchangeable with another

ligand L:

$$MCl_{n}^{(n-2)-} + L \stackrel{kf}{\leftarrow} MCl_{n-1}L^{(n-2-1)-} + Cl^{-}$$
 (II. 12)

The faster the ligand exchange reaction (the k_f) the more labile the complex is. In the opposite case, the complex is kinetically inert. For example $PdCl_4^2$ is labile ($k_f = 10^3 \text{ s}^{-1}$), whereas $PtCl_6^2$ is $Inert^{(29)}$ ($k_f = < 10^{-10} \text{ s}^{-1}$). Due to the scarcity of the data and the large number of elements described in the present work, no information on the kinetic behaviour of complexes is included.

Chloro-Species and Speciation Diagrams: Speciation diagrams are very useful graphical representations of the domain of stability of each complex as a function of the concentration (or activity) of the complexing chloride ligand. In the literature speciation diagrams have been published but a great many of them are not in agreement with each other. The reason is the different sets of stability constant data used by various investigators. In particular, a common problem is that the graphical constructions are made on the basis of thermodynamic stability constants. These diagrams imply then that activities are equal to concentrations (since they refer to I=0). This, however, is not the case in concentrated chloride solutions (since they refer to I=0). This, however, is not the case in concentrated chloride solutions (measured data or alternatively mass stability rather than thermodynamic constant values so as to closer represent real solution composition. Figures II.6-II.11 show respective diagrams for Cu(II), Fe(III), Zn(II), Pb(II), Sn(IV), Ag(I). Figures II.12-II.15 depict the diagrams found for Sb(V), Bi(III), Se(IV) and Te(IV).

Species Which do not Form Chloro-Complexes: Ni(II) does not form anionic chloro-complexes readily according to Warshawsky⁽³²⁾ and only exists as Ni²⁺ and perhaps NiCl⁺ in highly concentrated chloride solution⁽³³⁾. Arsenic (V) exists in acid medium as arsenic acid H₃AsO₄, which has little tendency to dissociate below pH 0⁽³⁴⁾:

$$H_3AsO_4 \rightleftharpoons H^+ + H_2AsO_4$$
 $K = 2.5 \times 10^4$ (II.13)

In the case of Se(IV) very few chlorocomplexes are mentioned in the literature. It seems only 12M HCl is capable of holding SeCl₄ and SeOCl₂ and these are unlikely to be encountered in a solvent extraction system⁽³⁵⁾. Hydrolysis of these species produces the selenous species, SeO_3^{2-} , which was found to exist in monomeric and dimeric form in perchloric medium at pH 0 by Barcza and Sillen⁽³⁶⁾. The species resembled (HSeO₃, H₂SeO₃), HSeO₃, (HSeO₃)₂ and (H₂SeO₃)₂.

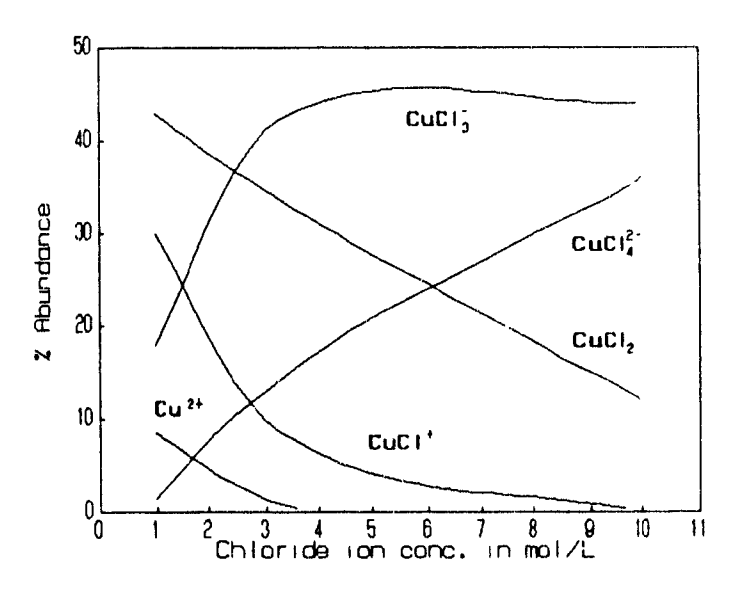


Figure II.6 Distribution of cupric chloride complexes⁽²⁶⁾ as a function of chloride ion concentration. Conditions: $@25^{\circ}\text{C}$, $[\text{Cu(II)}] = 6 \times 10^{4} - 6 \times 10^{3}\text{M}$, (non-corrected for ionic strength).

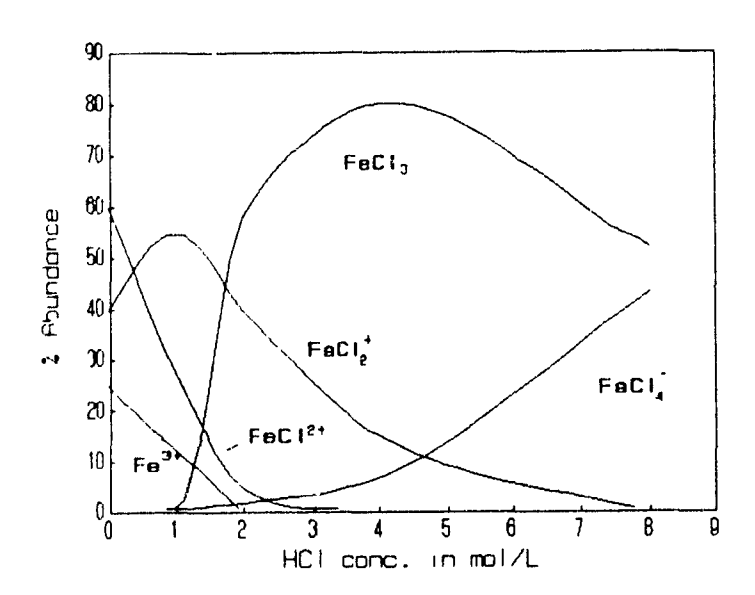


Figure II.7 Distribution of ferric chloride complexes⁽³⁷⁾ as a function of HCl concentration. Conditions: @20°C, [Fe(III)]=10⁻³M, (non-corrected for ionic strength).

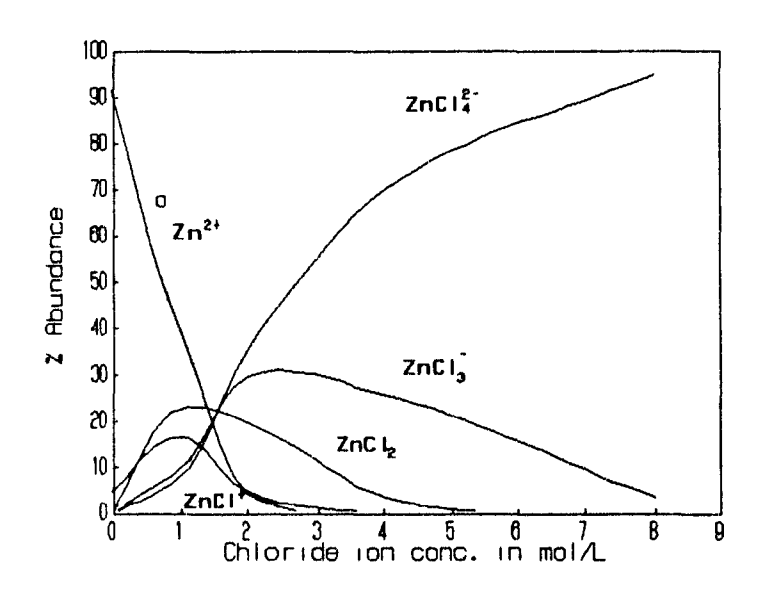


Figure II.8 Distribution of zinc chloride complexes⁽³⁰⁾ as a function of chloride ion concentration. Conditions: @25°C, [Zn(II)]=0.05M (diagram computed from stability constant data and corrected for ionic strength).

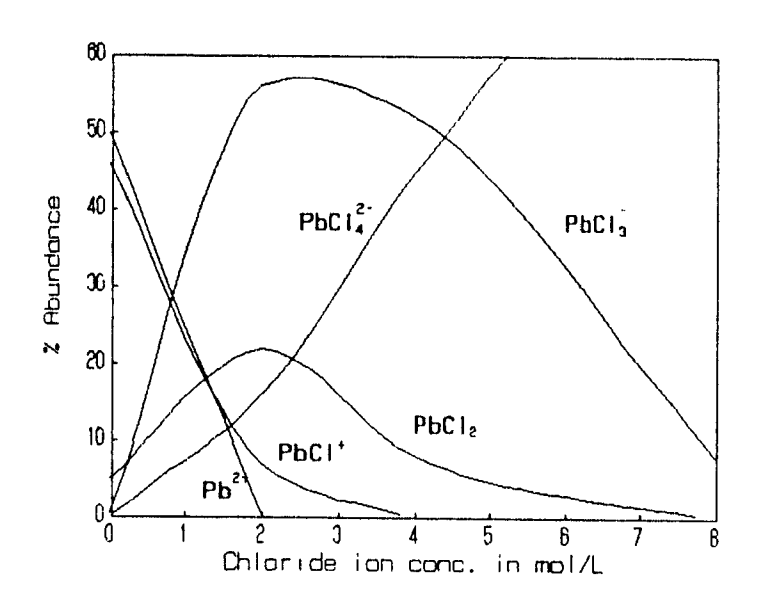


Figure II.9 Distribution of lead chloride complexes⁽³⁰⁾ as a function of chloride ion concentration. Conditions: @25°C, [Pb(II)]=0.05M (diagram computed from stability constant data and corrected for ionic strength).

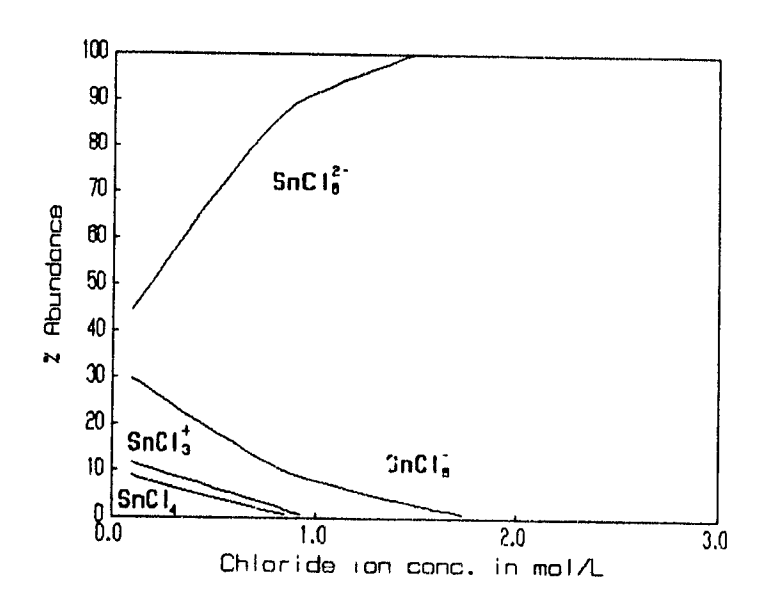


Figure II.10 Distribution of stannic chloride complexes⁽²⁷⁾ as a function of chloride ion concentration. Conditions: @25°C, I=5.0M HClO₄, [Sn(IV)]=0.003-0.01M.

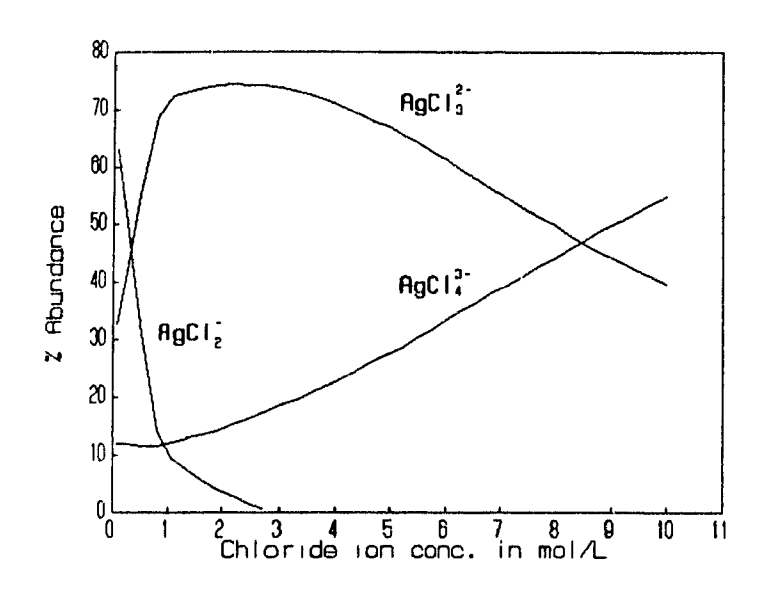


Figure II.11 Distribution of silver chloride complexes⁽³⁸⁾ as a function of chloride ion concentration. Conditions: @25°C (diagram computed from stability constant data and non-corrected for ionic strength).

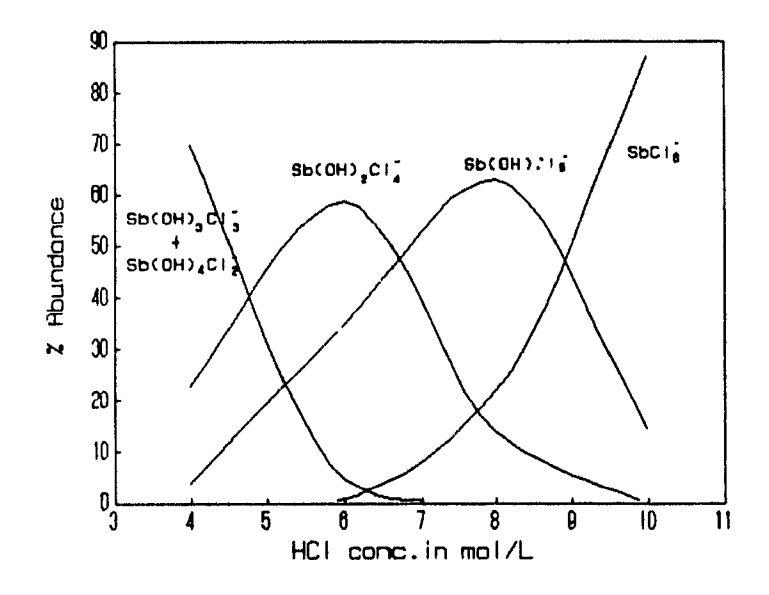


Figure II.12 Distribution of antimonic chloride complexes⁽³⁹⁾ as a function of HCl concentration. Conditions: @25°C, [Sb(V)]=2×10⁻⁴M, non-corrected for ionic strength.

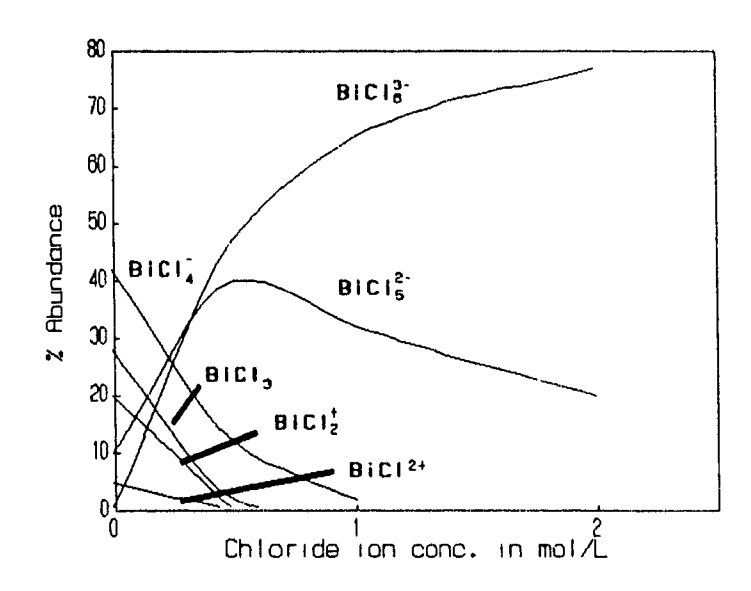


Figure II.13 Distribution of bismuth chloride complexes⁽²⁵⁾ as a function of chloride ion concentration. Conditions: @25°C, I=2.5M NaClO₄, [Bi(III)]=10⁻⁴M.

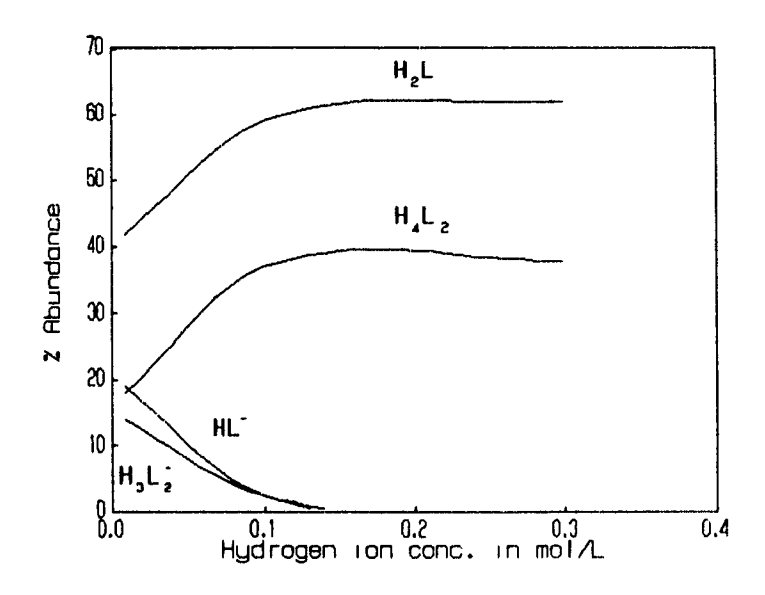


Figure II.14 Distribution of selenous complexes⁽³⁶⁾ as a function of hydrogen ion concentration. Conditions: @25°C, I=1M NaClO₄, L=SeO₃²·=0.1M.

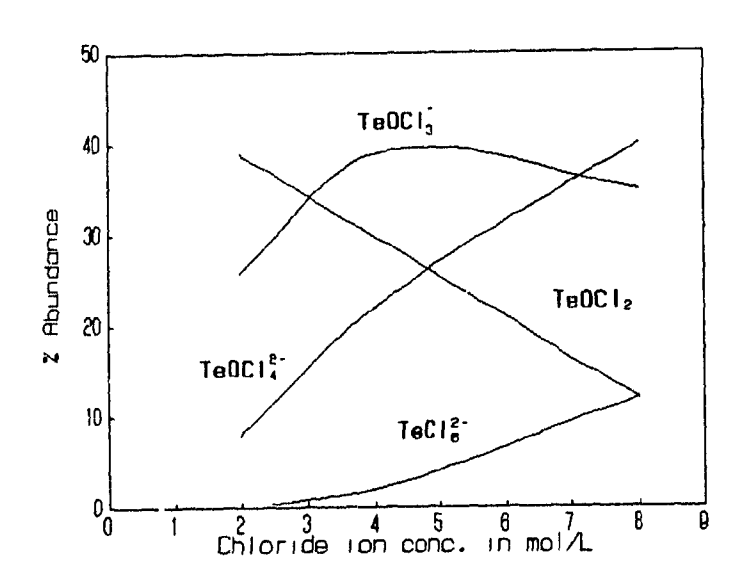


Figure II.15 Distribution of tellurous chloride complexes⁽⁴⁰⁾ as a function of chloride ion concentration. Conditions: @25°C, $[H^+]$ =const=0.5M, [Te(IV)]= 10^4 - 10^3 M.

II.4 Solvent Extraction Systems of the Impurity Elements

Only sporadic and incidental reference can be found in the technical literature on the deportment of impurity elements in industrial PGM solvent extraction circuits. It is important to review the general solvent extraction literature to obtain information on the nature of the extractable species of the impurity elements from aqueous chloride solutions. Before the literature is reviewed, the various mechanisms which may be encountered in solvent extraction are defined. The impurities are grouped in two categories: the base metals (Cu, Fe, Zn, Ni, Pb, Sn and including Ag) and the metalloids (As, Sb, Bi, Se, Te).

Classification of Extraction Mechanisms: Solvent extraction of metal species can take place via three different mechanisms⁽¹⁵⁾: the first class is known as *compound formation* and involves direct bonding of the organic extractant with the metal species itself, i.e., substitution of the chloride ion with the organic molecule occurs, and this is usually favoured by a labile chlorocomplex:

$$MCl_4^{2-} + 2HL_{(0)} \rightleftharpoons ML_{2(0)} + 2H^+ + 4Cl^-$$
 (II.14)

The second class, which is more common, is *ion-pair formation* and is characterised by the formation of an electrically neutral ion pair between an anionic chlorocomplex and a protonated basic organic reagent:

$$MCl_{m}^{n} + nBH^{+}Cl_{(0)} \rightleftharpoons MCl_{m}^{n} \cdot nBH^{+}_{(0)} + nCl^{-}$$
 (II.15)

The third class is called *solvation* and extracts neutral chlorocomplexes with an organic reagent which tends to solvate the outer sphere of the inorganic complex to varying degrees. The following equation shows a typical solvating scenario:

$$MCl_n^{\circ} + yS_{(o)} \rightleftarrows MCl_n.yS_{(o)}$$
 (II.16)

Solvent extraction systems: the base metals

Cu(II) Although copper has mostly been investigated in sulphate medium due to the commercial importance of this system⁽⁴¹⁾, researchers have looked at the chloride route as well. Christie et al.⁽⁴²⁾, report that Lix 63, an α -hydroxyoxime extracts copper as a neutral complex, probably CuCl₂ at low pH values, whereas above pH 1 the Cu²⁺ cation is probably the species extracted. Using a tertiary amine, Aliquat 336, Sato and coworkers⁽⁴³⁾, found that at greater than 4.0M LiCl, copper is strongly extracted, probably as CuCl₄²⁻ by an ion-pair regime:

$$CuCl_4^2 + 2R_3R'NCl_{(0)} \rightleftharpoons (R_3R'N)_2 CuCl_{4(0)} + 2Cl^-$$
 (II.17)

NOPC and Acorga CLX-20, n-octyl-3-pyridine carboxylate and pyridine dicarboxylic ester respectively, function as nitrogen donors via a mechanism which is similar to extraction of CuCl₂ with octanal oxime⁽⁴⁴⁾. The extraction mechanism for Acorga CLX-20 was reported to be:

$$CuCl2(a0) + 2RN(o) \rightleftharpoons CuCl2(RN)2(o)$$
 (II.18)

<u>Fe(III)</u> In the same paper⁽⁴⁴⁾, mention is made that ferric iron existing as FeCl₄ at greater than 4.0M chloride extracts strongly with increasing HCl/Cl concentrations. With Acorga CLX-20 the extraction mechanism, illustrated in eqn. II.19, shows how the ion-pair formation route is followed. Here the protonated form of the extractant (RNH⁺), instead of the neutral form, was postulated in the reaction:

$$RNH^{+}_{(0)} + FeCl_{4}^{-} \rightleftharpoons [(RNH^{+})(FeCl_{4}^{-})]_{(0)}$$
(II.19)

A similar observation with a quaternary amine showed that NR₄FeCl_{4(o)} was the extracted species between 1.9-2.7M HCl⁽⁴⁵⁾. The investigators noted that at low chloride ion

concentration the presence of sulphate ion decreased iron extraction. T. Sato et al. investigated the D2EHPA (di(2-ethylhexyl)phosphoric acid) system and mentioned that below 3.0M chloride, Fe³⁺ was the species extracted whereas in stronger HCl, a solvating reaction mechanism was postulated instead:

$$FeCl3(aq) + 3 HX(o) \rightleftharpoons FeCl3.3HX(o)$$
 (II.20)

Zn(II) In the development of the Zincex process for the recovery of zinc, solvent extraction is employed as a purification technique. In the flowsheet two solvent extraction circuits are incorporated in series⁽⁴⁷⁾. In the first one the ZnCl₄² anion is extracted from 1.9-2.7M Cl² feed liquor with Amberlite LA2, a secondary amine, as an ion-pair and the loaded amine solvent is stripped with water. Zn²⁺ is then extracted from the water strip liquor with D2EHPA via compound formation. Quaternary⁽⁴⁸⁾ and tertiary amines have also been found to extract from chloride media as well.

Ni(II) Literature reports very low tendency for Ni(II) to form chlorocomplexes^(32, 33). As a consequence Ni(II) is hardly extracted from chloride medium Rice and Smith⁽⁴⁹⁾ investigated acidic alkyl phosphorus extractants D2EHPA AND SME 418. These were good for Ni(II) only above pH 3.0 and 2.0M chloride, which is outside the range of recovery for PGM liquors. Groves and Redden⁽⁵⁰⁾ proposed solvation for nickel extraction in their ethylhexanal oxime (EHO) system. At 3.7M Cl, extraction via the following route was suggested:

$$Ni(H_2O)_4Cl_{2(aq)} + 4 EHO_{(o)} \rightleftharpoons Ni(EHO)_4Cl_{2(o)} + 4 H_2O$$
 (II.21)

This solvation extraction route contradicts nevertheless with the fact that Ni(II) does not form chlorocomplexes as stated above^(32,33). It might be speculated then that Ni(II) is extracted via compound formation instead. The strong affinity for anionic chlorocomplexes shown by Alamine 336 and amines in general is reflected in the

extraction results presented in Figure II.16⁽⁵¹⁾. The stronger the tendency for an element to form an anionic chlorocomplex, the more readily the extraction occurs.

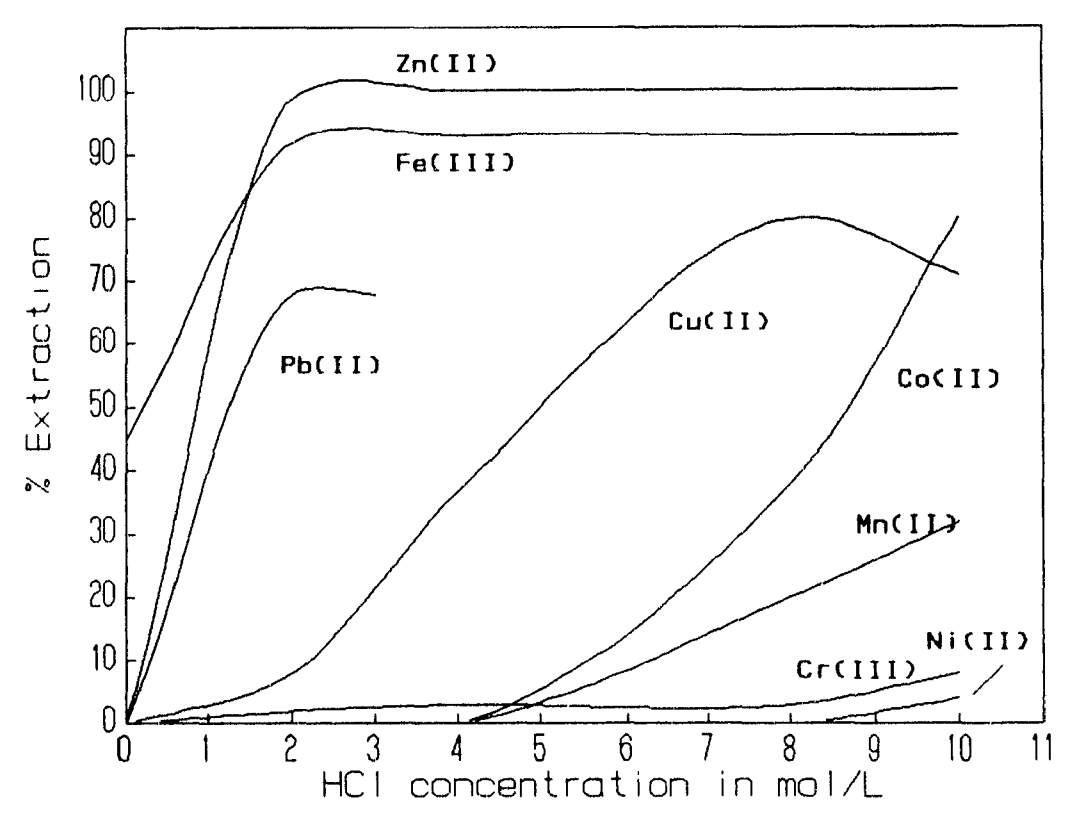


Figure II.16 Distribution of metal species⁽⁵¹⁾ in Alamine 336. Conditions: 25% Alamine 336, 15% dodecanol in Kerosene, $M_n = 1,000 \text{ mg/L}$.

<u>Pb(II)</u> Holdich and Lawson⁽⁵²⁾, completed a number of solvent extraction studies on the extraction of Pb(II). They reported results using D2EHPA, Versatic 10 (a tertiary carboxylic acid), Lix 34 (a sulphydryl quinoline derivative), 54 (a beta diketone) and 70 (a chloro-substituted aromatic hydroxyoxime), Alamine 336, Aliquat 336, as well as Kelex 100 (an akylated 8-hydroxyquinoline derivative) for chloride solutions from 0 to 5.0M HCl. They found that both Alamine 336 and Aliquat 336 showed reduced lead extraction with increasing chloride concentration; they attributed this observation to the fact that the PbCl₄²⁻ complex is not extractable above 4.0M chloride. The Kelex 100 and Lix reagents originally designed for copper extraction gave low distribution coefficients via chelation. McDonald *et al.* ⁽⁵³⁾, who had also worked with Aliquat 336 and Alamine

336 attributed the drop in extraction at 3-4M HCl as being due to steric interferences arising from the bulky PbCl₄²⁻ and PbCl₆⁴⁻ anions. As the existence of PbCl₆⁴ is highly unlikely, another possible cause for the observed behaviour in high chloride concentrations could simply be Le Chatelier's Principle:

$$PbCl_4^{2-} + 2R_3NH^+Cl_{(0)} \rightleftharpoons PbCl_4^{2-}(R_3NH^+)_{2(0)} + 2Cl^-$$
 (II.22)

<u>Sn(IV)</u> Golinski⁽⁵⁴⁾ reported the use of tributyl phosphate, TBP, for the extraction of Sn(IV) from hydrochloric acid. The following solvating mechanisms are suggested:

$$SnCl_{4(aq)} + nTBP_{(o)} \rightleftharpoons SnCl_4.nTBP_{(o)}$$
(II.23)

$$SnCl_6^{2-} + nTBP_{(0)} \rightleftharpoons (SnCl_6^{2-}).nTBP_{(0)}$$
 (II.24)

Tin extraction coefficients increased from 0.1 to 100 as HCl was increased from 0 to 8M. Moreover, there is reason to believe that ion-pair formation is likely at high HCl concentrations as opposed to simple solvation that the authors stated. Although TBP is a weakly basic molecule it is indeed capable of being protonated. Thus eqn. II.24 should be rewritten as follows:

$$SnCl_6^{2\cdot} + 2TBPH^+Cl_{(0)}^{\cdot} \rightleftharpoons SnCl_6^{2\cdot}.(TBPH^+)_{2(0)} + 2Cl^{\cdot}$$
 (II.25)

Other researchers, Sato and Kikuchi⁽⁵⁵⁾ reported that with D2EHPA, Sn(IV) below 2.0M is extracted by compound formation and proposed SnCl₂²⁺ as the extracted species:

$$SnCl_2^{2+} + (HX)_{2(0)} \rightleftharpoons SnCl_2X_{2(0)} + 2H^+$$
 (II.26)

Whereas at higher concentration of chloride, >2.0M, a solvating reaction was postulated:

$$SnCl4(aq) + (HX)2(o) \rightleftharpoons SnCl4.2HX(o)$$
 (II.27)

Selmer-Olsen⁽⁵⁶⁾, showed that Sn(IV) loads very strongly onto triisoctylamine (TIOA) between 0 and 10 M HCl. Sn(IV) tends to extract quantitatively at >1M HCl. Marcus⁽³⁵⁾, in fact proposes the loading of $SnCl_5$ and $SnCl_6$ ²⁻ with amines above 2.0M HCl. Figure II.17 shows the distribution of many impurity elements in the triisoctylamine system investigated by Selmer-Olsen⁽⁵⁶⁾.

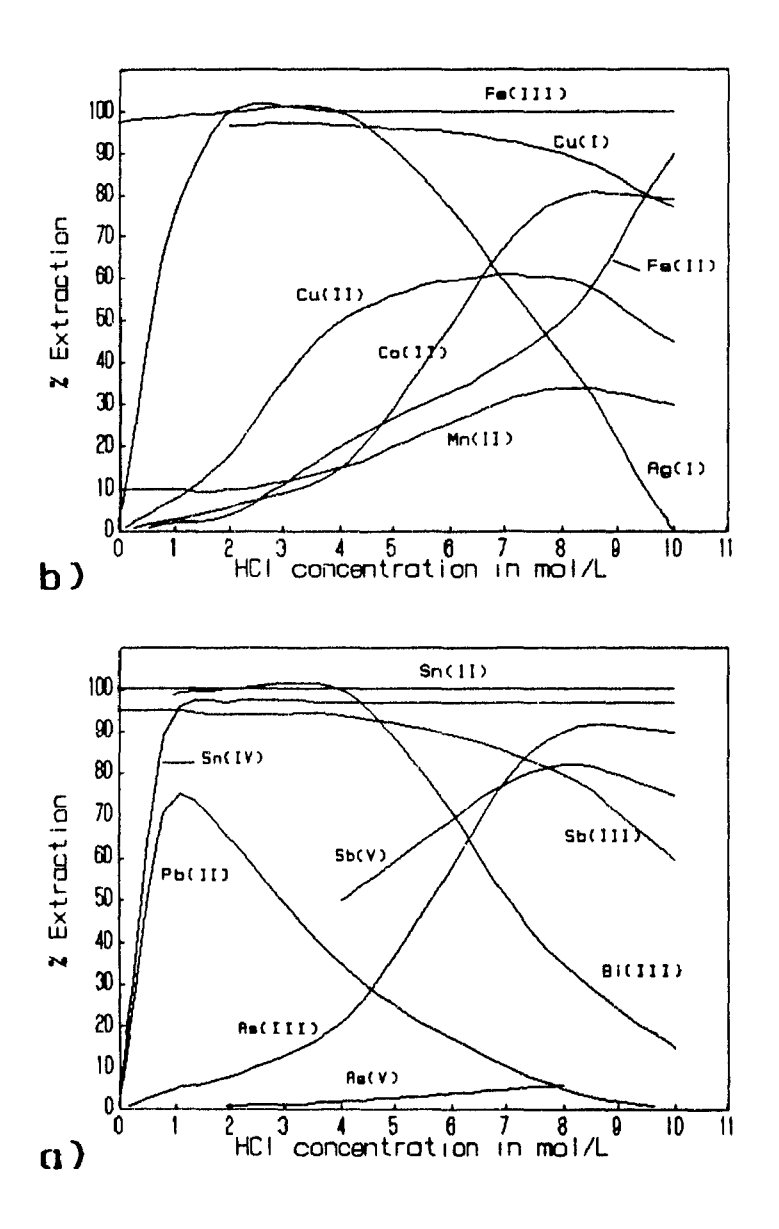


Figure II.17 Distribution of metal species⁽⁵⁶⁾ in TIOA as a function of HCl concentration, a) Sn, As, Sb, Bi, Pb and b) Fe, Ag, Cu, Co, Mn. Conditions: 20v% TIOA in CCl₄, aqueous phase=[Me]=0.1M.

Ag(I) Despite the low solubility of Ag(I) in chloride, Hay Liem and Zangen⁽⁵⁷⁾ experimented with trilaurylamine(TLA) using AKUFVE equipment in order to determine the complex chloro-species of Ag(I). Maintaining constant the chloride concentration at 1.0M they found that the anionic species AgCl₂, AgCl₃² and AgCl₄³ were present at 1:2:0.8 ratio and that these formed extractable ion-pairs of the type (BH⁺)₂(AgCl₃²). They did not produce results for other HCl concentrations Sevdić *et al.*⁽⁵⁸⁾, found that AgCl extracts at less than 0.03M chloride with BATP (0,0-di-n-butyl α-phenylamino-phenylmethane thiophonate), but at higher concentrations the complex anionic species did not extract. Data from Selmer-Olsen in Figure II.17 indicated that the AgCl₄³ species, expected to dominate at high HCl concentration, was not readily extracted with amine. This behaviour is analogous to that observed with Pb(II).

Solvent extraction systems: the metalloids

As(III/V) Most of the patents issued for the extraction of As(III/V) have been for solvating extractants such as TBP and have concentrated only on sulphate aqueous media^(59,60). Marcus⁽³⁵⁾, has reviewed As(III) extraction from chloride medium. Ethers extract AsCl₃ at 10M HCl whereas at lower concentrations the species resembles the type As(OH)₃₋₁Cl₁. Mention is made of the very improbable existence of AsCl₄. Extraction from chloride solution seems to be greater in the presence of HCl with 4-methylpentanone. In the case of As(V), H₃AsO₄ is the neutral complex extracted and is only slightly loaded onto long-chain amine. The amine extraction behaviour of As(III) and As(V) is depicted in Figure II.17a. Above 4.0M, As(III) begins to extract strongly in amine indicating the predominance of anionic species.

Sb(III/V) Antimony in chloride medium has been investigated with solvent extraction and one such study has involved the use of TBP. Bumbalek *et al.*⁽⁶¹⁾, have looked at Sb(III) and have found that it extracted strongly with TBP between 2.0 and 8.0M HCl

although they did not propose an extraction mechanism. SbCl₄ is the complex extracted as an ion pair with amines at 4.0M HCl according to Marcus' review⁽³⁵⁾. In the same review, Sb(V) was shown to have erratic behaviour as hydrolytic reactions are known to take place at less than 6.0M HCl. With diethyl and diisopropyl ether irreproducible results seemed to occur quite readily. In another study⁽⁶²⁾, with mesityl oxide (MeO) which is an unsaturated straight chain ketone, two species were proposed to be extracted at 3.0M Cl⁻. The first was a solvated species SbCl₃.MeO and the second was an ion-pair one represented as HSbCl₄.MeO. Data in Figure II.17a show that complexation seems to result for both states as they probably extract both by ion-pair formation in the full HCl range.

<u>Bi(III)</u> T. Sato⁽⁶³⁾ investigated the behaviour of Bi(III) with trioctylamine (TOA) and trioctylmethyl ammonium chloride (TOMAC). The results showed strong extraction below 2.0M chloride for both extractants, with a strong decrease at greater chloride concentration. The following equations show the possible mechanisms at 2.0M chloride:

TOA:
$$BiCl_4 + R_3NHCl_{(0)} \rightleftharpoons (R_3NH)BiCl_{4(0)} + Cl$$
 (II.28)

TOMAC:
$$BiCl_5^{2-} + 2R_3R'NCl_{(0)} \rightleftharpoons (R_3R'N)_2BiCl_{5(0)} + 2Cl^{-}$$
 (II.29)

At greater chloride concentrations, BiCl₃⁶ is thought of being not extractable. This might again be attributed to the Le Chatelier's Principle or to steric factors since 3 amine molecules per metal ion are required. Marcus' review⁽³⁵⁾ claims that solvating extractants produce poor results due to the strong chloro complexation of Bi(III), evidently due to the predominance of anionic species. This is seen in the case of TBP in Bumbalek's data shown in Figure II.18. No reports were found on Bi(V).

<u>Se(IV)</u> Most of the earlier extraction work dealt with solvating extractants. TBP and TOPO, trioctylphosphire oxide, produced distribution coefficients of > 100 at 12M HCl where selenium forms chloride species such as SeOCl₂ and SeCl₄ (35). Also, Jordanov (63)

states that above 3.0M HCl Se(IV) extracts at >80% with a variety of aliphatic monoketones, presumably by a solvating mechanism with proposed species Se(OH)₂Cl₂. Heddur and Khopkar⁽⁶⁴⁾ noticed that with trioctylphosphine oxide (TOPO), very strong chloride conditions, i.e, 6M HCl/7M LiCl, were required for Se(IV) extraction.

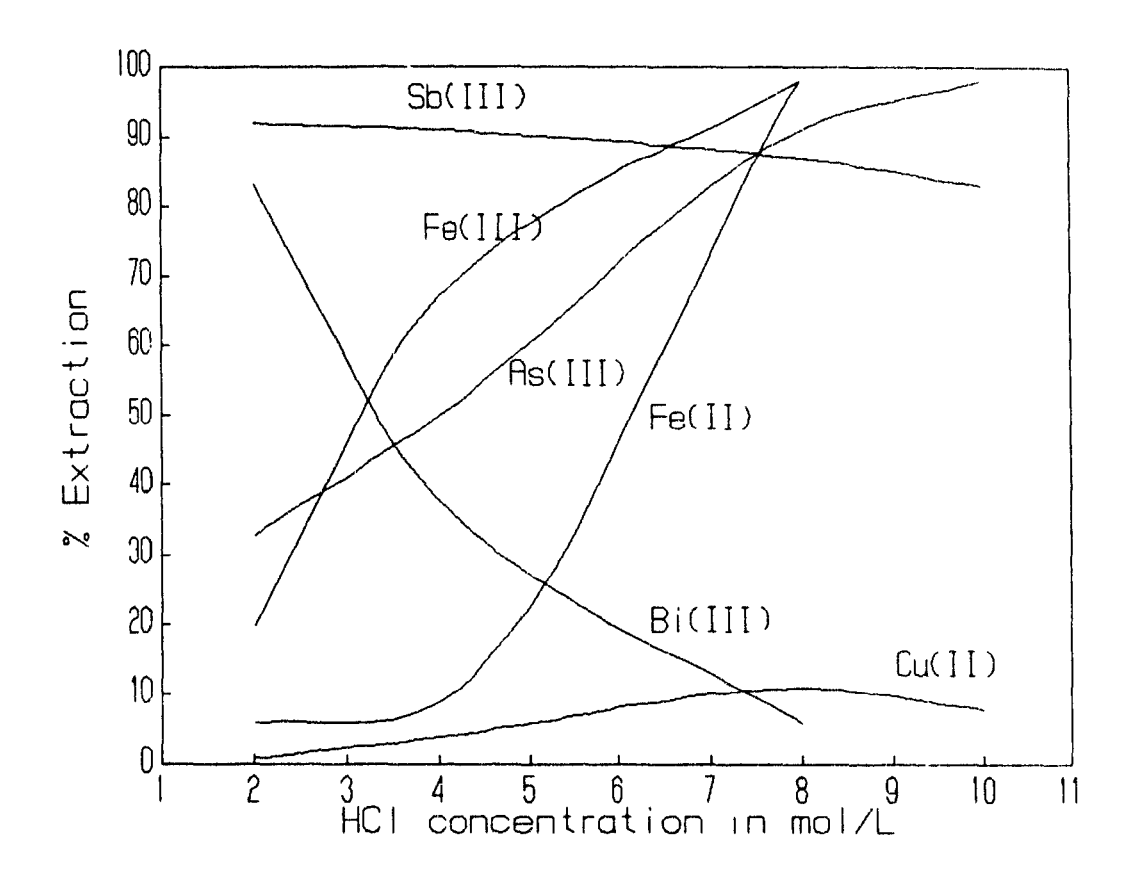


Figure II.18 Distribution of metal species⁽⁶¹⁾ as a function of HCl in TBP. Conditions: 40v% TBP in white spirit, Aqueous phase=Cu(II)= 1000 mg/L, Sb(III)=80,000 mg/L, Bi(III)=As(III)=Fe(II)+Fe(III)= 1750-3000 mg/L.

With methylisobutyl carbitol, and in perchlorate medium, 3.0M perchlorate was sufficient to achieve a D=10 for Se(IV), at < pH 2 according to Sekine *et al.* (66) So far, few researchers were successful in attempting to describe the mechanisms of extraction apparently due to the complexity of selenium chemistry. One of the few was the team led by Fisher (67), who described the extraction of selenous species with tri-n-octylammonium

chloride. The following two possible mechanisms were proposed for the region between pH 1.2-5.0:

$$1/2(H_2SeO_3)_{2(a_0)} + TOAH^+Cl^-_{(o)} \rightleftharpoons H_2SeO_3.TOAH^+Cl^-_{(o)}$$
 (II.30)

$$1/2(HSeO_{3}^{-})_{2} + TOAH^{+}Cl_{(0)}^{-} \rightleftharpoons HSeO_{3}^{-}.TOAH^{+}_{(0)} + Cl^{-}$$
 (II.31)

<u>Te(IV)</u> It has been suggested that the formation of Te(IV) chloro-complexes increase above 3.0M chloride with species such as $TeOCl_4^{2-}$ and $TeCl_{4+n}^{n-}$ dominating⁽³⁵⁾. TeCl_{4+n}ⁿ is not mentioned by other researchers (see diagram of Figure II.15) and its formation is not certain. These are the types of complexes postulated to have been extracted at 6M HCl with diethyl ether (D=0.5) and with TBP (D=200). TBP can be seen as extracting the said complexes (at least partly via ion-pair formation upon protonation) but diethyl ether must be extracting a neutral species, possibly TeOCl₂°. Another basic extractant, TOPO, has been reported to extract Te(IV) at pH 4 and 3.0M perchlorate⁽⁶⁶⁾ but as tellurous acid. In this case, the tellurous species is possibly extracted:

$$H_2TeO_{3(aq)} + TOPO_{(o)} \rightleftharpoons H_2TeO_3.TOPO_{(o)}$$
 (II.32)

Mabuchi and Okada⁽⁶⁸⁾ state that in their work on Te(IV), Te(OH)₃⁺, a hydrolysed species is extracted by compound formation between 1.0-3.0M HCl with dithizone (H₂Dz) a diphenylthiocarbazone. Like selenium few mechanisms of extraction were suggested with extractants as tellurium chloro-species have yet to be determined accurately.

Summary: The relevant published data applicable to PGM refining are summarised in Tables II.4 and II.5. The following main observations can be made with reference to the extraction of impurity elements from aqueous chloride liquors encountered in PGM refining. The ion-pair formation mechanism is the most common case for the extracted species. Thus, strong basic extractants (amines) extract strongly

Metal	Extractant	Extracted Species/Range	Mecha -nism	Ref.
Cu(II)	LIX 63	C: $Cl_2 < pH1 < Cu^{2+}$	S/CF	42
	ALIQUAT 336	$CuCl_4^{2-} > 4.0M Cl$	IP	43
	ACORGA CLX-20	$CuCl_2 > 4.0M Cl$	S	44
Fe(III)	ACORGA CLX 20	FeCl ₄ >4.0M Cl	IP	44
	QUAT. AMINE	FeCl ₄ 1.9-2.7M HCl	IP	45
	D2EHPA	Fe ³⁺ <3.0M Cl < FeCl ₃	CF/S	46
Zn(II)	AMBERLITE LA2 TLA	$ZnCl_4^{2-}$ 1.9-2.7M HCl $ZnCl_4^{2-}$ > 0.01M Cl	IP IP	47 48
Ni(II)	D2EHPA SME 418	Ni ²⁺ , >pH 3.0, " 2.0M Cl	CF CF	49
	ЕНО	$Ni(H_2O)_4Cl_2$, ~3.7M HCl	S	50
Pb(II)	ALAMINE 336	PbCl ₃ -, 0-5.0M HCl	IP	52
	ALIQUAT 336	PbCl ₃ -, 0.1-4.0M HCl	IP	53
Sn(IV)	TBP	SnCl ₄ < 4M HCl < SnCl ₆ ² ·	S/IP	54
	D2EHPA	SnCl ₂ ²⁺ < 2M Cl ⁻ < SnC ₁₄	CF/S	55
	TOA	SnCl ₆ ² ·, 0-10M HCl	IP	56
	TOA	SnCl ₅ > 2.0M HCl	IP	35
Ag(I)	TLA	$AgCl_3^2$, ~ 1.0M HCl	IP	57
	BATP	AgCl < 0.03M HCl	S	58

Table II.4 Summary of most relevant impurity element SX systems: extraction of base metals and silver from chloride liquors. Legend: CF= compound formation, IP= ion-pair formation and S= solvation.

Metal	Extractant	Extracted Species/Range	Mech- anism	Ref.
As(V)	TOA	H ₃ AsO ₄ , NO EXTRACTION in 1.0-8.0M HCl range	S exp- ected	35
Sb(V)	ТОА	Sb(OH) _n Cl _{5-n} -,3.0-10.0M HCl	IP	56
Bi(III)	TOA TOMAC	BiCl ₄ up to 2.0M Cl BiCl ₅ ² up to 2.0M Cl	IP IP	63
Se(IV)	TBP, TOPO Aliphatic Monoketones	SeOCl ₂ or SeCl ₄ at 12M HCl Se(OH ₂)Cl ₂ > 5.0N HCl	S S	35 64
	ТОА	H ₂ SeO ₃ , HSeO ₃ , pH1.2-5.0	S/IP	67
Te(IV)	ТОРО	H ₂ TeO ₃ , 3.0M ClO ₄	S	66
	TBP diethyl- ether	6M HCl, TeOCl ₄ ²⁻ " TeOCl ₂	IP S	35 36
	H ₂ Dz	0.1-3.0M HCl, Te(OH) ₃ ⁺	CF	68

Table II.5 Summary of most relevant impurity element SX systems: extraction of metalloids from chloride liquor. Legend: IP= ion-pair formation, S= solvation.

throughout the HCl range and weak basic extractants (TBP/TOPO) seem to extract to a significant degree only at higher Cl'/HCl concentrations, i.e., > 3.0M. Although the solvation mechanism is mentioned in several of the reviewed SX systems nevertheless it appears to be applicable only in the case of Se(IV) and to a lesser degree Sn(IV). The other cases are not directly relevant to PGM refining (for example, the extraction of H_2TeO_3 from 3.0M ClO_4). Compound formation is much rarer as chloride solutions tend to strongly complex most impurity elements. It appears then that a weak basic extractant such as the one used in this study (TN 1911) has lower potential for the extraction of impurity elements from strong chloride liquors.

CHAPTER III: EXPERIMENTAL

III.1 Apparatus and Reagents

Phase Mixing-Contacting: Both shake-out and mechanically-stirred solution tests were performed. Almost all the shake-out tests were carried out in 125, 250, 500, 1000 and 2000 mL Pyrex separatory funnels. The 125 mL ones were small enough to fit on the arms of a Burrell model 75 wrist action shaker available in the laboratory Minimum volume used was 10 mL for each phase in the case of the single metal tests whereas 20 mL was the norm for mixed metal tests. In the case of controlled pH tests, the set-up was quite different. A minimum of 60 mL liquid was poured into a 300 mL beaker fitted with a 1" teflon coated impeller and a single teflon baffle. Stirring speed was 350 r.p.m. Manual pH control was carried out by using a Fisher Accumet 810 meter with a corresponding pH probe. 1.0M NaOH and 8.0M HCl were used for pH adjustment and these were contained in two overhead burettes. Figure III.1 shows the laboratory assembly.

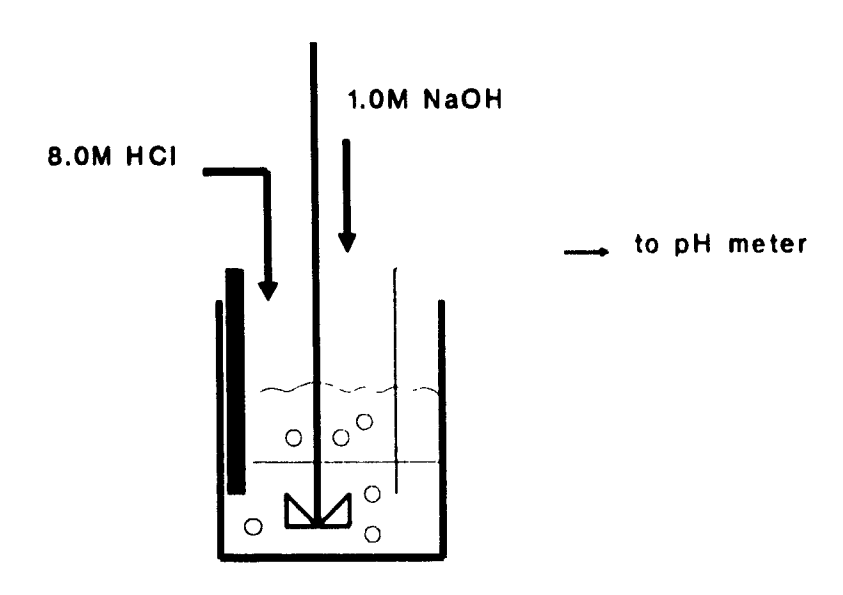


Figure III.1 pH control set-up for agitation tests.

Organic Phase: Some information on the chemical identity of the extractant and the other components of the organic phase is given in Table III.1.

Organic phase component	Composition	Average molecular weight	Purity	Supplier
REAGENT TN 1911	8-hydroxyquinoline R branch unsaturated, C#10-13	311	82%	Schering Berlin AG
MODIFIER Tridecanol	long chain alcohol C ₁₃ H ₂₇ OH	200	-	Harcros Chemicals
DILUENT Solvesso 150	97% aromatic 3% paraffinic	N/A	N/A	Esso

Table III.1 The chemical identity of the organic phase components.

The composition studied was the 5v% (0.13M) TN 1911-10v% (0.37M) tridecanol mixture. In the early part of the work (*Experiment 1*), a 5v% TN 1911-5v% (0.18M) tridecanol mixture was used and the modifier content was eventually raised to 10v% for the remainder of the experimental work to avoid any risk of phase disengagement problems. Before using the organic phase mixtures, they underwent a conditioning stage for the removal of water soluble impurities. It consisted of one 2.7M (100g/L) HCl contact followed by four water contacts all at an A/O=1 and 3 min agitation time.

Aqueous Phase: All single and mixed metal solutions were prepared using analytical grade reagents, distilled water and reagent grade HCl and HNO₃ (12 and 14M respectively). Chloride ion source was taken as MgCl₂. Aqua-regia at 1 HNO₃:3 HCl volume ratio was used for digestion in the case of solution preparation from elemental metal powders and in the case of oxide reagents. Also, whenever stannic salt was required, stannous chloride was oxidised by aqua-regia digestion. Table III.2 shows the

list of materials used in the experiments.

Reagent	Supplier		
ZnSO ₄ .7H ₂ O	A&C, American Chemicals Ltd.		
CuSO ₄ . 7H ₂ O	Anachemia		
$NiCl_2.6H_2O$	Anachemia		
SeO ₂	Mallinckrodt Chemicals		
$Fe_2(SO_4)_3.7H_2O$	Anachemia		
Pb°	Fisher Scientific		
Bi°	Cominco Inc.		
Sb ₂ O ₃	BDH		
As_2O_3	Fisher Scientific		
AgNO ₃	Fisher Scientific		
Te ^o	Aldrich Chemicals		
SnCl _{2wH2} O	Anachemia		
SnCl ₄ .5H ₂ O	Aldrich Chemicals		
Pt°	Johnson Matthey		
Pd°	Johnson Matthey		
KNa tartrate.4H ₂ O	Aldrich Chemicals		
NaOH	A&C Ltd.		
MgCl ₂	ACP Chemicals		
HCl	Mallinckrodt Chemicals		
H ₂ SO ₄	Aldrich Chemicals		
HNO ₃	Baxter (Canlab)		
-			

Table III.2 List of the reagents used in the experiments.

III.2 Experimental Procedures

Preliminary Tests with a Multi-Element Chloride Liquor: Among the earlier tests carried out in the laboratory were the ones done to investigate the distribution behaviour of several impurity elements upon coextraction of Pt-Pd from feed aqueous solutions of semi-industrial origin. This feed was prepared by diluting an industrial feed, coded RCMint-12-II, obtained from the Royal Canadian Mint in Ottawa, Ontario. A complete analysis is presented in Table III.3. It was a Au-free, Pt-Pd rich solution in the presence of a greater amount of Cu (14600 mg/L). This feed was also analysed for free acid by the EDTA masking technique (explained in Appendix A) and was found to hold 135 g/L or 3.7M HCl.

Element	Assay in mg/L
Pt	2500
Pd	5100
Ag	120
Fe	720
Cu	14600
Ni	960
Z n	860
Pb	1100
Na	5400
As	145
Sb	<3
Bi	<5
Se	<3
Те	15

Table III.3 Full assay of as-received Royal Canadian Mint solution (RCMint-12-II).

Dilution of the as-received solution reduced concentrations of Pd to 1,000 mg/L, Pt to 300 mg/L and Cu to 2,400 mg/L. The solution was "spiked" with various impurity elements with a target concentration of 1,000 mg/L $M_{\rm sq}$ in the following order: Pb and

Bi were added in the elemental form to boiling aqua-regia, and upon complete dissolution and vaporization to dryness, HCl and water were added, with stannous chloride together with ferric chloride following at a 2:1 molar ratio to oxidize stannous to stannic. Zinc sulphate, nickelous chloride, and trioxides of arsenic and antimony were added later, as well as some Pt single metal solution to increase the Pt concentration. Adjustment of the acid level was finally made to 0.70M (30 g/L) HCl. The procedure was repeated—for 2.33M (100 g/L) and 4.70M (200 g/L) HCl solutions. The prepared solutions were filtered through no. 42 Whatman paper for removal of any insolubles and analysed by atomic absorption spectrophotometry to determine accurately the impurity composition

The first series of tests were designed in the following manner: a) each of the three feeds was contacted with 5v% TN 1911-5v% tridecanol-Solvesso 150 for 3 min. at an A/O=1, b) a raffinate sample was removed and the organic volume adjusted to maintain the A/O ratio. Shaking was continued for a further 12 minutes to reach the 15 min. mark, and c) procedure (b) was repeated with agitation to 30 min

Single Element Tests, Extraction and Scrubbing: Further investigation of the behaviour of the impurity elements was done by carrying out single metal M_{aq} testing on each of the following: Fe(III), Cu(II), Zn(II), Pb(II), Sn(IV), Ag(I), As(V), Sb(V), Bi(III), Se(IV), Te(IV). Ni(II) was omitted from this list since it had exhibited nil extraction in preliminary tests. So, for each of the elements, four aqueous solutions holding 1,000 mg/L of M_{aq} were made up with different acid and chloride ion concentrations:

- (a) 1.3M (50 g/L) HCl
- (b) 1.3M (50 g/L) HCl + 2.0M MgCl₂
- (c) 2.7M (100 g/L) HCl
- (d) 4.0M (150 g/L) HCl

Loading experiments were carried out at an A/O=1 and 3 min. contact time. The organic phase loaded with 2.7M HCl feed was retained and in turn split into four streams for scrubbing with various selected solutions. These solutions were: distilled water, 2.7

and 8M HCl as well as $1.7M H_2SO_4$. Scrubbing was performed at A/O=1 and 3 min. contact time immediately following loading.

Some of the troublesome elements were subjected to further single metal tests using other scrubbing media. Thus, Sn(IV) was tested with chloride and hydroxide solutions, Sb(V) was subjected to scrubbing with KNa tartrate solution and Ag(I) was scrubbed with weakly acidic MgCl₂ solution.

Batch-Wise Simulation of a Counter-Current Circuit: In order to produce as representative data as possible for the design of a continuous counter-current circuit, the method proposed by Treybal⁽⁶⁹⁾ was used. Figure III.2 introduces the concept of batch contacting in a counter-current cascade fashion. The flow of aqueous is realised from left to right, whereas organic is in the opposite direction. A 5^(top) by 5^(right) batch contacting scheme is proposed for a 5-stage counter-current contact and this seems to recreate a situation close to the steady state. Volume and metal inventory had to be carefully worked out before conducting the experiment as multiple streams became necessary for simulating extraction, scrubbing and stripping circuits. A minimum volume of 20 mL was a requirement at the tail end of the circuit and was chosen to avoid significant errors with the mass balance.

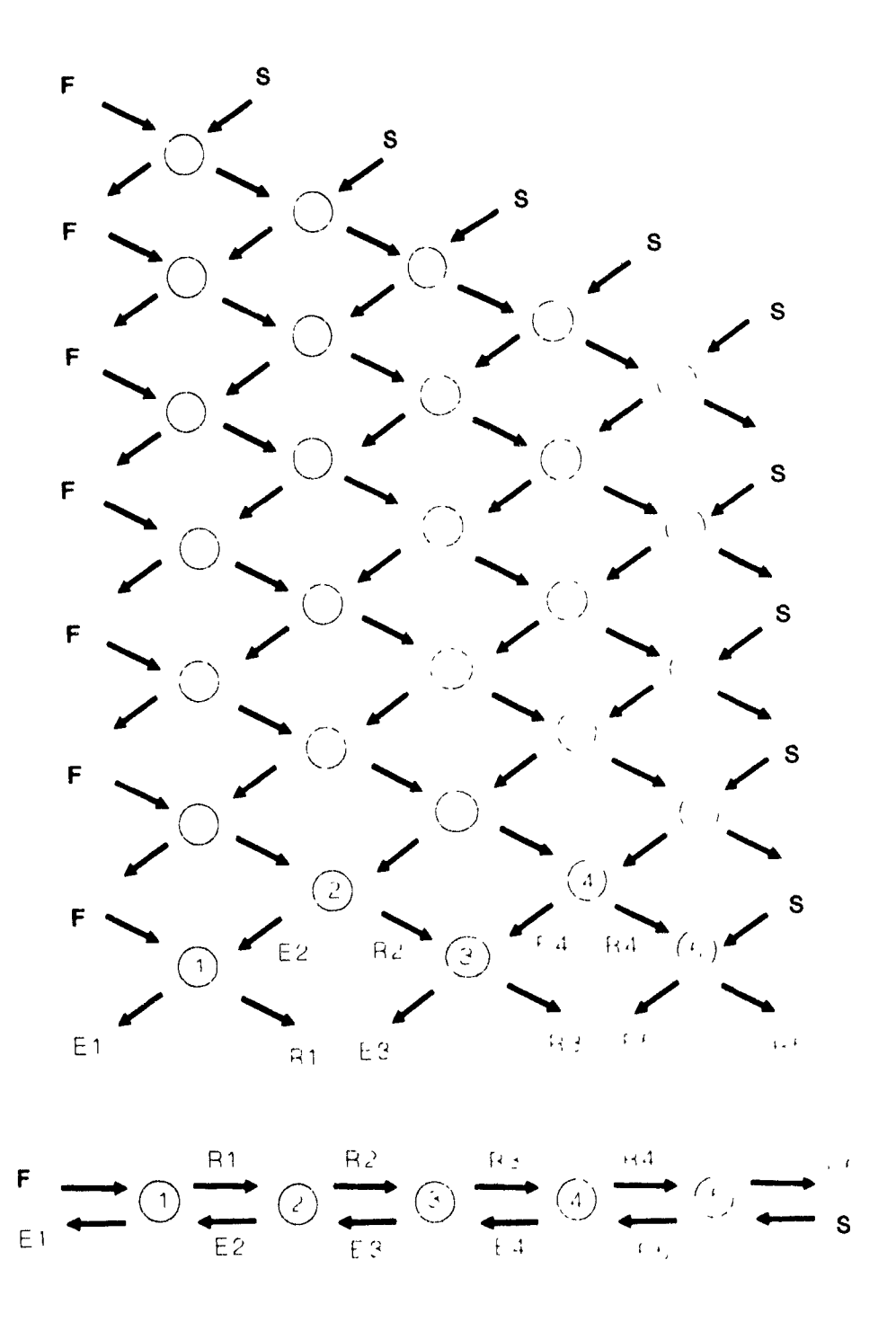


Figure III.2 Treybal's batch-wise simulation of continuous counter-current contacting. F = aqueous feed, S = fresh organic, E = loaded organic and R = aqueous raffinate.

III.3 Chemical Analysis

ŧ

Instrumentation: The adoption of flame atomic absorption spectrophotometric analysis (AA) was based on the view that it was the most rapid and sensitive technique considering the numerous elements to be analysed. All relevant information on the AA analysis of the impurity elements is summarised on Table III.4. An Instrumental Laboratories model 357 instrument fitted with double-beam system was used. Standard practice was to use an air-acetylene flame (2300℃) but Sn required a hotter flame and a nitrous oxide-acetylene flame was used for this element (~3000℃). Single element hollow cathode lamps were selected as source.

Sample and Standard Preparation: Aqueous solutions only were analyzed by flame atomic absorption which meant that mass balance could only be derived by balancing feeds and raffinates. In the case of the RC Mint shake-out tests, Experiments 1-2, standards were prepared in 1.5wt% HCl and 2,000 mg/L LaCl₃ to avoid suppressing interference from strong Na concentration, particularly in the case of Pt analysis. In the initial analyses, erratic readings were obtained for As and Fe and so further refinements were made to the technique for more confident analysis. All the remaining tests performed with mixed metal media were analysed by using the method of standard additions⁽⁷⁰⁾. The method of standard additions is based on the concept of spiking a sample solution several times with different amounts of standard solution, thus operating in a matched matrix environment and producing a linear relationship as well as an accurate determination for the particular spiked sample as well as other samples. Figure III.3 shows a typical graph correlating absorbance to the concentration of an unknown spiked sample x.

Element	Wavelength, λ (Bandpass, nm)	Linear Range, mg/L	Remarks	Reprodu- cibility
Ag	328.1 (1.0)	1 - 20	Air-C ₂ H ₂ , blue flame	good
As	193.7 (0.3)	1 - 15	BKG, Air-C ₂ H ₂ , bl. fl	poor
Bi	223.1 (0.3)	1 - 15	Air-C ₂ H ₂ , blue flame	good
Cu	324.7 (1.0)	1 - 5	U H H H	satisfact.
Fe	248.3 (0.3)	1 - 5	. 11 11 11	ft .
Ni	232.0 (0.15)	1 - 5	" " , " "	good
Pb	217.0 (1.0)	1 - 15		14
Pd	247.6 (0.3)	1 - 15	. , , ,	''
Pt	265.9 (0.5)	1 - 120	Air-C ₂ H ₂ , blue flame	satisfact.
Sb	217.6 (0.3)	1 - 30	Air- C_2H_2 , blue flame	good
Se	196.0 (1.0)	1 - 30	BKG, Air-C ₂ H ₂ , bl /l	poor
Sn	235.5 (0.5)	1 - 120	N ₂ O-C ₂ H ₂ , red cone	excellent
Те	214.3 (0.5)	1 - 25	Air-C ₂ H ₂ , blue flame	good
Zn	213.9 (1.0)	0.1 - 1.0	u u u u	"

Table III.4 Atomic absorption settings used for the elements on the IL 357 instrument. BKG = Background correction with deuterium lamp. Pt analysis from mixed metal solutions was followed by spiking with 2,000 mg/L La⁴⁺. Reproducibility: excellent (±1%) to poor (±10%).

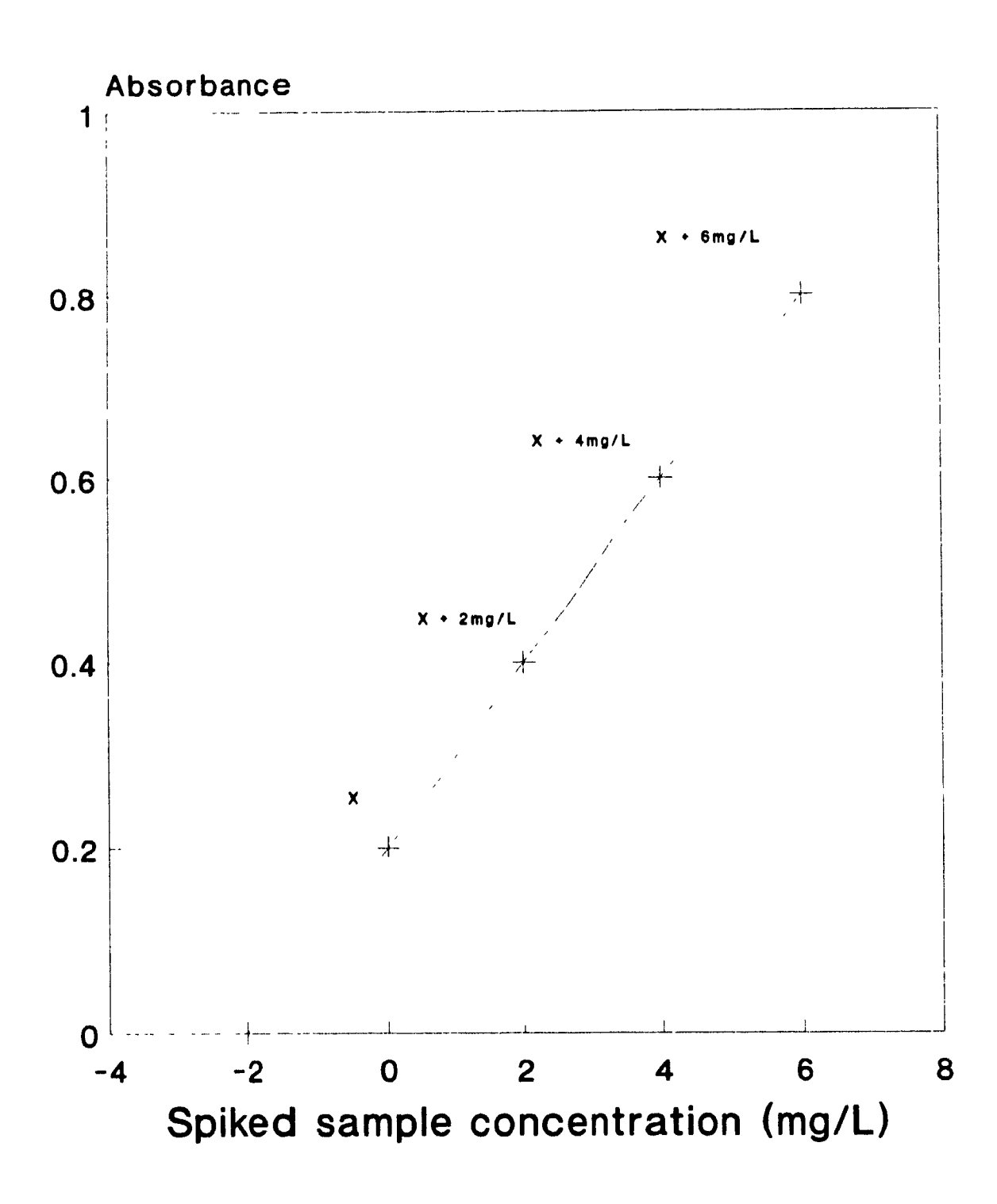


Figure III.3 The method of standard additions.

CHAPTER IV: RESULTS AND DISCUSSION

IV.1 Introduction

Three kinds of experiments were carried out as part of the study. In the first series of tests, the tendency for coextraction of the impurity elements along with Pt-Pd was observed, using a semi-industrial feed and a chosen solvent composition. Having established the behaviour of the elements in multi-element solution, the second series of tests involved single element extraction tests, which were useful in determining the distribution of the elements as a function of HCl concentration without the interference of possible crowding effects. Moreover, single element distribution tests in conjunction with information from the literature summarized in Chapter II made it possible to propose the operating extraction mechanisms and thereby understand the chemistry of the TN 1911-HCl system. In addition, a second objective was the development of scrubbing procedures for the removal of impurity elements from the loaded organic phase. The third and final part of the experimental section involved the design and testing of a flowsheet which incorporated some of the developed scrubbing procedures.

IV.2 Preliminary tests

In these tests, a semi-industrial feed liquor was prepared from a Royal Canadian Mint solution (Table III.3) spiked with several impurity elements. This feed solution was contacted with the investigated solvent (TN 1911/tridecanol/Solvesso 150) to assess the general trends in impurity element behaviour. Their distribution behaviour was examined in terms of HCl feed concentration and contact time.

At 5v% (0.13M) TN 1911 and 3 min. contact time, Figure IV.1 shows how metal extraction varies as a function of initial HCl concentration. The extraction patterns of both Pt(IV) and Pd(II) are the expected ones as HCl concentration is increased. The extraction of Pt(IV) increases as more organic is protonated whereas the extraction of Pd(II) decreases due to the higher hydrogen and chloride ion concentrations. The previously postulated⁽⁴⁾ extraction mechanisms explain their behaviour:

Protonation:
$$HL_{(0)} + HCl \rightleftharpoons H_2I.Cl_{(0)}$$
 (IV.1)

Chelation:
$$PdCl_4^{2-} + 2H_2LCl_{(0)} \rightleftharpoons PdL_2 + 4H^+ + 6Cl^-$$
 (IV.2)

Ion-pair formation:
$$PtCl_6^{2-} + 2H_2LCl_{(0)} \rightleftharpoons PtCl_6^{2-}(H_2L^+)_{2(0)} + 2Cl^-$$
 (IV.3)

However, the nil extraction of Pt(IV) at 0.7M HCl was unexpected and had to be further investigated and explained via a series of tests which are described in Appendix B. It was found that the observed suppression of Pt(IV) was due to the presence of Sn(II) added to the feed. As for the extraction of the impurity elements, the following observations can be made: Strong extraction of Bi(III), Sb(III) and Sn(II/IV) was seen to occur throughout the 0.7-5.5M HCl range. With Bi(III) and Sb(III), the tendency of extraction dropped with increasing HCl concentration. Similarly, Cu(II) extraction seemed to follow the same trend. In contrast, Fe(III) and to a lesser degree As(III) and Zn(II) were found to extract at increasing degree with increasing HCl concentration. It

.

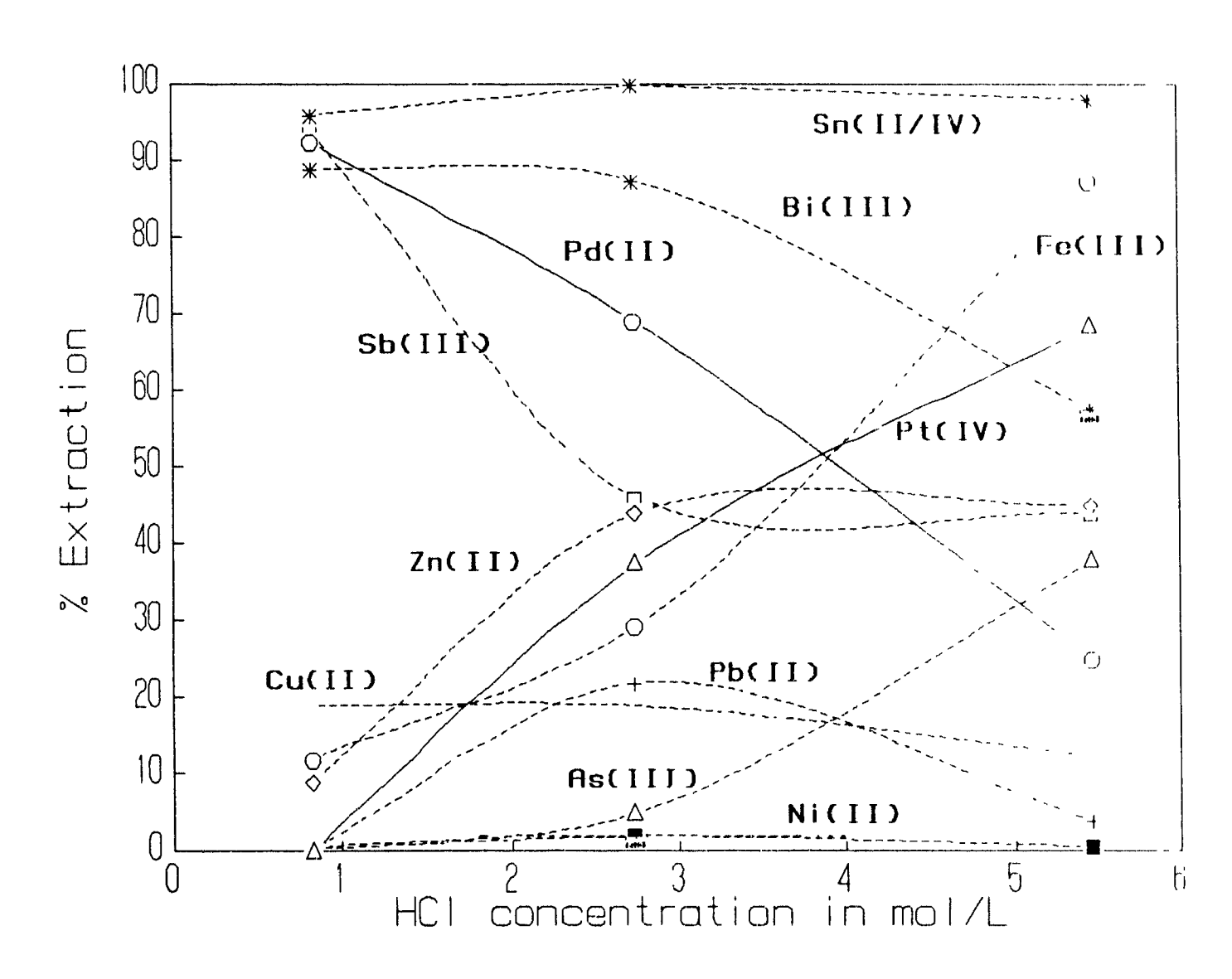


Figure IV.1 Distribution of impurity elements in 5v% TN 1911 as a function of HCl concentration (Experiment 1), conditions: $3 \text{ min., A/O} = 1, 25^{\circ}\text{C},$ $M_{\text{aq.}} = 1,000 \pm 200 \text{ mg/L}.$

should be noted that the analysis of As was at this point rather uncertain as readings were erratic (±20%). Pb(II) showed bell-shaped behaviour with highest extraction levels at 2 7M HCl while Ni(II) extraction was nil. Lastly, it was noted that no phase disengagement difficulties were encountered with these tests (phase separation times were less than 60 seconds).

Figure IV.2 shows the effect of contact time, at 0.7M HCl for 5v% TN 1911. As expected from Figure IV.1, two distinct groups of elements are observed at this acidity level: the first group consisted of Sn(II/IV), Bi(III) and Sb(III) coextracted along with Pd(II) whereas the second group exhibiting <20% extraction was constituted of As(III), Pb(II), Fe(III), Zn(II), Cu(II) and Ni(II). Pb(II) and Fe(III), as well as As(III), showed some increase in loading with contact time.

The suppressing effect caused b, the presence of Sn(II) on one hand, and the thermodynamic considerations (Table II.1), which suggest higher oxidation states for some of the elements involved, led to a new test. In this test the feed solution was spiked with As(V) and Sb(V) instead of the trivalent species. The higher oxidation states are more likely to prevail in real refining liquors as in most cases they are likely to originate from anode slimes treated under highly oxidizing conditions (potentials of the order of +1.00 V). Moreover, Se(IV) and Ag(I) were included in this test as well while stannic tin was not added since its suppressing behaviour was yet to be understood. The obtained results in Figure IV.3 points out some interesting differences with reference to Figure IV.1. First of all, the extraction of Pt(IV) was not suppressed this time; no Sn(II) was present. Bi(III) still loaded strongly, and Pb(II), Fe(III), Zn(II), Cu(II) and Ni(II) basically exhibited the same behaviour reported in the former experiment. A marked difference was the much reduced extraction of Sb(V) versus Sb(III) and As(V) versus As(III). These differences are better appreciated by considering Figure IV.4 on which the As(III)/(V) and Sb(III)/(V) results from the two tests are plotted. As for the new tested impurities Ag(I) and Se(IV), the former showed significant coextraction ($\sim 60\%$) despite its low solubility at concentrations below 4.0M HCl (~100 mg/L) while the latter exhibited less than 20% extraction throughout. Contact time was found again not to have a significant effect with the notable exception of Fe(III) and to a lesser degree Sb(V).

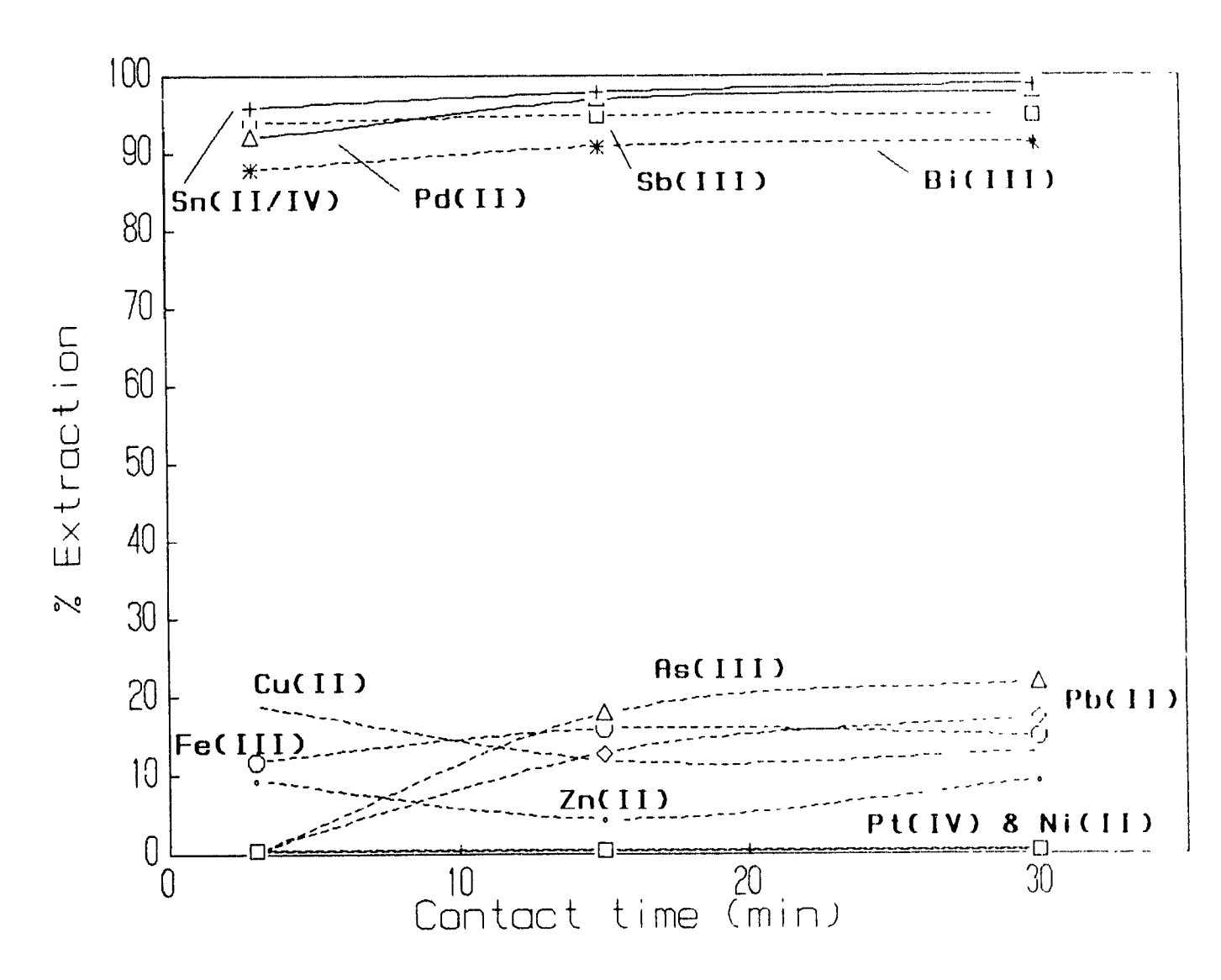


Figure IV.2 Distribution of impurity elements in 5v% TN 1911 as a function of contact time (Experiment 1), conditions: 0.7M HCl, A/O=1, 25° C, $M_{\text{aq}} = 1,000 \pm 200 \text{mg/L}$.

These preliminary experiments provided the basic trends vis-à-vis the contamination potential of the various impurity elements present in an industrial Pt-Pd chloride feed used in a solvent extraction circuit employing TN 1911 extractant. In order to further characterise the distribution of these impurity elements and thereby develop strategies for their control, individual testing of the elements was conducted.

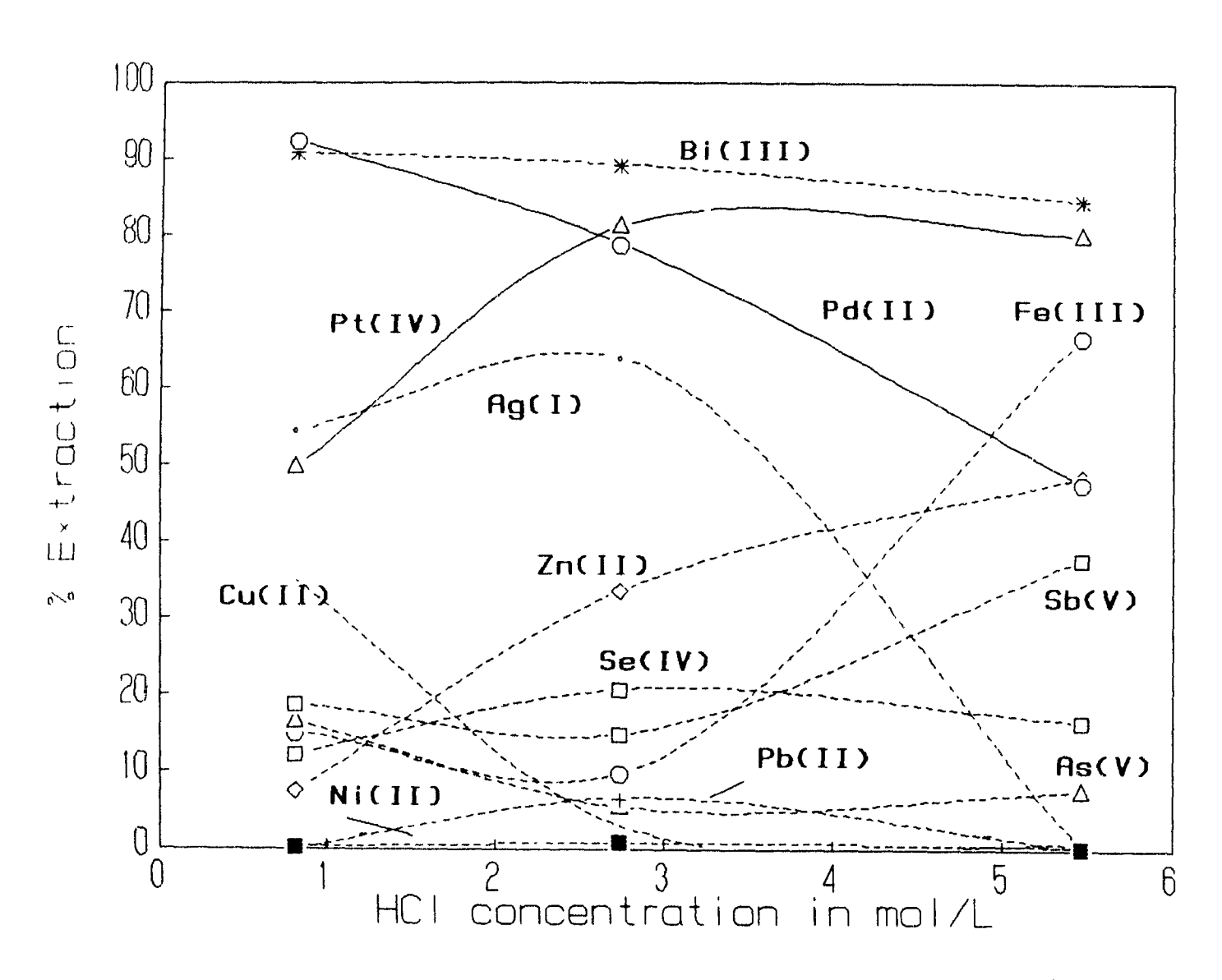


Figure IV.3 Distribution of impurity elements in 5v% TN 1911 as a function of HCl concentration (Experiment 2), conditions: 3 min., A/O=1, 25°C, M_{aq.i}= 1,000±200 mg/L, with the exception of [Ag(I)] = 30 mg/L.

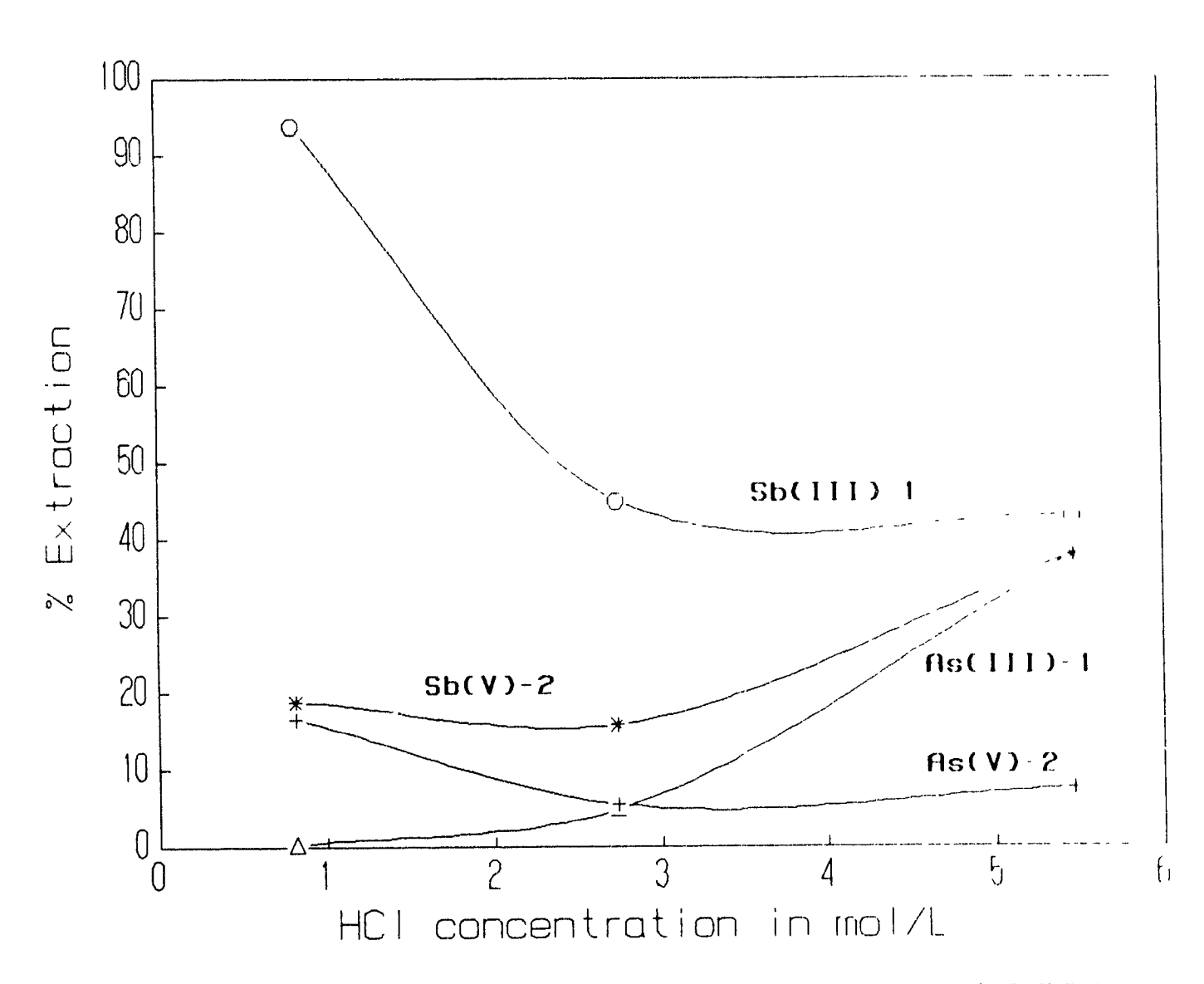


Figure IV.4 Extraction behaviour of Sb(III), As(III), Sb(V) and As(V) in 5v% TN 1911 as a function of HCl concentration (Experiment 1 & 2), dash/number refers to experiment. Conditions: 3 min., A/O=1, 25°C, M_{aq.i}= 1,000±200 mg/L.

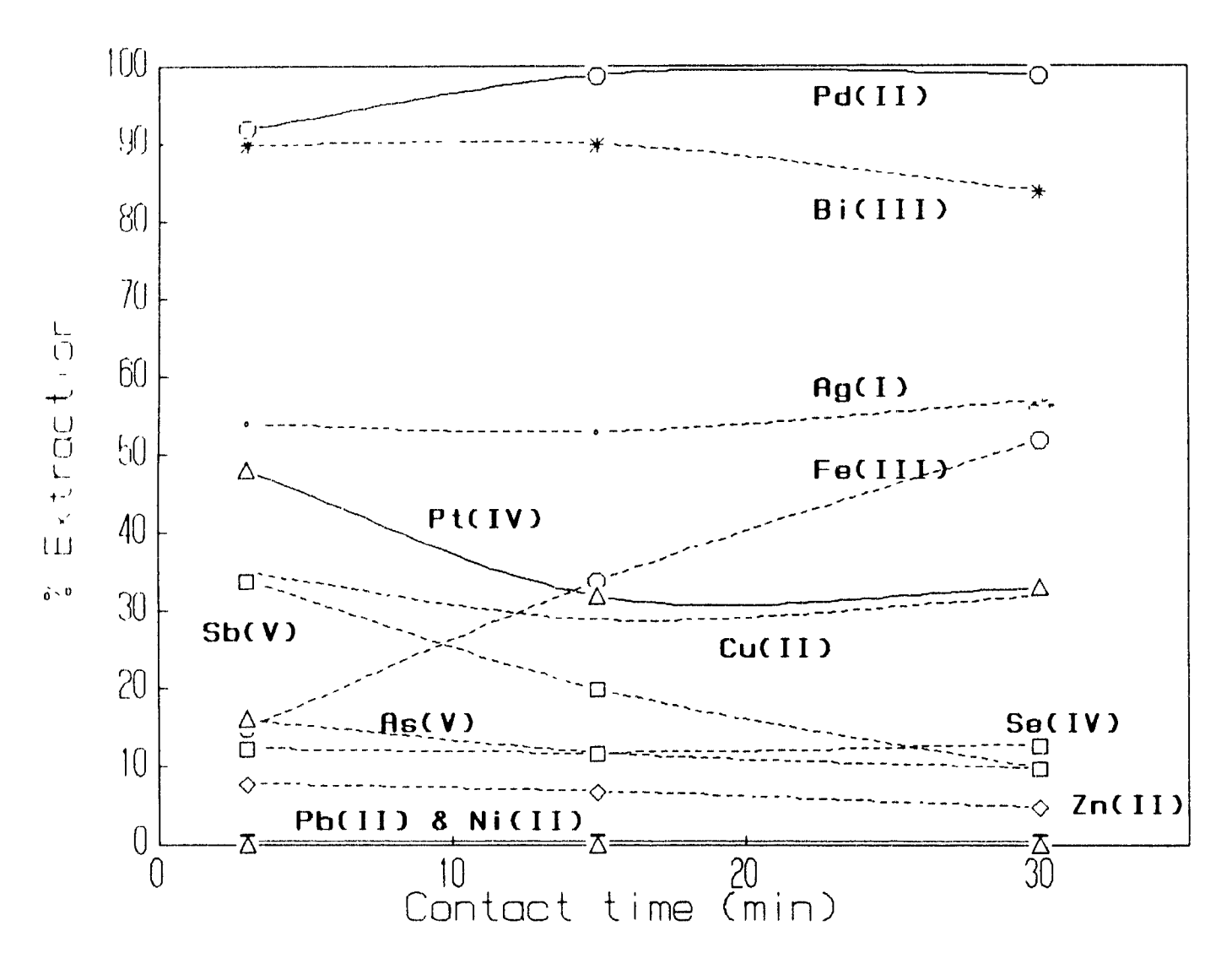


Figure IV.5 Distribution of impurity elements in 5v% TN 1911 as a function of contact time (*Experiment 2*), conditions: 0.7M HCl, A/O=1, 25°C, $M_{aq,1} = 1,000 \pm 200 \text{ mg/L}.$

IV.3 Single Element Distribution Behaviour during Extraction

Introduction: The behaviour of the impurity elements was further studied by carrying out single metal extraction tests. The impurity elements studied were Fe(III), Cu(II), Pb(II), Zn(II), Sn(IV), Ag(I), As(V), Sb(V), Bi(III), Se(IV) and Te(IV) Ni(II) was omitted from this list since it exhibited nil extraction in preliminary tests

Extractions were carried out for the range 1.3 to 4 0M HCl and the results were plotted in graphical form, with distribution coefficient (defined as metal concentration in organic/metal concentration in aqueous) on the ordinate and hydrochloric acid concentration on the abscissa. An additional test at 1.3M HCl was performed in which 2.0M MgCl₂ was added to evaluate the effect of chloride ion during extraction. The results appear on the following pages. As a measure of comparison between the impurity element distribution data and the Pt/Pd distribution data, single metal tests were conducted as well for Pt(IV) and Pd(II). The results are shown in Figure IV 6.

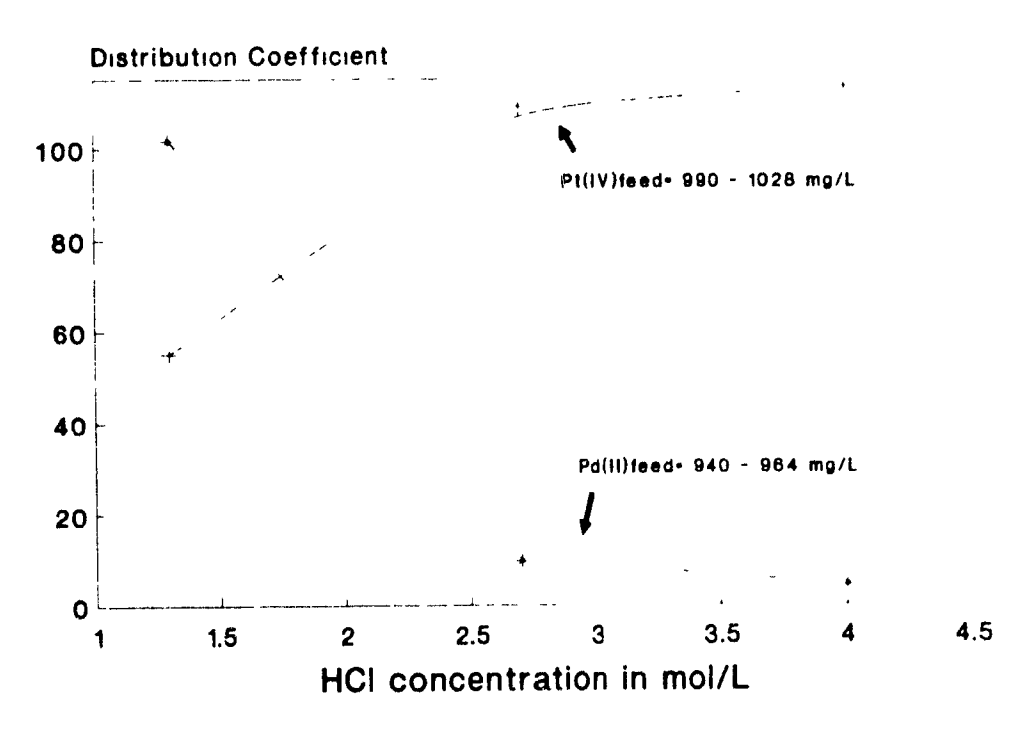


Figure IV.6 Single metal plot of Pt(IV) and Pd(II), 5v% TN 1911, A/O=1, 3 mm.

The depicted trends agree with the multielement results (Figures IV.1 and IV.3) and previously published data⁽⁴⁾. Below, the individual impurity elements are discussed and possible extraction mechanisms for each of them are postulated.

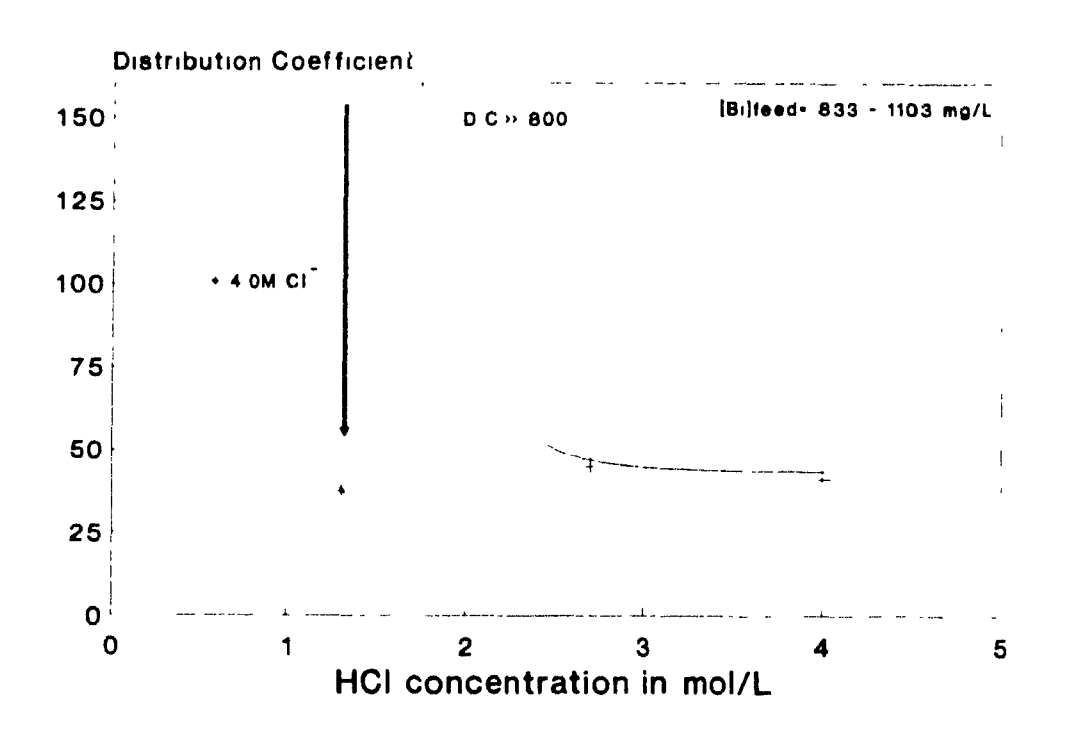


Figure IV.7 Single metal plot of Bi(III), 5v% TN 1911, A/O=1, 3 min.

Bi(III) As the single metal extraction plot in Figure IV.7 shows, Bi(III) is strongly extracted through the entire HCl range of investigation, with a tendency to lower distribution coefficient values at greater HCl or chloride ion concentration. This pattern is also observed with tri-iso-octylamine^(6.3) which extracts Bi(III) as an ion-pair above 0.5M HCl where Bi(III) forms anionic chlorocomplexes (see Figure II.12. Apparently the BiCl₄/BiCl₅² are extracted readily while the BiCl₆³ which dominates above 2.0M HCl is extracted at a lesser degree. Steric hindrance and/or possibly slow ligand exchange kinetics may be the probable causes of this phenomenon.

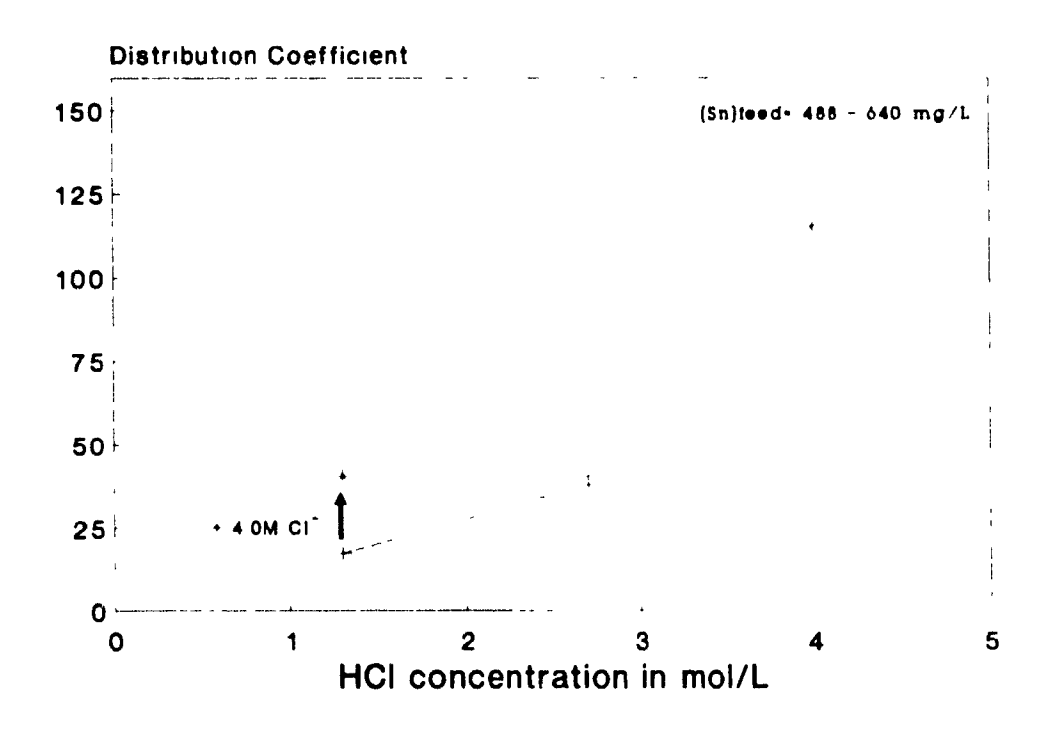


Figure IV.8 Single metal plot of Sn(IV), 5v% TN 1911, A/O=1, 3 min.

Sn(IV) With Sn(IV), strong loading is again observed. In other basic extractants strong extraction is also observed like with triisooctylamine⁽⁵⁶⁾ at >2M HCl and with TBP⁽⁵⁵⁾ at >>2M HCl. At such acid concentrations anionic chlorocomplexation is strong $(\log \beta_n > 3.70 \text{ at } I = 5.0^{(28)})$ and apparently the SnCl₆² is extracted via an ion-pair formation mechanism. This evidence is supported by the abundance of SnCl₆² in Figure II.10 at >1.0M Cl. This same mechanism is believed to occur in the present system as well.

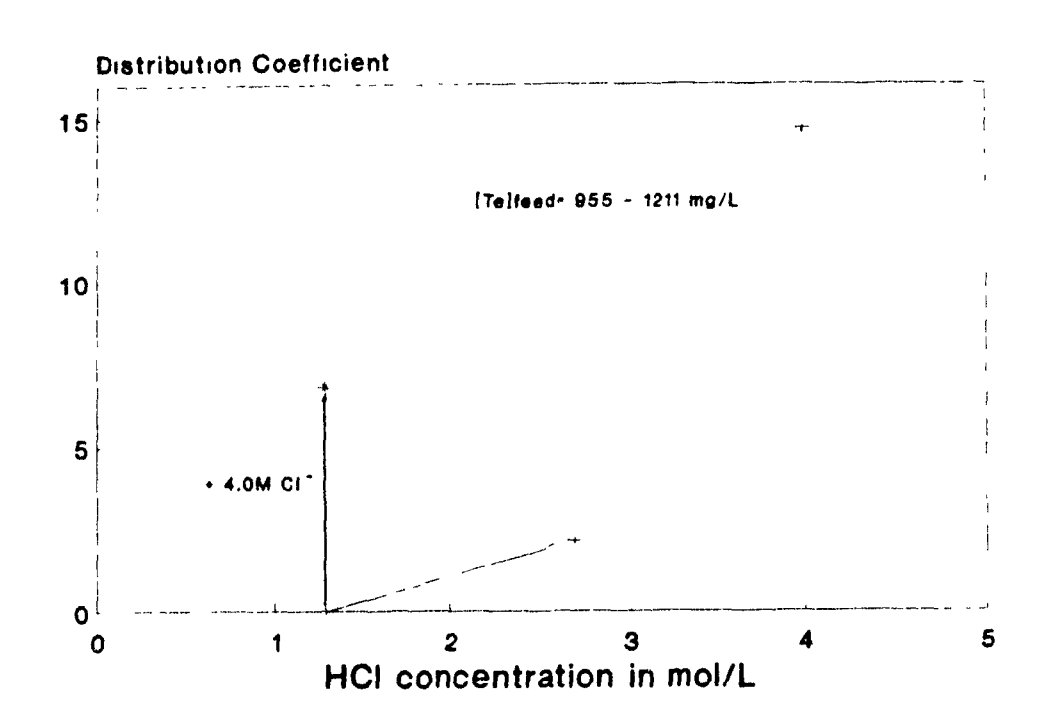


Figure IV.9 Single metal plot of Te(IV), 5v% TN 1911, A/O=1, 3 min.

Te(IV) Te(IV) shows strong extraction with TN 1911 above 2.0M HCl. In strong chloride solutions, i.e., >6M HCl, the weak basic extractant TBP has been reported to extract strongly probably as $\text{TeOCl}_{4^{2^{-}}}/\text{TeCl}_{4+n}^{n}$ via ion-pair formation⁽³⁷⁾. Nabivanets *et al.* (40) indeed showed such species to be present above 3.0M HCl (Figure II.15). As these complexes are very strong (log β_n values >3.24 at I=7) the respective D values are high at 4.0M HCl and equivalently at 4M Cl⁻/1.3M HCl with TN 1911. It is therefore hwhly likely that an ion-pair formation is taking place in the system under study.

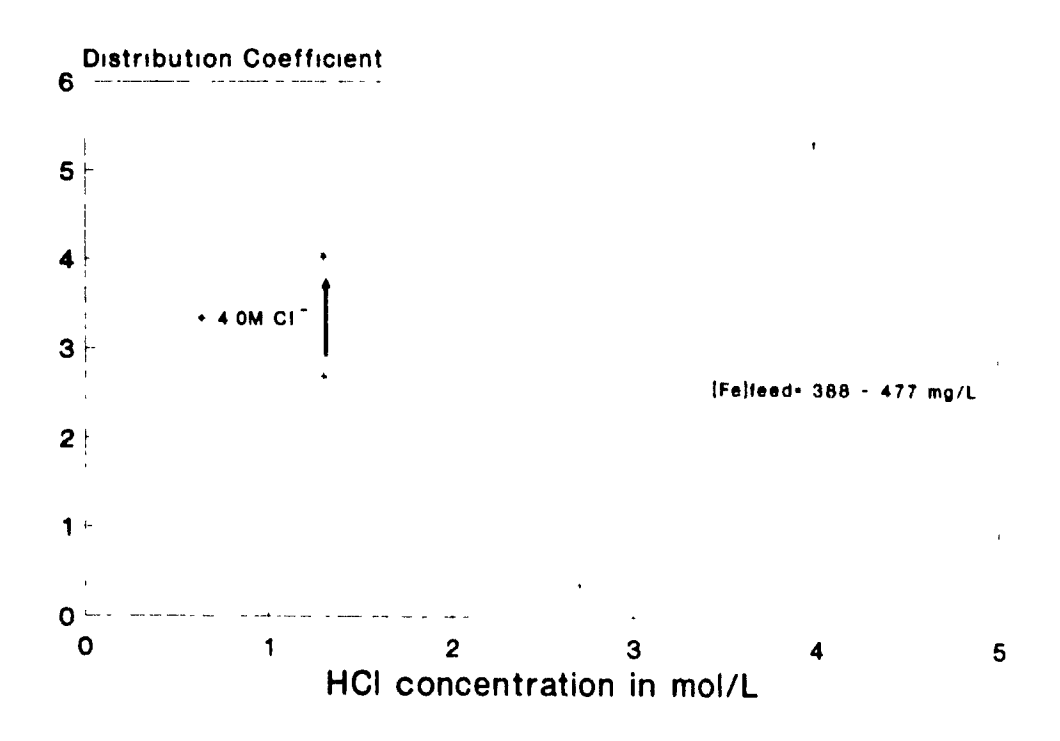


Figure IV.10 Single metal plot of Fe(III), 5v% TN 1911, A/O=1, 3 min.

Fe(III) In the case of ferric iron a minimum is observed around 2.7M HCl. Below 2.7M HCl, it is possible that Fe³⁺ is extracted by cation exchange like in the DE2HPA system⁽⁴⁶⁾. However, other cationic species, namely FeCl⁺² and FeCl₂⁺, exist and are more abundant as seen in Figure II.7. Neglecting the exchange of chloride ion with the organic anion ligand, it is likely then that these may load by cation exchange Above 2.7M HCl the FeCl₃° dominates with the simultaneous appearance of the I·eCl₄ anion, and as a solvation mechanism is less likely with the solvent used here, an ion-pair formation mechanism possibly begins to take place ^(44,45).

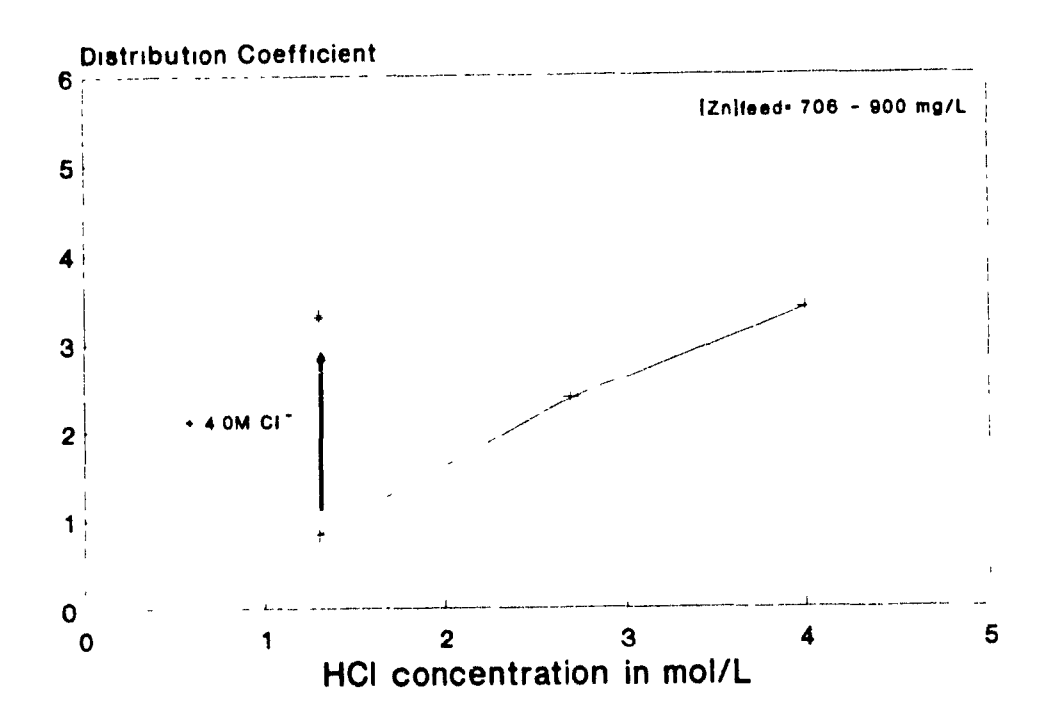


Figure IV.11 Single metal plot of Zn(II), 5v% TN 1911, A/O=1, 3 min.

Zn(II) An almost linear relationship is evident in Figure IV.11 and Zn(II) loading is clearly controlled by chloride ion concentration. The amine systems reported^(47,48), showed that at >0.01M and up to 2.7M HCl Zn(II) is extracted by ion-pair formation and most likely as the ZnCl₄²⁻ anion. This species becomes the most abundant above 2.0M HCl (Figure II.8). The most likely route of extraction with TN 1911 extractant is therefore by ion-pair formation.

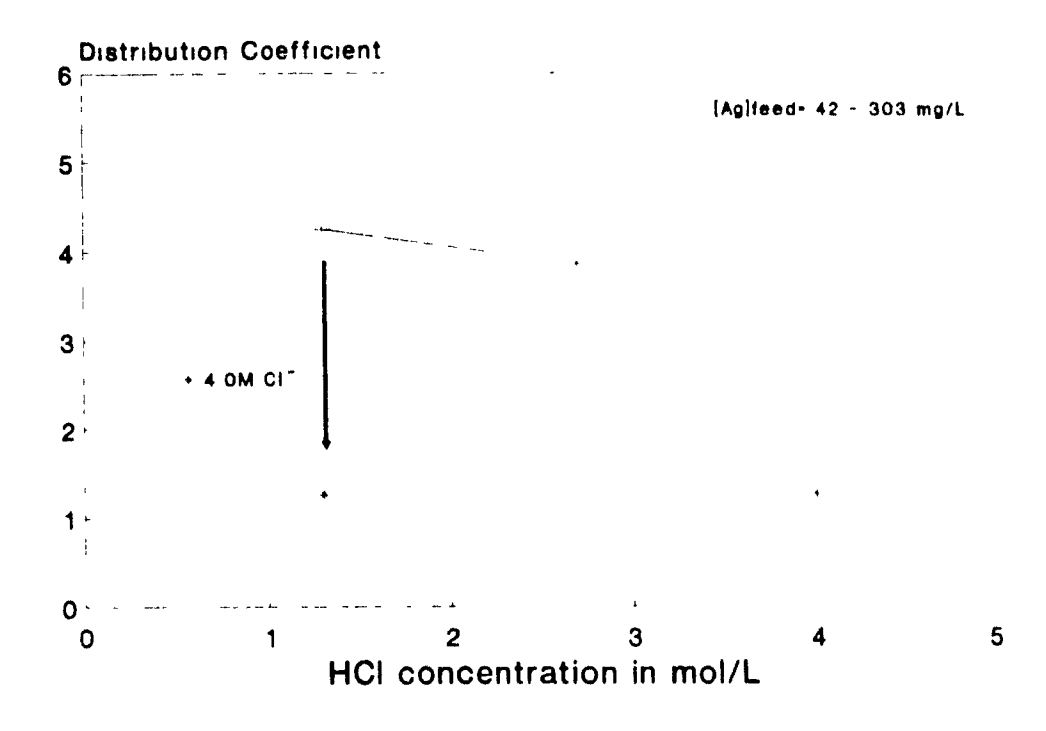


Figure IV.12 Single metal plot of Ag(I), 5v% TN 1911, A/O=1, 3 min

Ag(I) As for Ag(I), the same trend is observed as with Bi(III) Ag(I) forms strong chlorocomplexes ($\log \beta_n > 3.22$ at $I = 0^{(26)}$) which are known to extract via ion-pair formation (as for example $AgCl_3^2$ is extracted at 1 0M HCl with an amine^(5/1)) Apparently, this also happens in the case of 8-hydroxyquinoline derivatives. The speciation diagram found for silver shows that at >1.0M Cl, $AgCl_4^3$ begins to predominate (Figure II.11). The latter anion being too bulky and thus less extractable may produce a decrease in extraction and preferential extraction of acid instead⁽⁵¹⁾.

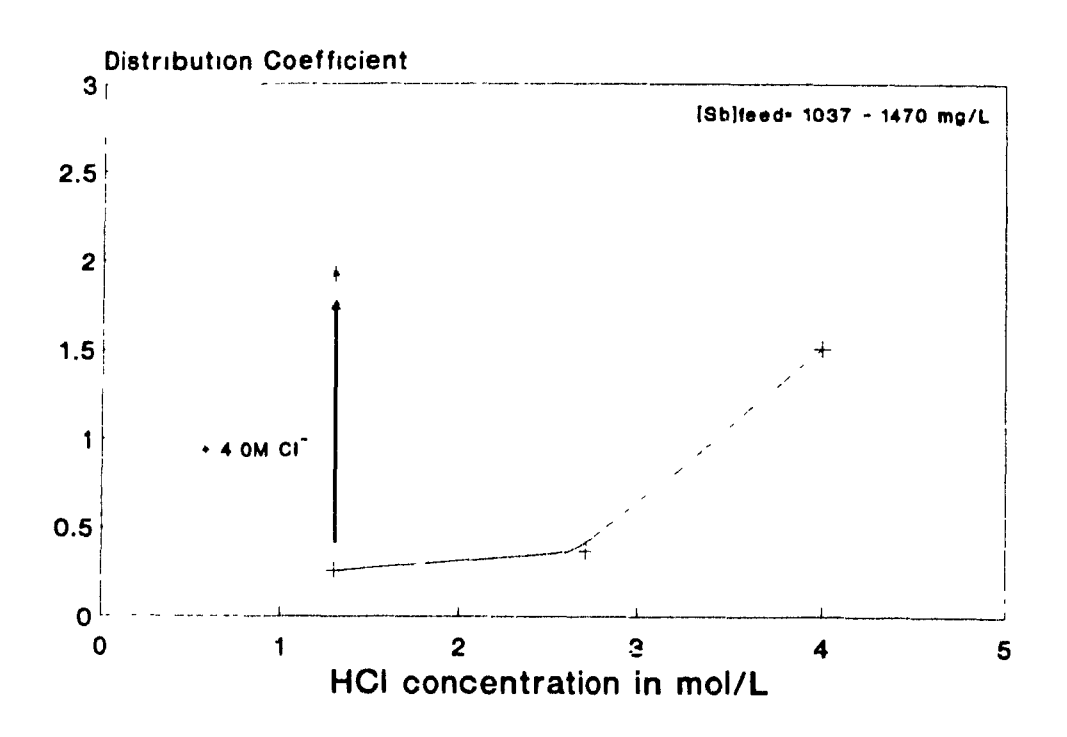


Figure IV.13 Single metal plot of Sb(V), 5v% TN 1911, A/O=1, 3 min.

Sb(V) Antimony in the (V) oxidation state seems to follow an ion-pair formation route, like for Zn(II), as it is highly dependent on chloride ion concentration. The same was found to be true in the amine system⁽⁵⁶⁾. It is true that Sb(III) forms quite strong chlorocomplexes ($\log \beta_n > 2.00$ at I=0) and although stability data was not found for the (V) state, evidence from mixed metal tests show stronger loading for the (III) state thus probably weaker anionic chlorocomplex formation for the Sb(V) (Figure IV.4). In fact, the chlorocomplexes which do exist for the Sb(V) are in the form Sb(OH)_nCl_{5-n} (79) (Figure II.12) in the HCl range of interest, and probably are extracted via ion-pair formation with TN 1911.

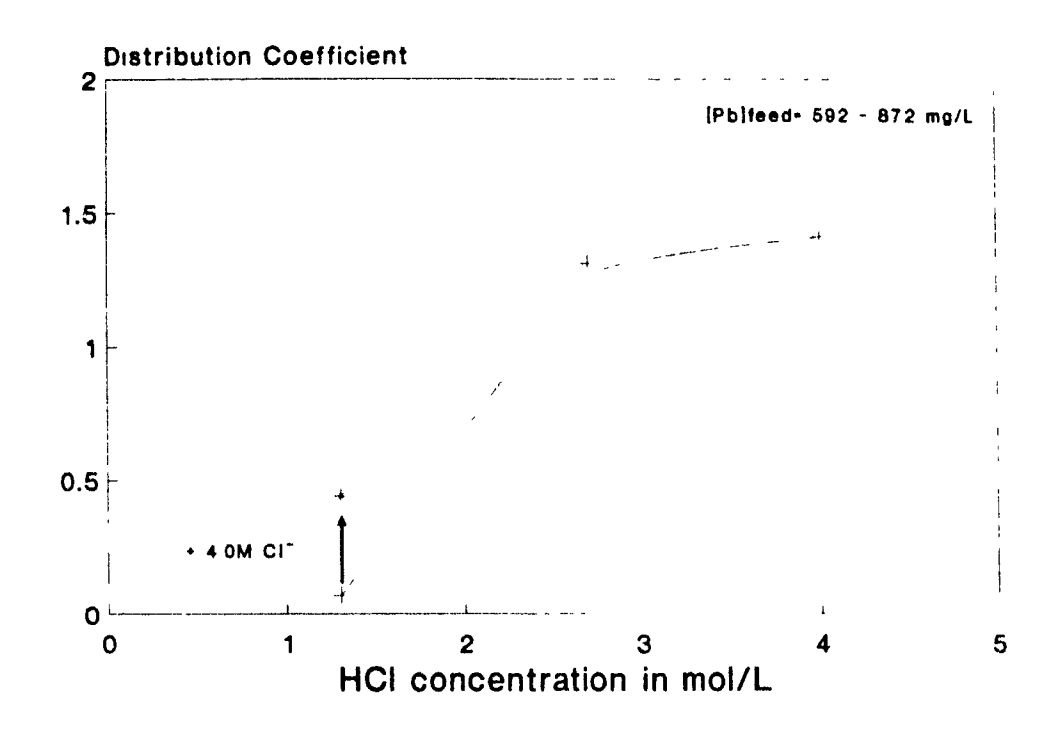


Figure IV.14 Single metal plot of Pb(II), 5v% TN 1911, A/O=1, 3 min.

Pb(II) Pb(II) also behaves very much like Zn(II) and an increase in extraction with increasing acid concentration is observed. Amine systems have been reported to extract strongly⁽⁵²⁻⁵³⁾ via the ion-pair route. The extracted species is believed to be the anion PbCl₃. It is most likely that the same mechanism applies to TN 1911 as well.

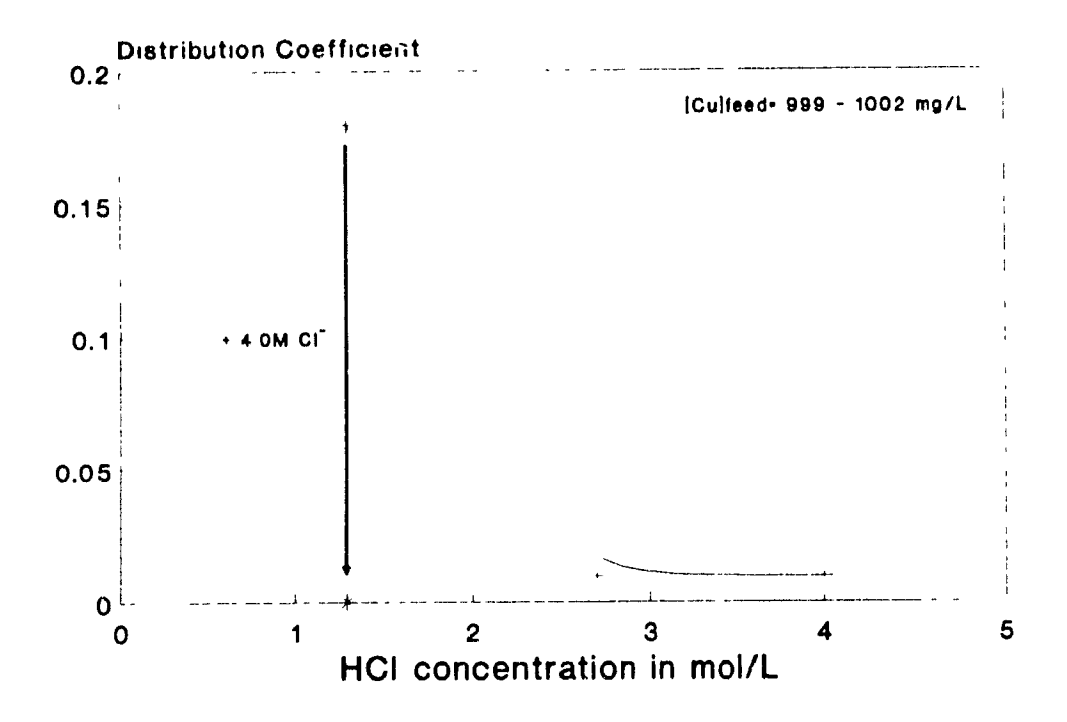


Figure IV.15 Single metal plot of Cu(II), 5v% TN 1911, A/O=1, 3 min.

<u>Cu(II)</u> In the HCl range 1.3-4.0M, cop; adding is very low with D<0.2. Cu(II) has a rather strong tendency to form chlorocomplexes (Table II.3). In fact at >1.0M chloride, the chlorocomplexes CuCl², CuCl₂ dominate. It appears therefore that Cu(II) is extracted by compound formation as established with other chelating extractants⁽⁴²⁾. The low presence of Cu²⁺ and CuCl⁺ in combination with the high acidity of the system explains the weak extraction of Cu(II).



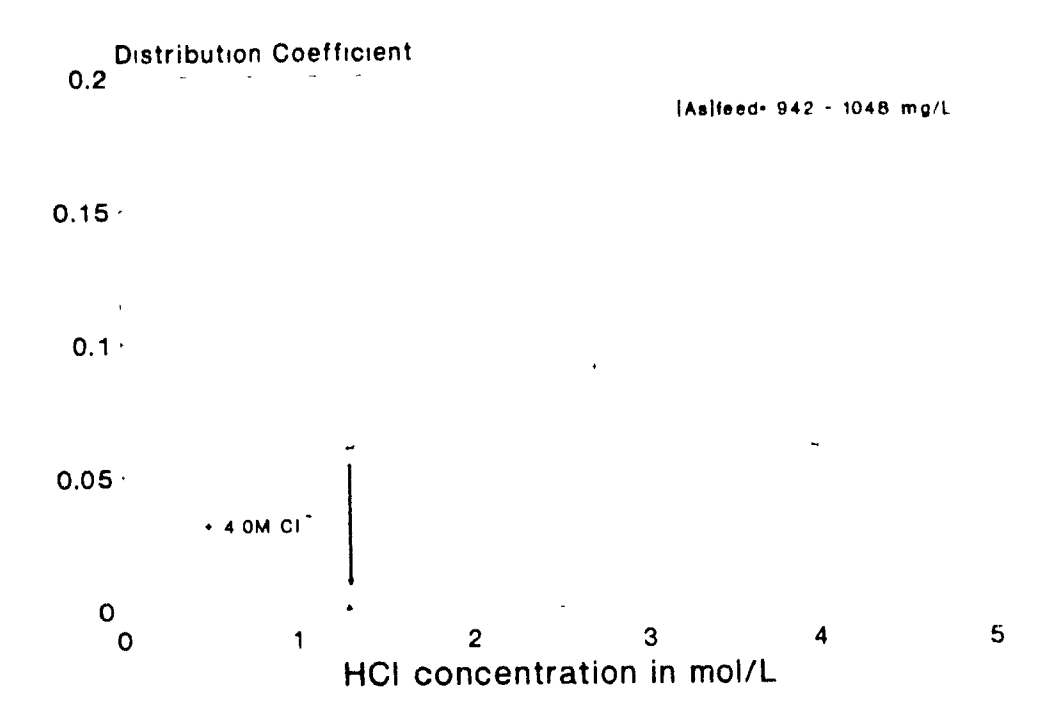


Figure IV.16 Single metal plot of As(V), 5v% TN 1911, A/O=1, 3 min.

As(V) As(V) does not form chlorocomplexes in the range investigated and according to Figure IV.16, extraction is negligible and quite difficult to measure as atomic absorption analysis produces erratic readings. In the acid region As(V) exists as $H_4AsO_4^{\circ\circ}$, arsenic acid, which has little tendency to dissociate $(K_1 = 2.5 \times 10^{4})^{(31)}$. Very slow extraction of As(V) has also been reported for an amine⁽⁵⁶⁾. In practical terms it can be assumed that extraction of As(V) is negligible with TN 1911.

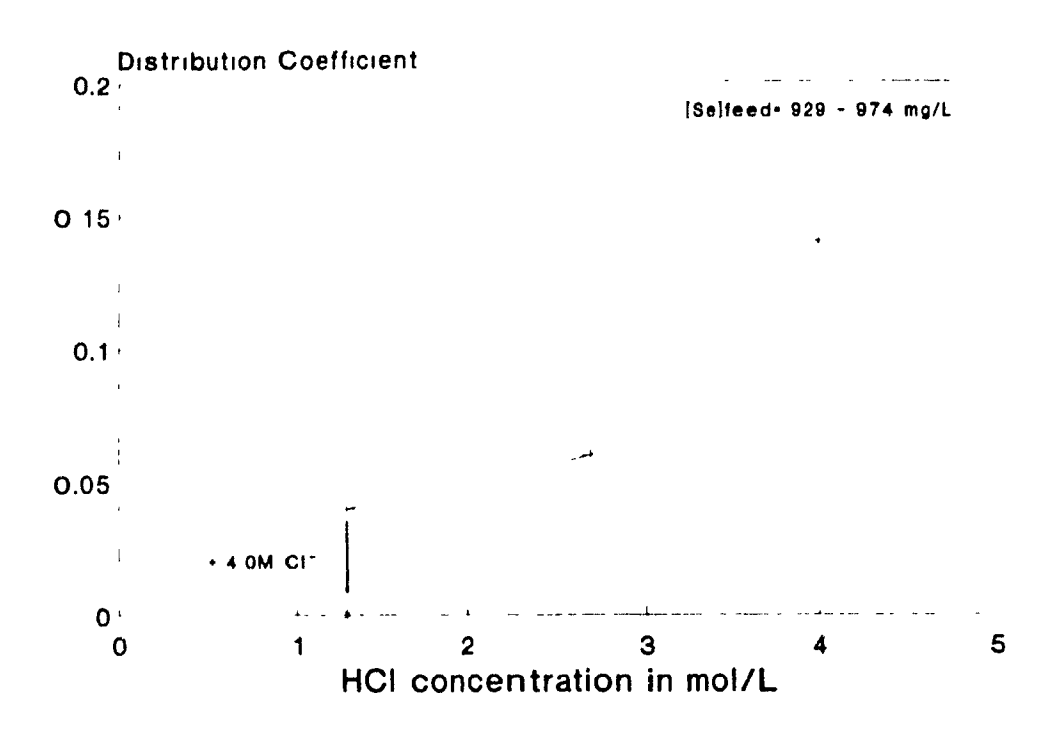


Figure IV.17 Single metal plot of Se(IV), 5v% TN 1911, A/O=1, 3 min.

<u>Se(IV)</u> As for Se(IV), similarly to As(V), very low extraction was observed and D < 0.15 was found to occur (Figure IV.17). Extraction being negligible, and determination with atomic absorption analysis intricate, makes it difficult to judge the true level of loading - and this is particularly true for 4.0M chloride ion concentration. Any extraction may be due to the dissociation of H_2SeO_3 into anionic species such as SeO_3^2 , $HSeO_3$ (Figure II.14) which extract via the ion-pair formation mechanism.

Summary of observations: By examining the graphs of Figures IV 7 to IV 17, the various impurity elements could be classified in three categories: those showing the highest values of distribution coefficient (D>25) such as Bi(III) and Sn(IV), moderate values (0.5 < D < 15) exhibited by Te(IV), Fe(III), Zn(II), Ag(I), Sb(V) and Pb(II), and lower values (D < 0.15) for Cu(II), As(V) and Se(IV). As a general rule, higher extractions were observed with increasing acidity and chloride ion concentration, with bismuth and silver being the exceptions. Iron was the only element which showed a minimum in the acid range 1.3-4.0M while Cu(II) extraction clearly decreased with increasing HCl/Cl concentration. Table II 4 summarizes the observations and includes postulated mechanisms for the elements in the HCl range 1.3-4.0M with the extractant TN 1911.

Element	Distribution coefficient (1.3-4.0M HCl)	Most abundant chlorocomplex	Postulated mechanism with TN 1911
Bı(III)	800 - 50	BiCl ₄ /BiCl ₅ ²	IP
Sn(IV)	20 - 110	SnCl ₆ ²	IP
Te(IV)	0 - 15.0	TeOCl ₄ ² /TeCl _{4+n} ⁿ	IP > 2.0M
Fe(III)	0.3 - 5.4	Fe ³⁺ /FeCl ²⁺ /	CF < 2.7M < IP
		$FeCl_2^+ < 2.7M < FeCl_4$	
Zn(II)	1.0 - 3.2	ZnCl ₄ ²	IP
Ag(I)	4.3 - 1.2	AgCl ₃ ²	IP
Sb(V)	0.25 - 1.9	Sb(OH) _n Cl _{5 n} ⁿ	IP
Pb(II)	0.1 - 1.4	PbCl ₃	IP
Cu(II)	0.18 - 0	Cu ²⁺ /CuCl ⁺	CF < 2.0M
As(V)	< 0.1	H ₃ AsO ₄	S
Se(IV)	< 0.15	SeO, ² /HSeO,	l IP

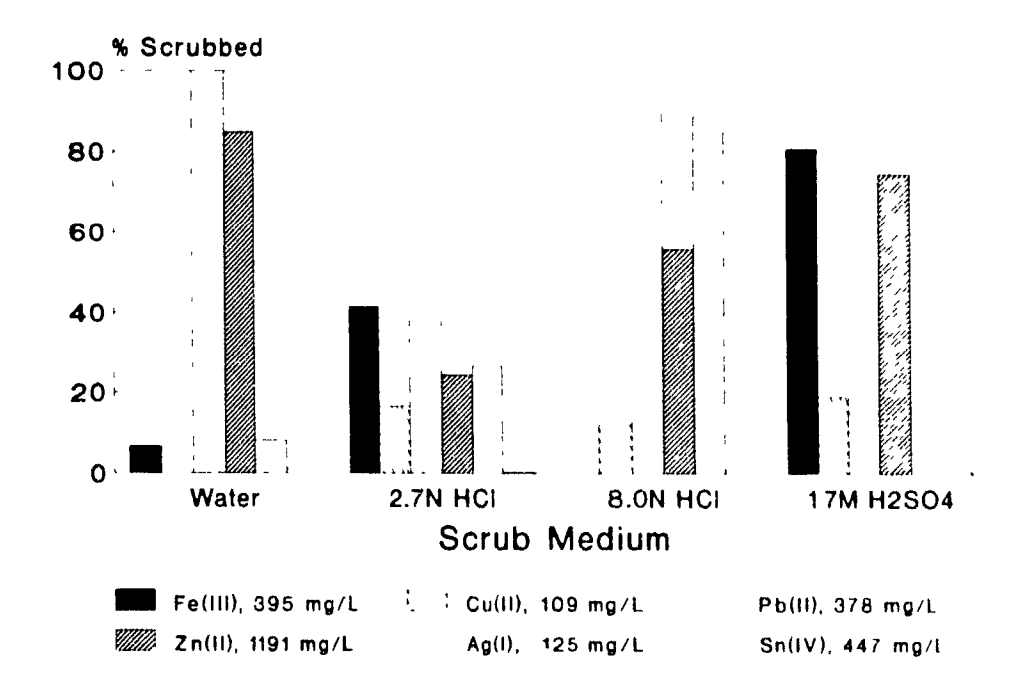
Table IV.1 Summary of single metal extraction observations and postulated mechanisms. CF=compound formation, IP=ion-pair formation, S=solvation.

IV.4 Single Element Distribution Behaviour During Stripping/Scrubbing

Having studied the behaviour of the impurity elements by investigating their extraction with 5v% (0.13M) TN 1911, information was made available for the selection of scrubbing media based on the dependency of the distribution coefficients on the acid and chloride ion concentration. Moreover, upon testing the various stripping/scrubbing media, it was possible to verify the postulated extraction mechanisms in section IV.3. Single-metal loaded organics loaded at 2.7M HCl were subjected to the following shake-out tests performed at ambient temperature (25°C), A/O=1 and 3 minute contact time:

- (i) distilled water, simulating Pt stripping
- (ii) 8M HCl, simulating Pd stripping
- (iii) 2.7M HCl as scrubbing medium
- (iv) 1.7M H₂SO₄ as scrubbing medium

A solution of 2.7M HCl was selected as a scrubbing medium based on the findings of the preliminary testwork with semi-industrial solution (Figure IV.3). It seems that at this acidity, the distribution coefficient is maximal for Pt/Pd whereas many of the impurities, namely Fe(III), Cu(II), Sb(V). As(V) and Se(IV) exhibit a minimum. Strong sulphuric acid at 1.7M concentration was adopted as a scrub solution for Zn(II) and perhaps Cu(II), Ag(I) as well as Bi(III) which showed lower distribution coefficients at higher acid strength. It was thought that the sulphate/bisulphate anions would be capable of destabilizing the anion chlorocomplexes which were mostly responsible for the extraction of the impurities with TN 1911 thus facilitating their removal from the organic phase. The results are reported in bar chart form in Figure IV.18.



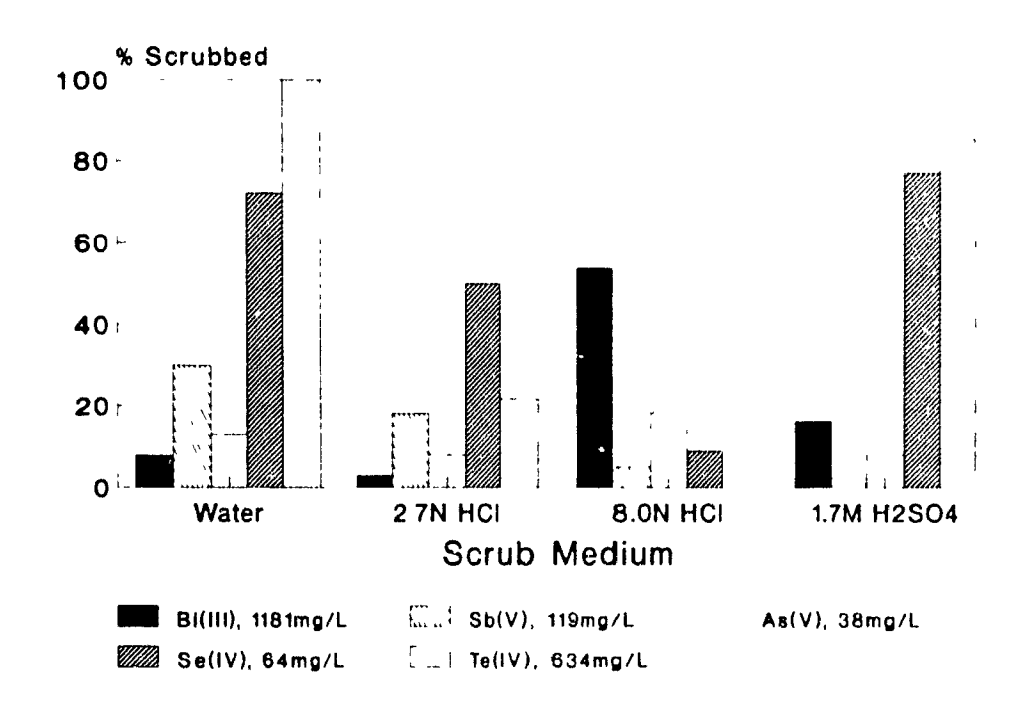


Figure IV.18 Deportment of impurity elements in four scrub/strip solutions with 5v% TN 1911 @ 25° C, A/O=1, 3 min. (Metal concentrations refer to loaded organic phase. Organic loaded with 2.7M HCl, $C_{M_{aq,i}} = 1,000 \pm 260 \text{ mg/L}$).

Contact with H₂O: Contact with distilled water at initial pH 4.5 produced a final raffinate pH of 0.7 which was much lower than pH 2.0, the optimum Pt strip liquor pH⁽³⁾. Hence, a significant amount of acid was transferred from the organic to the aqueous phase. Since pH control was not used it can only be said that the elements Pb(II), Zn(II), Se(IV) and Te(IV) appear to have a tendency to report to the Pt strip solution. Bi(III), despite its low percentage removal (10%), still remains classified as a potentially troublesome element in Pt stripping since it might report in significant concentrations (< 100mg/L) The removal of Pb(II), Zn(II) and Te(IV) from the loaded organic phase by H₃O contact is in agreement with the postulated extraction mechanisms, i.e., ion-pair formation in Table IV 1 Hence upon contact with water, the extractant is deprotonated and the anionic metal species can no longer remain in the organic phase. Moreover, the anions ZnCl₄², PbCl₄ and TeOCl₄² are likely to partly lose their chloride ions and become neutral or cationic and thus not extractable. The behaviour of Sb(V) can be understood in the same way. In the case of selenium, the selenous anion HSeO₄ is likely to gain a proton upon water contact, to be transformed into H₂SeO₃° and will thus be removed from the organic phase Ag(I) did not respond to water contact and this may be due to the low chloride ion content of water which is not able to keep Ag(I) in solution due to low solubility. On the other hand, Fe(III) and Cu(II), due to their postulated compound formation extraction do not respond to water stripping. Of particular interest is the behaviour of Bi(III). The latter, based on the postulated ion-pai. formation mechanism (Table IV.1) was expected to be removed via the deprotonation of the extractant. This however occured only at a marginal degree of about 10%. It is possible that upon deprotonation of the extractant and release in the aqueous acidic phase, the latter is back-extracted by TN 1911 in the form of a chelate:

$$B_1Cl_4 . H_2L^+_{(0)} \rightleftharpoons B_1Cl_2^+ + HL_{(0)} + H^+ + 2Cl$$
 (IV.4)

$$B_1Cl_2^+ + 3HL_{(0)} \rightleftharpoons B_1L_{3(0)} + 3H^+ + 2Cl^-$$
 (IV.5)

The extraction of Bi(III) via chelate formation from H_2SO_4 media (>1.0M H_2SO_4) with

Kelex 100—analogous to the TN 1911 system— has been known to occur^{CD}. Finally the behaviour of Sn(IV) is to be discussed at the end of this section.

Contact with 8M HCI: the results show that there is potential for significant transfer of a number of impurity elements and particularly Pb(II), Zn(II), Ag(I) and Bi(III) in the Pd strip liquor. In reference to the postulated extraction mechanisms (Table IV 1), the observed stripping/scrubbing behaviour with 8M HCI can be understood if the CI constituent of HCl is considered. Thus with increasing CI (or equivalently HCI) the simple extracted species are converted to higher chlorocomplexes possessing \geq 2 charge which are less extractable due to steric hindrance. For example, PbCl₄ is converted to PbCl₄²/PbCl₆⁴, AgCl₃³ to AgCl₄³ and BiCl₄/BiCl₅³ to BiCl₆³ which are known to be less extractable (52.53.57.63). The above reasoning can however not be applied to the case of Zn(II) stripping with 8M HCl, as Zn(II) does not form complexes higher than ZnCl₄² and thus no explanation can be given at this point. On the other hand, the failure of Cu(II) and Fe(III) to be stripped with 8M HCl, despite their presumed presence in the organic phase as chelates (see Table IV.1), is attributed to the formation and back extraction of high anionic chlorocomplexes CuCl₄² and FeCl₄ as ion-pairs

It is evident, therefore, from the presented results that a number of the impurity elements have the potential of contaminating the Pt and Pd strip liquors and this has to be prevented by devising scrubbing schemes for their prompt removal

Contact with 2.7M HCI: 2 7M HCI was partly successful in the removal of Fe(III), Zn(II), Te(IV) and Se(IV). The obtained results are in general agreement with the extraction data. In Table IV.2 the respective distribution coefficients and levels of expected and observed removal of each metal are compared. Considering that the metal and free extractant concentration were not exactly the same and that the kinetics of reversibility are ignored, the obtained levels of scrubbing are deemed reasonable. Significant discrepancy occurred with selenium but most of all with copper. This might well be due to slow scrubbing kinetics, or due to errors associated with the analytical determination of metal concentrations with flame AA.

М	Extraction D $M_{\rm org}/M_{\rm aq}$	Scrubbing D $M_{\rm org}/M_{\rm aq}$	Expected Percent Scrubbing based on D_{EXT}	Obtained Percent Scrubbing	Agree- ment
Fe(III)	0.5	1.5	65	40	Good
Pb(II)	1.3	0.9	40	53	Good
Zn(II)	2.2	3.5	33	22	Good
Ag(I)	4.0	3.2	20	24	Good
Bi(III)	50	32	2	3	Good
Te(IV)	2.4	3.8	29	21	Good
Sb(V)	0.3	4.5	76	18	Poor
As(V)	0.09	15.7	92	6	Bad
Se(1V)	0.05	1.0	95	50	Poor
Cu(II)	0.01	5.7	99	15	Bad

Table IV.2 Comparison of distribution coefficients at 2.7M HCl obtained from extraction and scrubbing tests. For $D_{\rm EXTRACTION}$, $M_{\rm aq~initial} = -1,000 \, {\rm mg/L}$ except for Ag(!) (~100 mg/L) and for $D_{\rm SCRUBBING}$, $M_{\rm org~initial} < 1,000 \, {\rm mg/L}$ except for Bi(III) and Zn(II) (see Figure IV.18).

Contact with 1.7M H_2SO_4 : Strong sulphuric acid was a more efficient scrub medium as it achieved >70% removal of Fe(III), Zn(II), Te(IV) and Se(IV). The H_2SO_4 scrubbing action with the exception of Cu(II) again is explained as follows: Fe(III) is removed from the organic because its chelate complex (FeL₃) is stripped by H^+ , while its ion-pair (FeCl₄ H_2L^+) is stripped by converting FeCl₄ to non-anionic species via the diluting action of HSO_4/SO_4^2 amons. The latter explanation is presumed to apply in the case of Zn(II) (ZnCl₄² \rightarrow Zn²⁺) and Te(IV) (TeOCl₄² \rightarrow TeO⁺) as well. The corresponding Pb(II) and Ag(I) were not scrubbed probably due to their known insolubility in sulphate medium. In the case of Se(IV), the extracted anion HSeO₃ can

be thought of as being converted to neutral selenous acid (Figure II 17) in the presence of high H⁺ concentration. The same did not apparently happen with the 8M HCl solution due to the possible interference of Cl ions.

Scrubbing of Sn(IV): In all the above contacts, Sn(IV) was found not to respond. As indicated in section IV.2 the Sn(IV) extraction results seem to suggest that the element is extracted via an ion-pair formation mechanism, i.e.,

$$SnCl_6^{2-} + 2H_2L^+Cl_{(0)} \Rightarrow SnCl_6^{2-}(H_2L^+)_{2(0)} + 2Cl^-$$
 (IV.6)

It was therefore expected that either H₂O (via deprotonation of the extractant) or H₂SO₄ (through ligand exchange of SnCl₆² to non-anion species) would strip Sn(IV) from TN 1911. This, however, was not the case

It was decided to attempt the removal of Sn(IV) by using a variety of selected H₂SO₄, MgCl₂ and NaOH solutions. The only solutions which showed some effect were those with 0.5-1.0M NaOH. With the latter solutions, up to 25% of loaded stannic tin was removed after a 3 min contact as seen in Figure IV.19. Disengagement time was found to be faster for the 1.0M NaOH test at less than one minute. Emulsion formation was observed only in the 2.0M case. Thus, the 1.0M NaOH solutions was retained for further testing. A 6-stage test was then conducted to see whether Sn(IV) could be at least removed even with the inconvenient approach of numerous stages using fresh NaOH for each stage. Figure IV.20 shows that greater than 75% of Sn(IV) was in fact removed, with the 6-stage cross-current contacting test. Next the effect of contact time was investigated. The outcome of this test is illustrated on Figure IV.21, which shows that over 90% of Sn(IV) was successfully removed implying a kinetically controlled reaction. No emulsion emulsion formation was observed in these tests.

The chlorocomplex apparently resisted conversion into cationic/neutral species

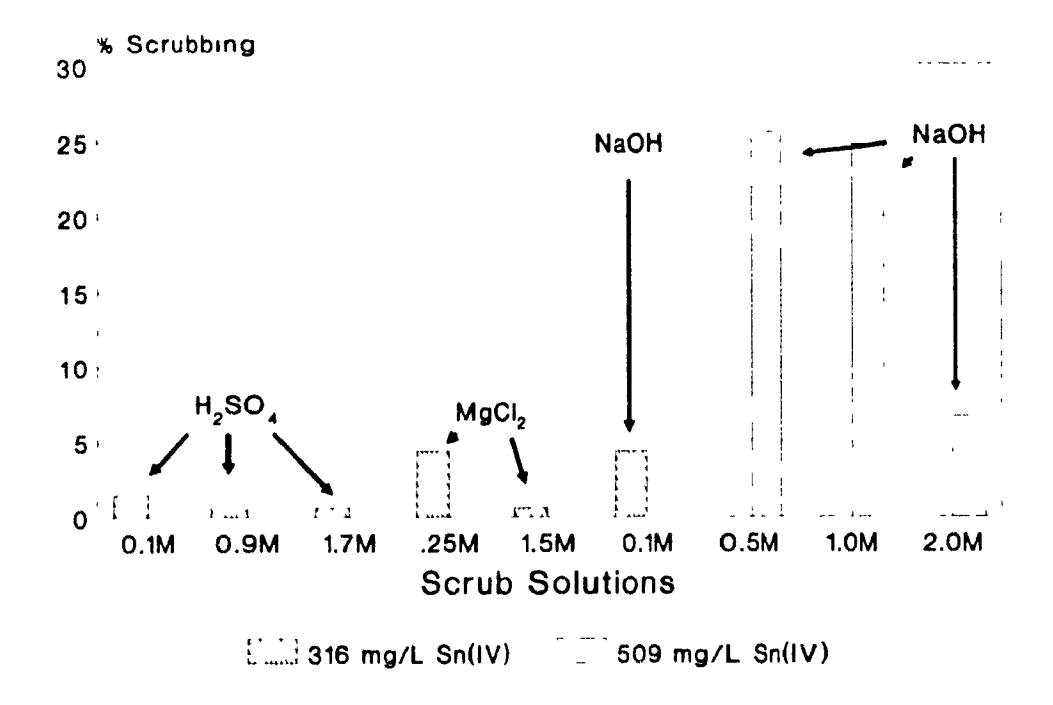


Figure IV.19 Scrubbing Sn(IV) from loaded 5v% TN1911 single metal tests, A/O=1, 3 min., 25°C.

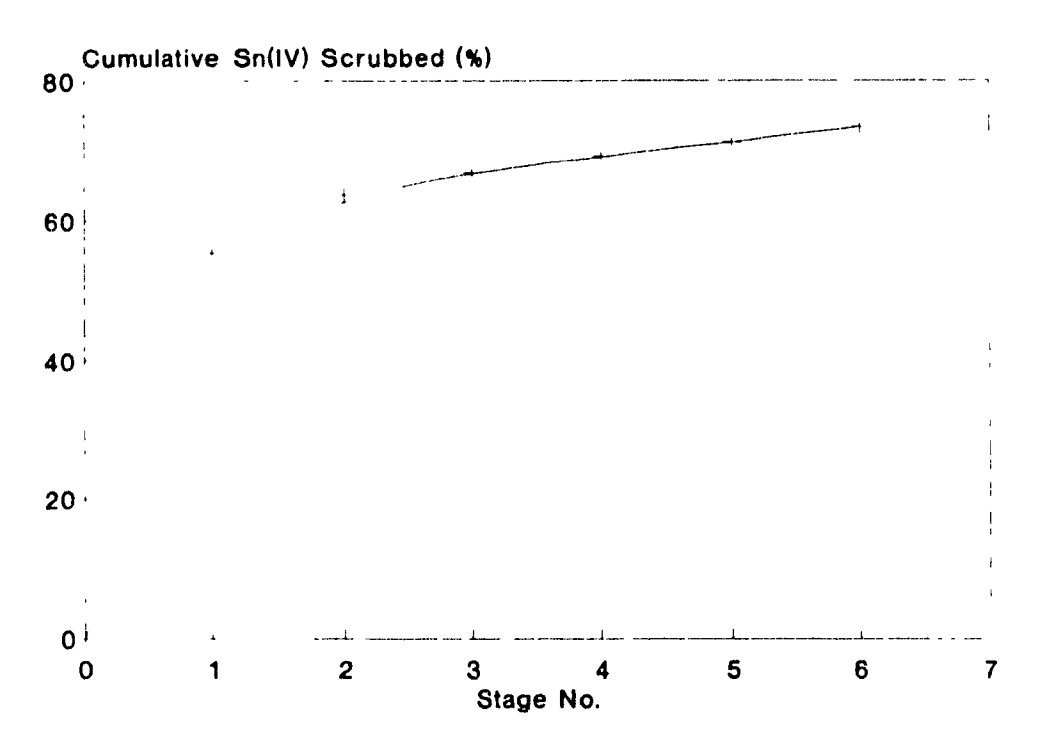


Figure IV.20 Sn(IV) six-stage scrubbing using 1.0M NaOH solution 5v% TN 1911, A/O=1, 3 min., 25° C, $[Sn(IV)]_{(o)}$ = 455 mg/L.

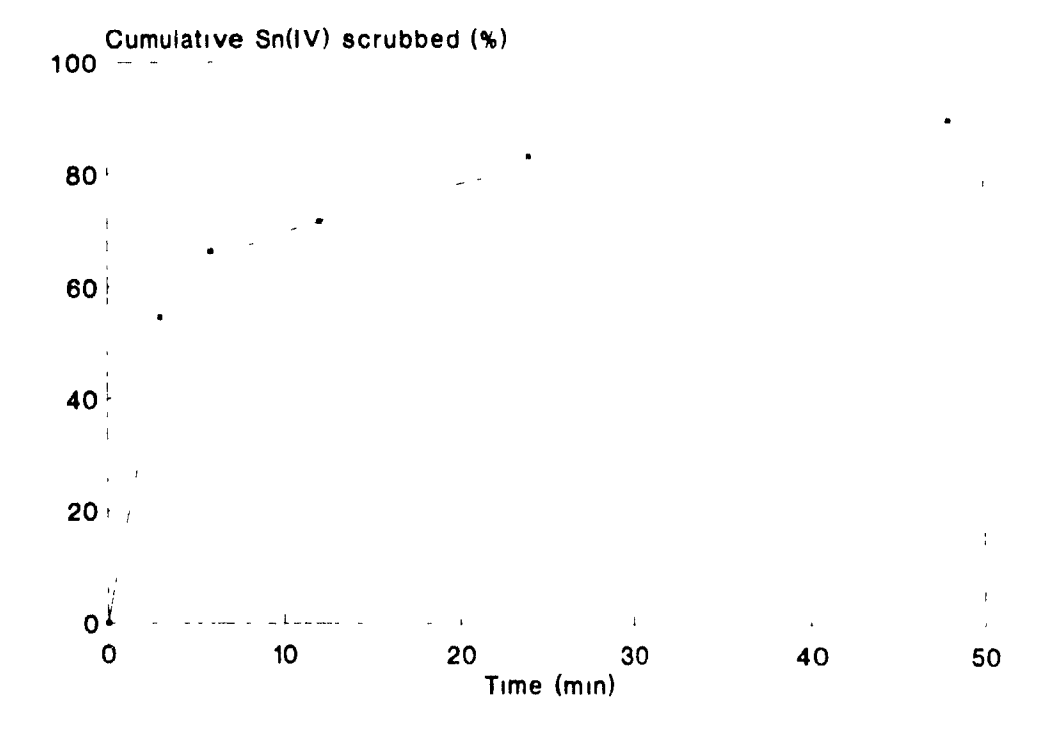


Figure IV.21 The effect of contact time on the removal of Sn(IV) using 1.0M NaOH. 5v% TN 1911, A/O=1, 25° C, $[Sn(IV)]_{(o)} = 455$ mg/L.

through the removal of Cl ions due to its thermodynamically stable character⁽²⁷⁾. The effectiveness of NaOH can be attributed to be the successful exchange of Cl ions for OH to form $Sn(OH)_n^{(4-n)}$ species. In fact investigators⁽⁷²⁾ have found that 0.05M Sn(IV) forms stable monomeric species in solution without any turbidity, when adjusted to >0.3M NaOH. Another plausible interaction may be an acid-base reaction between $SnCl_4$ and the base as the former is known to be a very strong Lewis acid⁽⁷³⁾. Through longer contact times with NaOH, the tin problem was resolved. Attention was then given to some of the other problem impurities such as Ag(I) and Sb(V).

Chloride Scrubbing: The single metal test on Ag(I) (Figure IV.12) showed effective suppression of extraction at high chloride concentration. This clue led to testing two scrub solutions: 2.0M MgCl₂ and 0.1M HCl+2.0M MgCl₂ which represent strong chloride ion and weak acid/strong chloride. According to the obtained results the weakly acid scrub medium proved effective in removing Ag(I).

MEDIUM	Feed Ag(I)	% Scrubbed
0.1M HCl+2.0M MgCl,	30 mg/L	61.0
2 0M MgCl,	30 mg/L	23.0

Table IV.3 Scrubbing results for Ag(I) using strong chloride ion in solution. 5v% TN 1911, A/O=1, 3 min., 25°C. Mixed metal organic phase: Pd 400, Cu 60, Ag 30, Bi 1730 (in mg/L).

The effective scrubbing of Ag(I) via the action of chloride ion is in agreement with the postulated extraction mechanism of Ag(I) which calls for lower extraction of Ag(I) when the higher chlorocomplex $(AgCl_4^3)$ dominates.

Scrubbing of Sb(V): A spectrophotometric study by Gentry and Sherrington⁽⁷⁴⁾, revealed that the extraction of Sb(V) could be partially suppressed in the presence of 2% sodium potassium tartrate. Limited testing of KNa tartrate salt was attempted on single metal solutions of Sb(V) and results showed that one contact of 3 min. at an A/O=1 with 0.1M tartrate was sufficient for almost 50% removal of Sb(V) (Table IV.4). Phase separation was close to 5 min. and emulsion problems were experienced only at higher tartrate concentrations.

[KNa tartrate] in mol/L	% Sb(V) Scrubbed	Remarks
0.1	46.0	phase sep.: 5 min.
0.2	16.0	stable emulsion
0.4	14.0	stable emulsion
0.8	18.0	stable emulsion

Table IV.4 Sb(V) scrubbing with KNa tartrate solutions from 5v% TN 1911. Conditions: A/O=1, 3 min., 25°C, [Sb(V)]_o= 109 mg/L (loaded from single metal solution at 2.7M HCl).

The Effect of Scrubbing on Pt and Pd: The single metal scrubbing results showed that HCl and H₂SO₄ solutions would indeed be adequate in the removal of most of the impurity elements. As the loaded organic would also contain Pt and Pd, it was important to consider whether significant losses would occur during scrubbing. Organics were therefore loaded using the same methodology as described in Section IV.3. Then, they were subjected to scrubbing for different contact times and HCl/H₂SO₄ concentrations. Table IV.5 shows the results.

In the case of Pt/HCl, losses were not affected by time of contact (3 and 15 min.) or acid concentration (1.5–3.5M HCl) and remained constant at <1.6%. The Pt-HCl scrub results are in very good agreement with the single metal plots (Figure IV.6). According to the results in the latter figure, $D_{\rm Pt} > 60$ at 1.5M HCl which suggests that less than 2% of the Pt(IV) remained in the aqueous phase. With Pd/HCl, losses were effected only at greater than 2.5M HCl. At 3 min. contact time, 6% loss was registered at 2.5M HCl; that increased to 15% at 3.5M HCl. Longer contact resulted in very little change, with 4% and 18% losses respectively. These values are again in agreement with Figure IV.6 which gives $D \sim 20$ at 2.5M HCl and D = 6 - 7 at 3.5M HCl. For these D values, 5 and 15% removal of Pd(II) is expected as is found in Table IV.5. The data collected therefore showed that an HCl scrub solution lower than 2.5M would be effective in selectively removing the impurity elements, with only minor losses of Pt-Pd and that contact time (up to 15 minutes) does not affect PGM losses.

In the case of $\rm H_2SO_4$ scrubbing, the effect of acid concentration, between 0.1 and 1.7M, was investigated only for 3 minute contacts. The lowest losses were observed at the highest acid concentration (1.7M) both for Pt (1.5%) and Pd (0.3%). The greatest losses were for Pt at 0.1M $\rm H_2SO_4$ with 57% going to the aqueous scrub phase $\rm A.0.1M$ sulphuric acid would approximately correspond to pH 1.00 and this is the region of Pt stripping which is above pH 0.7. The corresponding loss for Pd in 0.1M sulphuric acid solution was 3.5%. Overall therefore, adoption of a dual acid scrubbing acid approach using 2.0M HCl and 1.7M $\rm H_2SO_4$ is expected to effectively remove the impurities and

Scrub solution	$\mathrm{C}_{Pt_{aq,mg/I}}$		CPd _{aq,n}	ng/l
(C in mg/L) A/O=1	3 min.	15 min.	3 min.	15 min
C _{Morg} = 874 Pt 1003 Pd				
1.5M HCl 2.5M HCl 3.5M HCl	11 9 11	14 9 11	15 63 152	3 41 178
См _{огд} = 1118 Pt 967 Pd				
0.1M H ₂ SO ₄ 0.9M H ₂ SO ₄ 1.7M H ₂ SO ₄	750 30 16	-	35 3 3	-

Table IV.5 Pt-Pd single metal scrubbing tests in HCl and H₂SO₄ solution.

prevent contamination in the Pt and Pd strip liquors with negligible losses of Pt and Pd.

Summary: The data presented in this section was useful in two ways: (i) in developing scrubbing schemes for the common impurity elements encountered in industrial chloride leach liquors; and (ii) in understanding the underlying extraction/stripping mechanisms. It is evident that further tuning of these procedures would be required in order to select more suitable scrubbing conditions for maximal removal of impurities with minimal losses of Pt/Pd. It is also important to note that in multi-element solutions the elements, including the PGMs, may behave differently due to the phenomenon of crowding.

IV.5 Flowsheet Design Considerations

<u>Introduction</u>: The extraction and scrubbing data which had been generated in the earlier tests was used to design and test a flowsheet for the clean separation of Pt and Pd. Scrub steps were incorporated in the circuit based on the behaviour of the impurity elements with different scrub solutions.

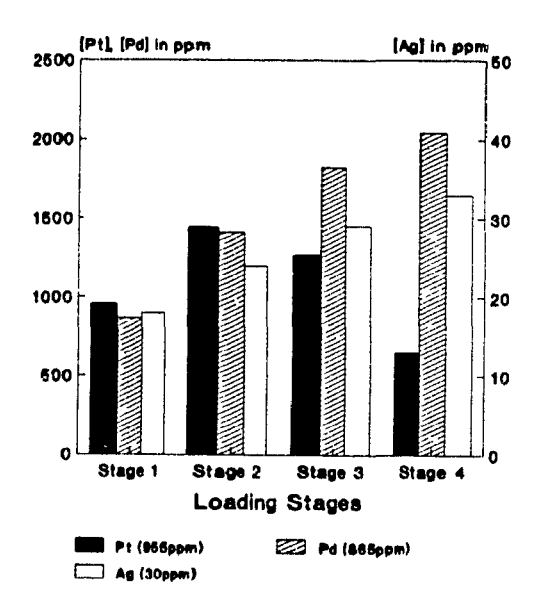
Selection of Synthetic Feed and Extraction Conditions: Before looking at potential scrub solutions, it was essential to select a feed HCl concentration which would maximize Pt/Pd extraction and perhaps reduce the coextraction of many of the impurity elements encountered in the Pt strip solution. Making this selection was rather straightforward: by examining the single metal extraction results for Pt(IV) and Pd(II) (Figure IV.7), a common region of strong coextraction for Pt and Pd was identified at 100 g/L (2.7M) HCl. This same acidity point produced a minimum in Fe(III) and little or no Cu(II) extraction. As(V) and Se(IV) also exhibited distribution coefficients lower than 0.1.

Having made the selection of the feed acid concentration, it was rather unrealistic to accept that 1,000 mg/L of each of the impurities would be present in a typical refinery feed. PGM refining liquors vary greatly both in terms of composition and concentrations. Table IV.6 shows the compositions of two industrial liquors which were available in the laboratory as well as the composition of the feed prepared specifically for this work. It was decided to include first of all, elevated concentrations of Cu and Ni, 3,000 mg/L of each, as a typical feed may originate from a copper or a nickel refinery. The remaining impurity elements would each be present at 500 mg/L except for Ag which would typically occur at around or below 100 mg/L due to its low solubility in aqueous solutions. Pd being more abundant than Pt was set at 3,000 mg/L and Pt at 1,500 mg/L.

METAL	Noranda ⁽⁵⁾	R.C. Mint (#RCMINT-12-II)	McGill (March 1991)
Pt(IV) Pd(II) Ag(I) Fe(III) Cu(II) Ni(II) Zn(II)	713 6814 69 154 2120 no assay no assay	2500 5100 120 720 14600 960 860	1.50C 3000 100 500 3000 3000 500
Pb(II) Na(I) As(V) Sb(V) B1(III) Se(IV) Te(IV)	274 no assay no assay < 1 133 89 no assay	1100 5400 145 <3 <5 <3 15	500 no assay 500 500 500 500 500

Table IV.6 Typical refinery feeds vs McGill synthetic feed. Concentrations in mg/L.

As for the the number of extraction stages, previous work(4) involving the construction of isotherms had determined two stages to be sufficient both for Pt and Pd. Before this number of extraction stages was adopted it was thought useful to evaluate the deportment of the impurity elements when consecutive contacts with the same organic are performed. Under this contacting scheme, any tendencies for crowding could be better detected. The results are depicted in Figure IV.22. According to the top bar diagram of this figure, after two contacts, Pt begins to drop and Pd loading increases. Similar behaviour has been observed in a parallel study conducted by Côté⁽¹⁵⁾. In terms of the impurity elements we can mention the following observations. firstly, the elements Ni(II), Pb(II), Se(IV) and Te(IV) are either effectively not extracted or simply do not build-up in the organic phase as the contacts increase. These elements should therefore not be problematic in a solvent extraction circuit. Secondly, the loading of Fe(III), Cu(II), As(V), Sb(V) and most notably Sn(IV) keep increasing with contact stage and need to be watched, and thirdly, Bi(III) was the only impuriswhich eventually showed a drop in loading after two contacts. A two-contact extraction scheme was adopted for Pt/Pd coextraction despite the co-loading of some of the impurities. For feeds with different Pt/Pd molar ratios different conditions might have to be devised.



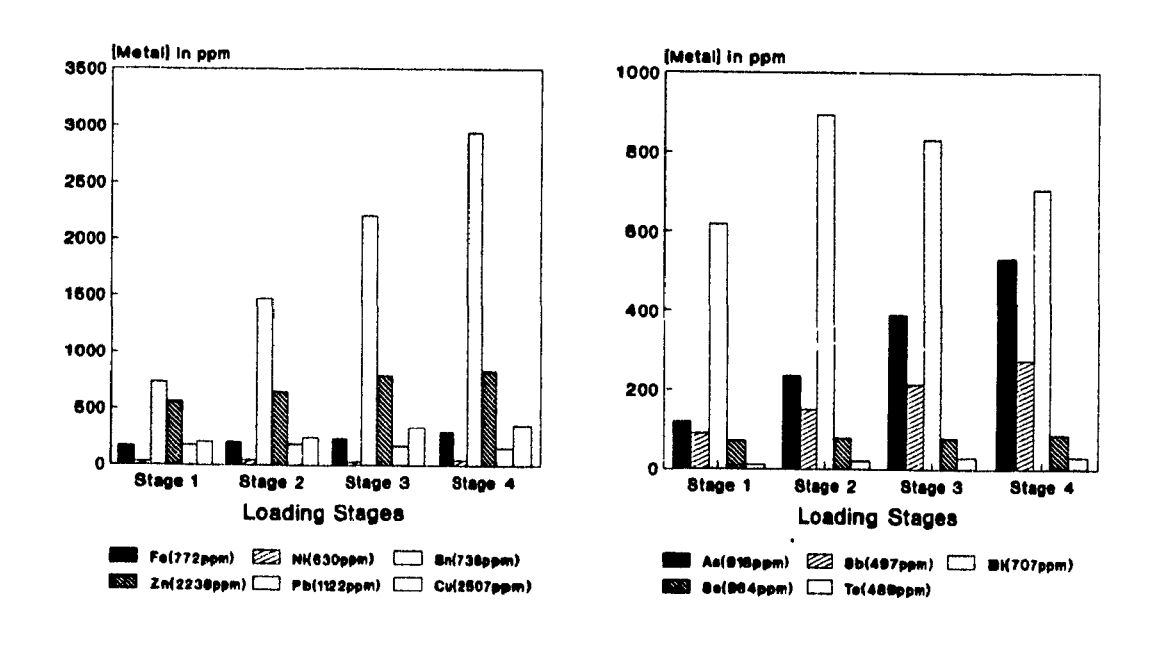


Figure IV.22 4-stage loading of 5v% TN 1911.

Conditions: A/O=1, 3 min., 2.7M HCl feed, impurity element concentrations appear in legends.

Selection of Scrub Solutions and Conditions: Based on the single metal scrub results in Section IV.4, Table IV.7 was prepared to classify the impurity elements according to their contamination potential. Thus elements reported to strip liquors at high concentrations (>100 mg/L) were classified as having high contamination potential while those reporting at <100 mg/L had lesser contaminating potential. Impurities reporting at less than 20 mg/L are not included in this table as this level is taken as the "threshold of cleanliness" (76). The table shows the importance of cleaning the organic of its impurity species prior to Pt/Pd stripping. In particular, Pb(II), Zn(II) and Te(IV) should be removed prior to Pt stripping, while Ag(I) and Bi(III) could be dealt with after Pt stripping but before Pd stripping.

Impurities reporting to:	High Contamination Potential > 100 mg/L in strip liquor	Low Contamination Potential < 100 mg/L in strip liquor
Pt strip solution	Pb(II) Zn(II) Te(IV)	Se(IV) Bi(III) Fe(III) Sb(V)
Pd strip solution	Pb(II) Zn(II) Ag(I) Bi(III)	-

Table IV.7 Classification of impurity elements according to their potential to contaminate the PGM strip liquor. Conditions: 5v% TN 1911 with Feed [HCl]=2.7M, 1000 mg/L M_{ag}.

The Design of the HCl Scrub: In order to further optimize the HCl scrubbing step, data was generated, based on distribution coefficient values obtained in the single metal extraction experiments (Section IV.4). In principle, this value, is independent of the phase volumes, and for the extraction stage is defined as:

$$D_{E} = \frac{[M]_{org}}{[M]_{aa}} \tag{IV.7}$$

The distribution coefficient in its rigorous definition is determined at the equilibrium state and for a reversible single transfer reaction. However, for all practical purposes it can be used to obtain data useful in designing the flowsheet. It is obvious that the data will be valid only for the impurity elements that seem to attain fast and reversible equilibrium. As it is shown later in this section many of the impurities tested seem to obey this requirement. It is with caution that this analysis should be approached. For scrubbing or stripping, D is defined as:

$$D_{s} = \frac{[M]_{aq}}{[M]_{ore}} \tag{IV.8}$$

where D_s is the distribution coefficient for stripping/scrubbing. For a pair of metals, say Pt and an arbitrary impurity element M, the ratio of the two distribution coefficients defines a new quantity:

$$S_{f_{M|n}} = \frac{D_{S_M}}{D_{S_n}} \tag{IV.9}$$

where S_f is a measure of the degree of separation between Pt and M and is known as the separation factor⁽⁷⁷⁾. The greater the S_f , the better the removal selectivity between the impurity element and Pt. D_S values were therefore calculated for Pt and each of the impurity elements at 1.5, 2.5 and 3.5M HCl and S_f values have been determined. Using the respective D_S values and through A/O ratio manipulations, the efficiency of impurity element selective removal was estimated $vis-\hat{a}-vis$ Pt. Appendix C provides details of the these calculations.

The data shown in Tables IV.8 and IV.9 describe what theoretically should occur in HCl scrubbing at 1.5 and 2.5M HCl respectively if the distribution coefficient is respected for all the impurity elements. The absolute concentrations are given in Appendix C. Also found in Appendix C is data for the 3.5M HCl which is excluded from the present discussion due to unacceptably high losses incurred for Pd at this concentration.

It is interesting to note that the calculated distribution data for Pt are in good

METAL	CM _{org} (mg/L)	S _f Pt/M	M _{removed} A:O=0.5 (in %)	M _{removed} A:O=1 (1n %)	M _{removed} A:O=2 (1n %)	M _{removed} A: O=3 (in %)
Pt	990	N/A	< 1.0	2	3	5
Pd	923	N/A	1	1	1	1
Se	60	1550	93	97	97	100
As	93	886	96	93	96	98
Cu	105	388	76	87	93	94
Pb	565	248	20	80	89	92
Sb	286	248	20	80	89	92
Те	714	78	38	56	71	79
Zn	697	52	29	45	63	71
Fe	231	25	17	29	44	55
Ag	80	14	11	19	33	41
Sn	972	3	2	4	8	12
Bi	980	< 0.1	0	0	0	0

Table IV.8 Predicted scrubbing data for 1.5M HCl solution. Conditions: single 3 min. contact on 5v% TN 1911. Last four columns depict removal efficiency (levels of loading were taken from single element extraction tests at 2.7M HCl; Section IV.3).

agreement with the experimentally obtained scrubbing data reported earlier in Table IV.5. Thus according to Table IV.5, Pt losses were <1.6% throughout the 1.5 to 3.5M HCl range at A/O=1 agreeing well with the computed losses (<2%). This confirms that for Pt(IV) the D value holds for extraction and scrubbing. Most of the impurity elements seem to follow this rule with the most notable exceptions being Cu(II); experimental

METAL	CM _{org} (mg/L)	S _f Pt/M	M _{Removed} A:O=1/2 (in %)	M _{Removed} A:O=1 (in %)	M _{Removed} A:O=2 (1n %)	M _{Removed} A:O=3 (in %)
Pt	990	N/A	< 1.0	1	2	3
Pd	923	N/A	2	4	7	11
Cu	105	2857	93	96	99	100
Se	60	1667	89	95	97	100
As	83	1111	76	91	96	98
Sb	286	286	59	74	78	89
Fe#1 #2	231	231	40 64	57 82	72 93	81 97
Pb#1 #2	565	83	29 50	45 70	63 86	72 92
Te#1 #2	714	45	18 30	31 52	49 73	58 81
Zn#1 #2	697	45	19 34	31 52	48 73	58 83
Ag#1 #2	80 60	25	11 21	20 36	33 55	41 67
Sn	972	3	1	3	5	7
Bi	980	2	4	2	4	6

Table IV.9 Predicted scrubbing data for 2.5M HCl scrubbing solution. Conditions: single 3 min. contact on 5v% TN 1911. Last four columns depict removal efficiency. For Fe, Zn, Pb, Ag, Te cumulative % data for 2-stage contacts is shown as well (levels of loading were taken from single element extraction tests at 2.7M HCl - Section IV.3)

scrubbing data at 2.7M HCl produces <20% removal (Figure IV.18, whereas at 2.5M the D values predict 87% removal. Setting aside this observation and commenting on the data of tables IV.8 and IV.9, it can be deduced that the best separations were achieved for Pt - As(V), Se - $\frac{1}{2}$) and Cu(II) at 2.5M HCl as $\frac{1}{2}$, >1,000. This is equivalent to saying that high degrees of removal are expected for each of these impurity elements Sn(IV) and Bi(III) on the other hand are predicted not to be effectively scrubbed with HCl.

The scrubbing data for the various A/O ratios show that in general, as the A/O increases, the degree of impurity removal is greater. Absolute losses of Pt and Pd losses increase with A/O ratio, so it was essential to determine a limit for the purposes of flowsheet design. The limit was set at 5% of 1,000 mg/L for Pt and Pd Experimental scrubbing data in Table IV.5 shows a loss of 6% for A/O=1 at 2.5M HCl which meant that in our selection an HCl concentration of < 2.5M would have to be considered. At the same time going down to 1.5M HCl but raising A/O to 3, Pt losses are equally high (5%). This narrowed down the scrubbing conditions to < 2.5M HCl and < A/O=3

Table IV.7 summarises the most troublesome of the impurities, namely Pb(II), Te(IV), Fe(III), Zn(II), Bi(III) and Ag(I). By focusing on these data it can be seen that the best set of removal conditions (>60% removal) for Pb, Zn and Te after one contact are A/O=2 and 1.5M HCl. Unfortunately, only 33% of the silver is removed under these conditions with bismuth not showing any tendency for removal. At the same time, Fe(III) removal tends to increase from 44% to 72% as HCl concentration increases from 1.5M to 2.5M HCl. Based on these facts, 2.0M HCl was selected to strike a compromise between the advantages of the higher and lower concentrations. The A/O ratio was thus taken as 2:1 to push the impurities out and also avoid any significant PGM losses. Longer contact time, e.g., 15 min., was also adopted as an extra measure to ensure satisfactory impurity element removal. To further remove remaining Zn, Te and Bi from the HCl scrubbed organic phase, sulphuric acid scrubbing was considered to follow HCl scrubbing.

The Design of the H₂SO₄ Scrub: Similar analysis on the basis of distribution coefficients, as was done with the HCl scrub was not possible since data was not

available for the extraction of Pt(IV) and Pd(II) from H₂SO₄ media. Instead data from Table IV.5 was used which suggests low PGM losses at high H₂SO₄ concentration. To complement this data an additional experiment was carried out to choose the best A/O ratio for sulphuric acid scrubbing. For this test, metal-bearing organic with B₁, Zn and Te was scrubbed at three different A/O ratios using 2.0M H₂SO₄. Table IV.10 shown below suggests that any zinc and tellurium remaining in the organic would be almost completely removed after a 3 min. contact, irrespective of the phase ratios.

ELEMENT	CM _{org ,mitual} (mg/L)	A/O=1 (%)	A/O=2 (%)	A/O=5 (%)
Bi(III)	901	13	43	88
Zn(II)	749	95	99	85
Te(IV)	369	84	85	85

Table IV.10 Multi-element scrubbing test with 2.2M H₂SO₄. Conditions: 5v% TN 1911, 3 minute contact.

In the case of bismuth an anomalous behaviour is observed in the sense that percent removal of Bi(III) does not seem to follow the same distribution law (*D* varies with A/O - this might very well be due to the fact that D was not determined under equilibrium conditions or because Bi exhibits limited solubility in in sulphuric acid solutions). Thus, high A/O ratios seem to strongly favour Bi(III) scrubbing as % removal rises quite sharply from 13 to 88% when ratio changes from 1:1 to 5:1. Having thus observed this behaviour in H₂SO₄ solutions, it was decided to choose an A/O ratio of 3/1 as higher ratios would result in significant losses of Pt/Pd. Moreover, a two-contact approach was adopted to ensure efficient removal not only of Bi(III) but also of other impurities not removed by the HCl scrub, and notably Cu(II) and Fe(III).

The Design of Other Scrubbing Steps: As a precaution against Ag leaking into the Pd

strip liquor, a scrubbing step was contemplated after Pt stripping. 0.1M HCl/2.0M $MgCl_2$ had been found to be effective for >60% removal after 3 min. contact at an A/O=1 (Table IV.3). These conditions were therefore adopted Finally, to deal with Sn(IV), which remains unaffected by the preceding scrubbing steps and stripping contacts, and to avoid buildup in the recycled organic, a caustic scrub was added after Pd stripping. The conditions for the scrub were 1.0M NaOH at an A/O=1 for a 60 min. contact time.

PGM Stripping Conditions: As pH control should be exercised during Pt(IV) stripping with water a contact time of 15 min was selected to facilitate pH control at pH 1.5-2.0³⁰ with the addition of base. A single contact stage at A/O=0.5 was adopted to concentrate the Pt. In the case of Pd, six stages at an A/O=1, with 3 min contacts each were selected⁽⁴⁾. Figure IV.23 shows the flowsheet designed by including the incorporated scrubbing steps. This flowsheet was tested in the laboratory as described in the next section.

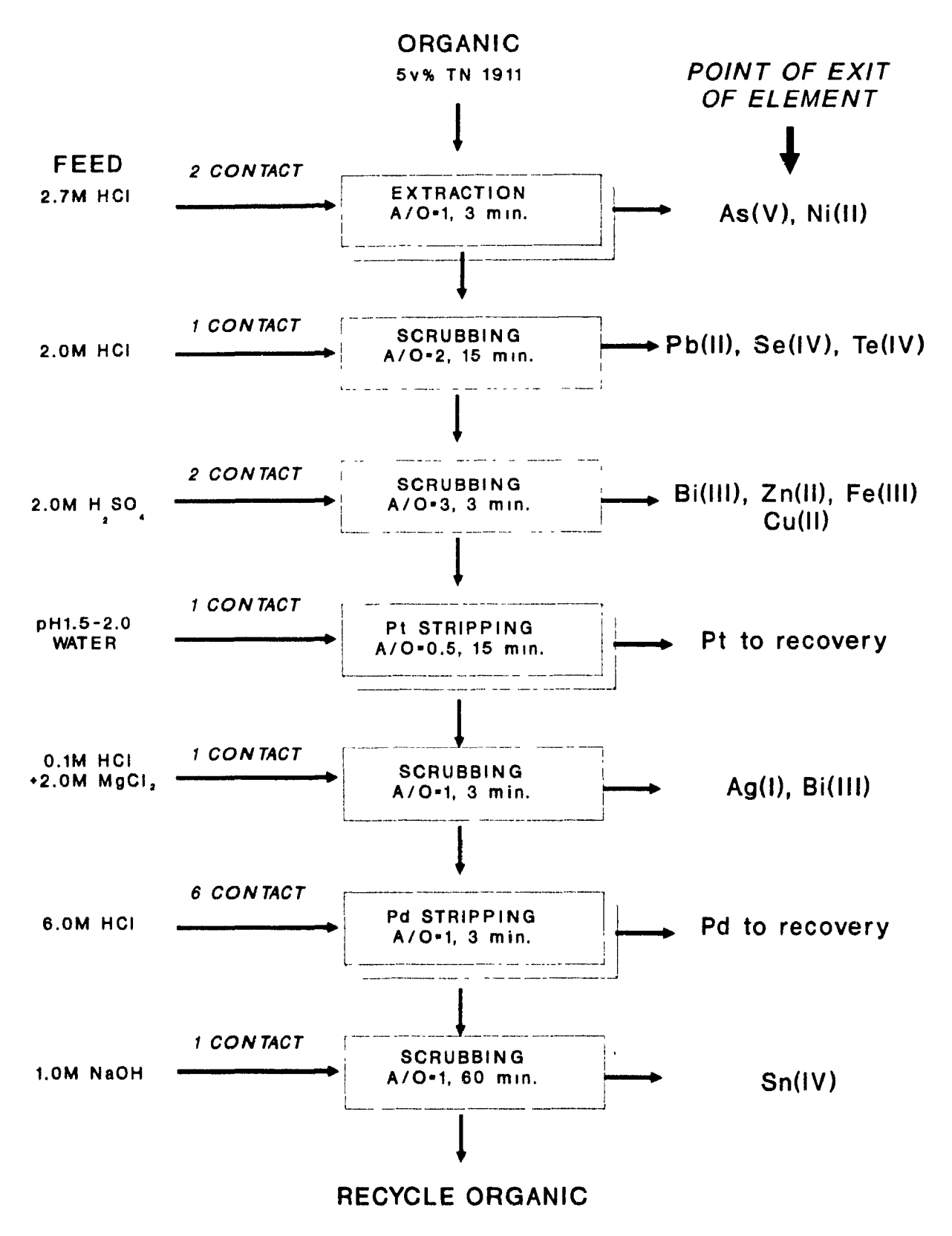


Figure IV.23 Tentative flowsheet designed for testing in the laboratory the effectiveness of the incorporated scrubbing steps.

IV.6 Bench-Scale Simulation of the Tentative Flowsheet

The continuous piloting of a process flowsheet was practically impossible in the present study due to (i) the prohibitive high costs in obtaining large volumes of PGM liquors, and (ii) the absence of a pilot-plant facility at McGill University. Only limited testwork was attempted with the primary objective to verify the effectiveness of the scrubbing procedures.

It must be emphasized that the ultimate definitions of all the contacting steps making up the process flowsheet should be made separately for each specific industrial feed using continuous piloting (as there is considerable variation in feed composition from refinery to refinery). The present bench-scale work attempts to establish in a generic rather than a feed-specific manner the steps one can take to control impurity elements from contaminating Pt and Pd strip liquors.

Adapting the Flowsheet into a Treybal Cascade: For the simulation of the tentative flowsheet the Treybal array was adopted. As explained in Section III 2 it consisted of multiple batch contacts which simulate the steady-state performance of a counter-current contacting circuit. Only the extraction, H₂SO₄ scrubbing, and Pd stripping steps were tested with this cascading technique as the Pt stripping, HCl and NaOH scrubbing steps adopted involved single contacts. Extraction and H₂SO₄ scrubbing were to appear as 2 x 2 cascades whereas a 6 x 6 array was needed for Pd stripping. The complete flowsheet in Treybal form appears in Figure IV.24. Mass balancing was performed for all the elements and the obtained results are discussed below in terms of a number of factors with particular focus on:

- a) purity of PGM strip solutions;
- b) effectiveness of scrub solutions;
- c) extent of steady-state attainment;

- 1
- d) physical difficulties experienced; and
- e) design of improved flowsheet.

Purity of PGM strip solutions: The Pt and Pd solutions collected contained low levels of impurity elements. The Pt strip was in fact 99.4% Pt with 6 mg/L Zn, being the most abundant impurity element, and 1 mg/L each of Ag, Sb, Se, Te. As for the Pd strip solution, it was 99.6% pure with Fe the most abundant impurity element (4mg/L) and 1 mg/L each of Cu, Se, and Zn. These strip solutions would normally immediatly report

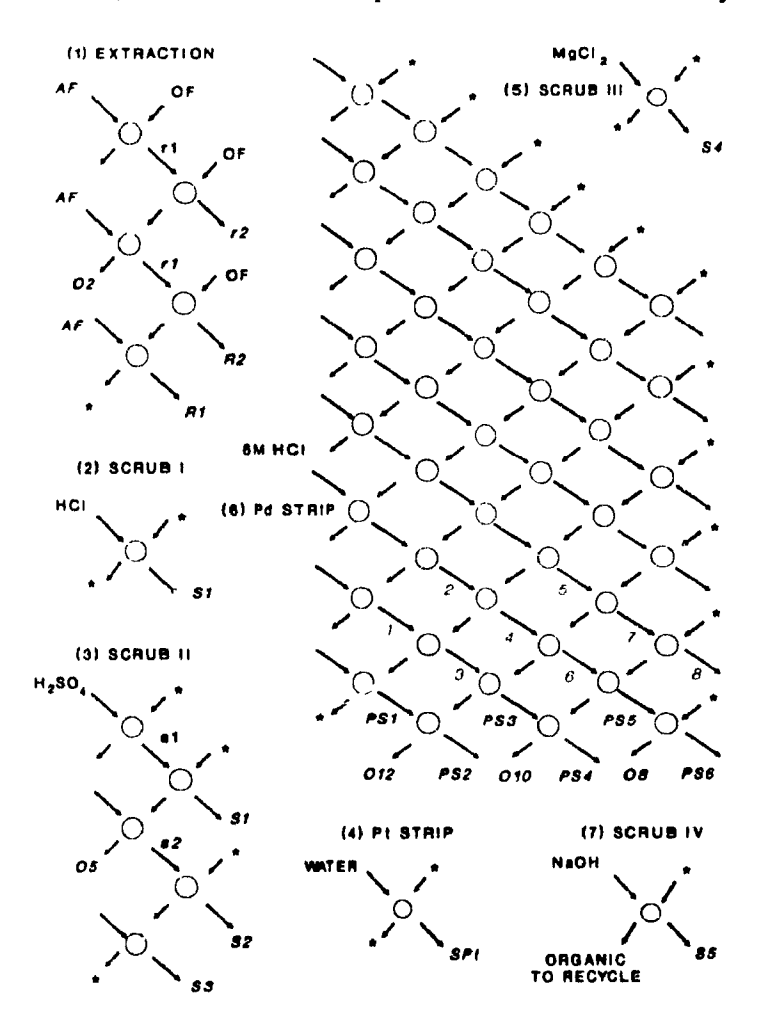


Figure IV.24 Adapting the Treybal cascade to the tentative flowsheet. Analysed streams appear in *italics*, flow of organic is denoted by an asterisk and SCRUB I= 2.0M HCl, SCRUB II= 2.0M H₂SO₄, SCRUB III= 0.1M HCl + 2.0M MgCl₂, SCRUB IV= 1.0M NaOH. AF/OF refer to aqueous and organic feeds respectively and S, R, s and r all indicate aqueous streams.

precipitation as di-ammonium salts followed by calcination or alternatively to solution reduction. These additional steps to obtain the metals in their pure form were not attempted here. However, it is clear from the purity of the strip liquors that the tested impurity control scrub steps in combination with the downstream selective precipitation steps would be effective in achieving typical refinery target purities.

Effectiveness of Scrubbing: A useful way of looking at the effectiveness of the scrub solutions was by drawing plots of metal concentration in organic as a function of circuit step. Three separate plots appearing in Figures IV.25 to 27 were constructed. The first shows the behaviour of the most strongly extracted impurities, Zn(II), Te(IV), Pb(II) and Bi(III); the second features the weakly loaded ones, Ag(I), Ni(II), Se(IV), As(V); and the third is with the remaining Sn(IV), Sb(V), Fe(III) and Cu(II).

By examining these plots, it becomes evident that the 2.0M HCl scrub removed greater than 50% of Zn(II), Te(IV), Pb(II) as well as Ag(I) Sc(IV), Ni(II) and Cu(II). The single metal tests, which were for 2.7M HCl at A/O=1 and 3 min. contacts, had predicted ~50% removal of Pb(II), Fe(III) and Se(IV), with lesser amounts of Te(IV) and Ag(I). The greater A/O (=2) and the longer contact time was indeed beneficial for Zn(II), Te(IV) and Cu(II) removal. With the two-stage sulphuric acid scrub, Bi(III) was totally removed as were also remaining amounts of Zn(II), Te(IV) and Pb(II). The overall results did correspond to the findings in the single metal experiments, in particular for the elements Zn(II), Se(IV) and Te(IV). In the case of B₁(III), the results were also as predicted, but the removal of Fe(III) and Cu(II) was not as effective as expected. The same can be said for the 0.1M HCl + 2.0M MgCl₂ scrub step. Although not conclusive, the results from this step indicated marginal removal of impurities (16 mg/L Zn and 7 mg/L Ag). Therefore, there is no justification for the inclusion of this scrub step in an ultimate flowsheet except in special circumstances where Ag(I) problems need to be addressed. In the case of 60 min/1.0M NaOH all the Sn(IV) and 45% of Sb(V) were scrubbed. The final organic phase contained some Pt (87 mg/L) and Pd (81 mg/L), as well as Sb (40.5 mg/L) and Cu (49 mg/L). Pt and Pd stripping was incomplete indicating further tuning would be required in the future so as to recover all

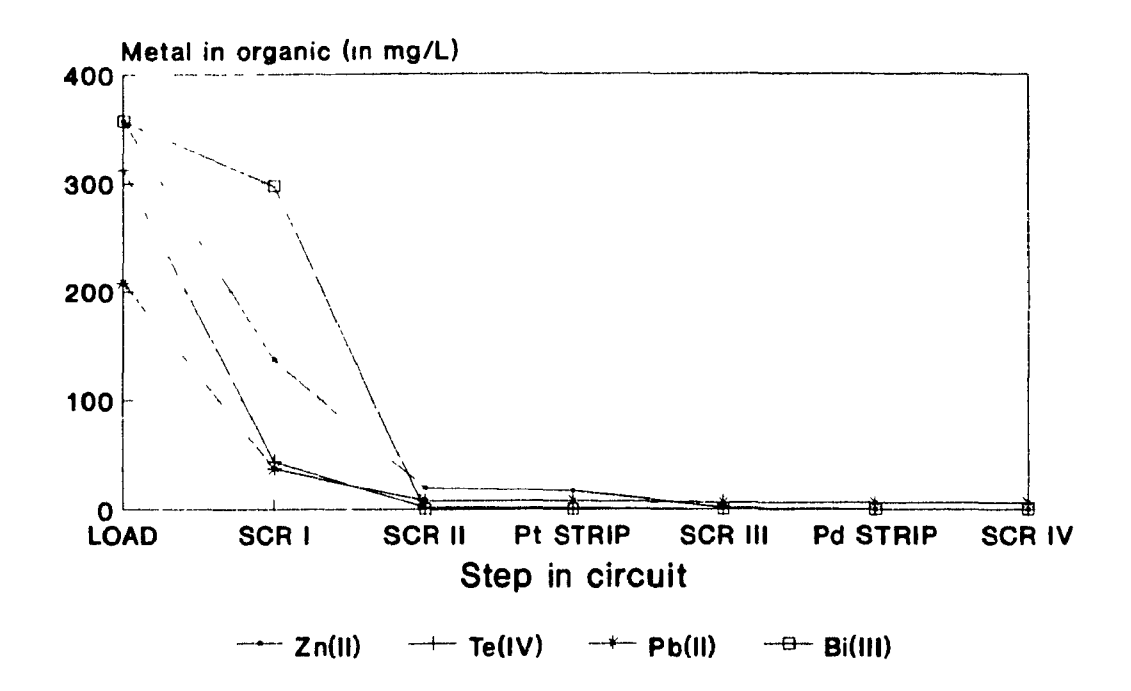


Figure IV.25 Effectiveness diagram for the strongly extracted impurities: Zn(II), Te(IV), Pb(II) and Bi(III). (SCR I= 2.0M HCl/1 contact, SCR II= 2.0M H₂SO₄/2 contacts, SCR III= 0.1M HCl+2.0M MgCl₂/1 contact, SCR IV= 1.0M NaOH/1 contact).

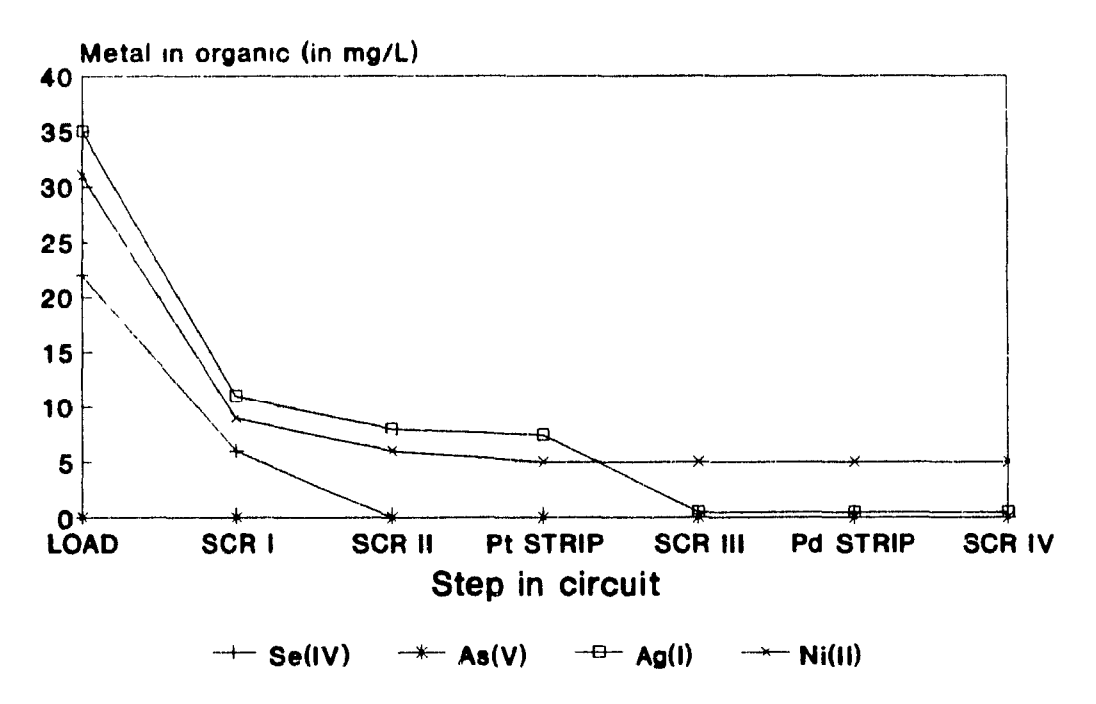


Figure IV.26 Effectiveness diagram for the minor impurities: Se(IV), As(V), Ag(I), and Ni(II).

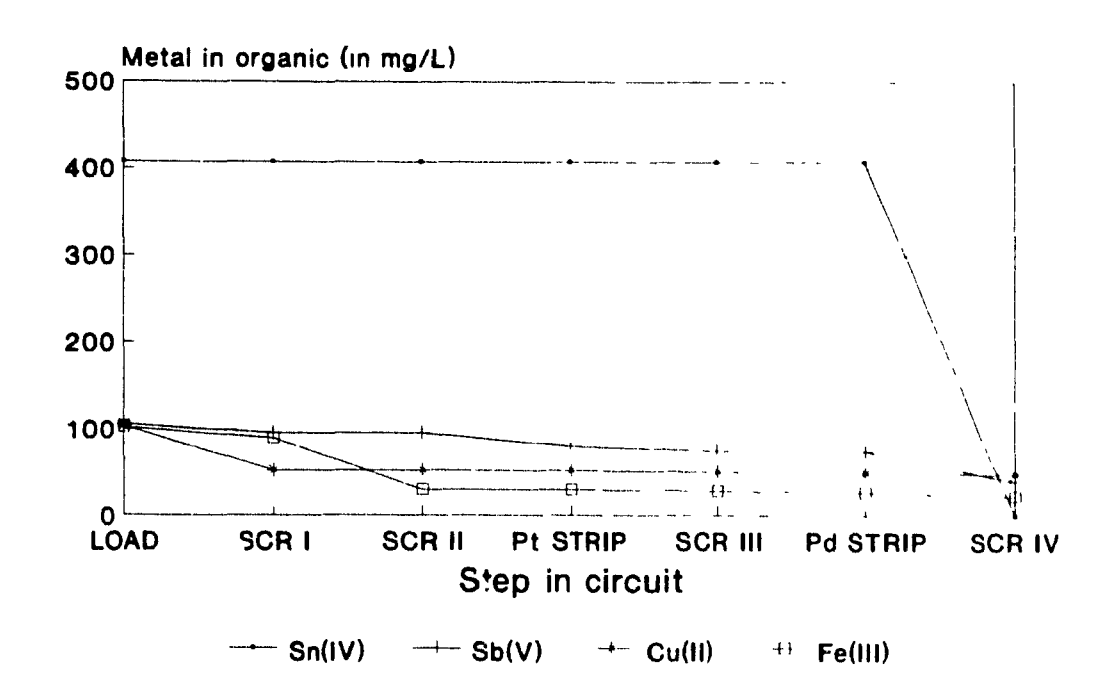


Figure IV.27 Effectiveness diagram for the other elements: Sn(IV), Sb(V), Cu(II), and Fe(III).

the values from the organic phase.

Extent of Attainment of Steady-State: Two different cascade sizes were selected for the simulation of the flowsheet, 2×2 and 6×6 . One way of finding out whether steady-state was attained, was to look at the assays for parallel streams. A 10% discrepancy between two values was chosen as the criterion for evaluating the attainment of steady-state. Looking at Figure IV.28 it can be seen that both for Pd and Zn there is some evidence that the steady-state is being approached especially if we consider the aqueous stream assays.

Figure IV.29 shows the sulphuric acid cascade results for B₁ and Zn which follow the same trends. The 10% margin of error criterion was therefore not met in the 2×2 case. A 2×4 cascade in the case of two contact stages would have probably reproduced results closer to a steady state.

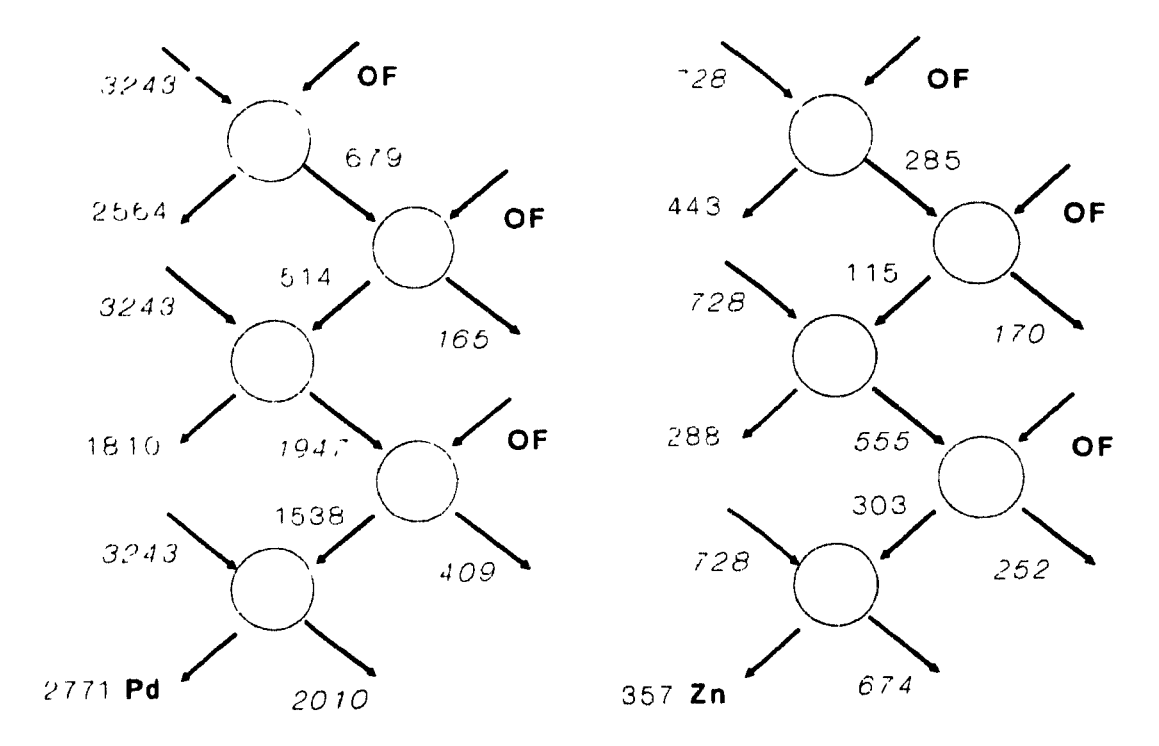


Figure IV.28 Treybal diagram assays: extraction of Pd(II) and Zn(II) (numbers shown are concentrations in mg/L). Conditions: A/O=1, 3 min.

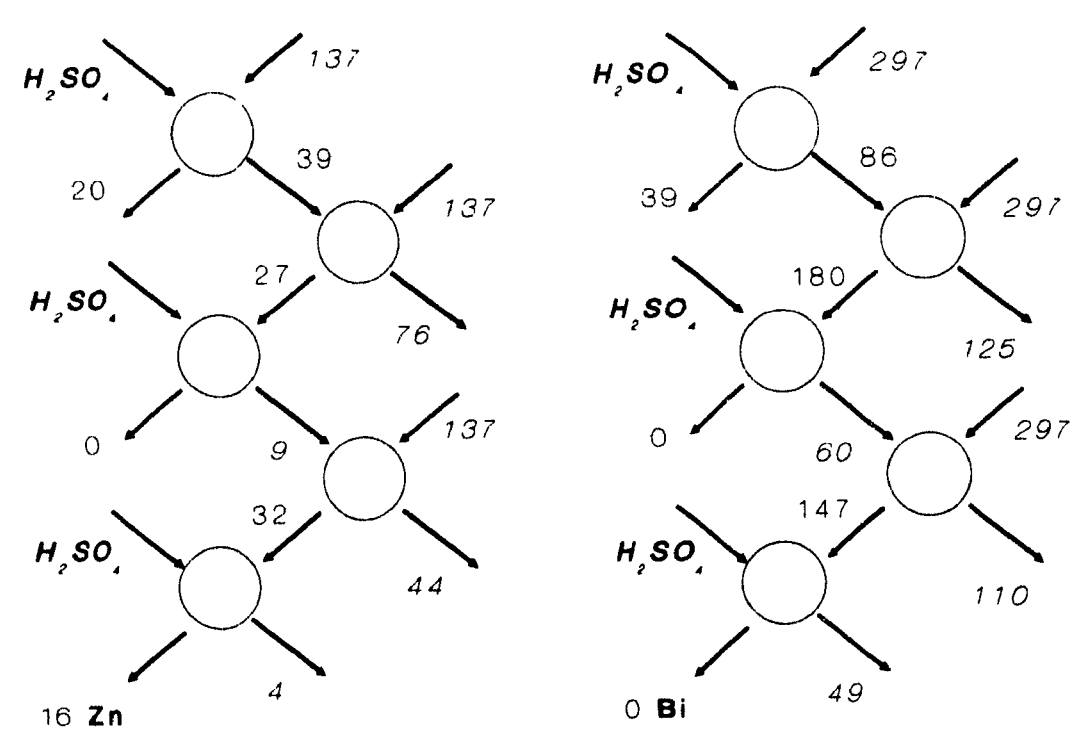


Figure IV.29 Treybal diagram assays: H_2SO_4 scrubbing of Zn(II) and Bi(III) (numbers shown are concentrations in mg/L). Conditions: A/O=3, 3 min.

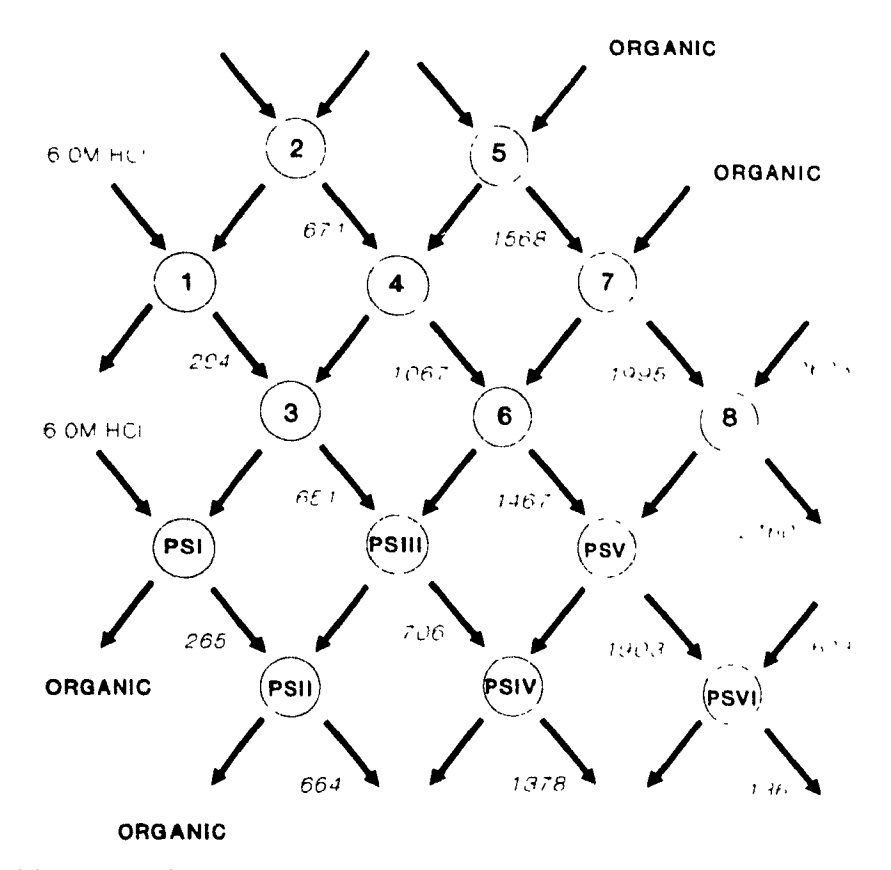


Figure IV.30 Treybal diagram assays: Pd stripping with 6.0M HCl. PS = I-VI indicate final 6 contacts in 6×6 array (numbers shown are concentrations in mg/L). Conditions: A/O=1, 3 min.

Figure IV.30 shows the bottom portion of the 6 x 6 Pd stripping cascade. All parallel aqueous streams agree with the margin criterion, except for the streams exiting batch contacts 4 and PSIII. A good approach to steady-state was therefore attained in this case.

Physical Difficulties Experienced: Phase disengagement difficulties were only encountered in the very last stage, involving the alkaline scrub with 1.0M NaOH. A stable emulsion was produced after the 60 min. contact which had not been observed during single metal testing. A disengagement time of one day was necessary to produce a clear phase for analysis. Later it was found that contacting the organic phase with water after Pd stripping, would remove acid, thus favouring an enhanced phase separation (and remedying the problem). Of course, for feeds not containing Sn(IV), NaOH would not

be necessary and the accompanying problems would not be encountered. In the case of feeds containing Sn(IV), maybe periodic bleed-off of a portion of the solvent (to prevent metal build-up) with special centrifugal separators would need to be exercised.

The Design of a Revised Flowsheet: On the basis of this part of the work, the flowsheet in Figure IV.23 was revised and a new version appears in Figure IV.31. The modifications made to the flowsheet were few, but nethertheless of importance:

- a) In the extraction operation a higher A/O ratio (3/2 instead of 1/1) and a longer contact time (5 min. instead of 3 min.) are thought to be a better choice as they well concentrate the PGM values and result in improved Pd extraction the latter is a function of time⁽⁴⁾.
- b) To improve the efficiency of HCl scrubbing, two stages of 5 min. each instead of one of 15 min. are adopted.
- c) Perform Pt stripping in two stages of 5 min. each, as the simple stage was hardly sufficient in the trial carried out in the laboratory. Also, reduce the contact time from 15 min. to 5 min. The kinetics of Pt extraction/stripping are effectively very fast and limited by the speed of pH adjustment control⁽⁴⁾.
- d) An increase in contact time of 3 to 5 min. is perceived to be beneficial to Pd stripping due to slow kinetics.
- e) The 0.1M HCl + 2.0M MgCl₂ scrub stage is eliminated as Ag(I) and Bi(III) seem to be effectively removed in the preceding steps.
- f) Adjust H₂SO₄ scrubbing contact time from 3 to 5 min. to maintain a consistent contact time period per stage throughout the circuit. And finally,

1

I

g) Conduct scrubbing of Sn(IV) with NaOH (although not shown) after the Pd stripped organic is washed with water to remove its acid content. In this way phase separation problems (emulsion formation) are greatly eliminated.

In summary, the modifications made were to (i) enhance Pd extraction, (ii) improve the effectiveness of the two acid scrubs and (iii) improve Pt stripping. This new flowsheet still needs to be tested and optimised.

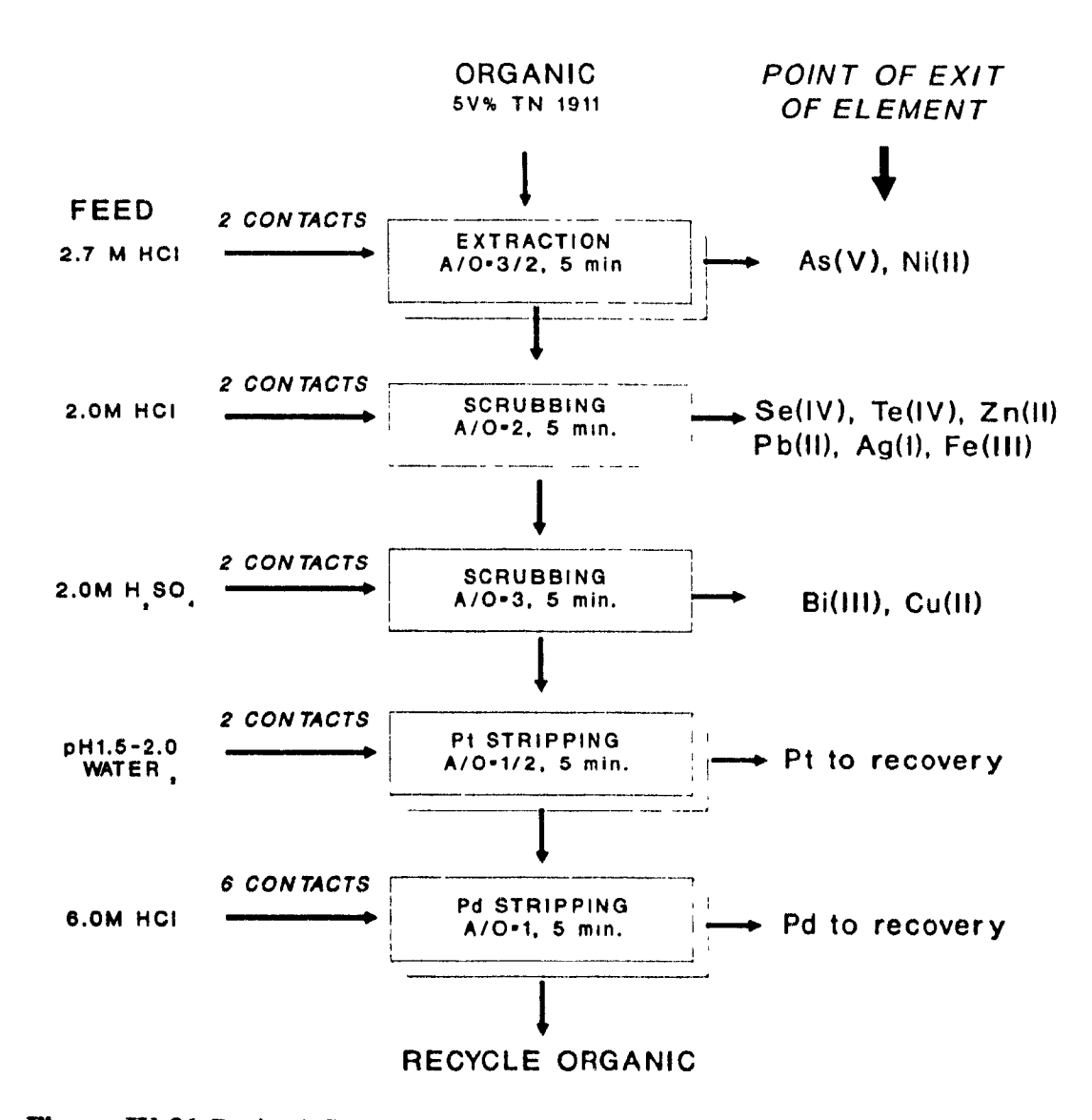


Figure IV.31 Revised flowsheet designed for the refining of Pt and Pd using TN 1911.

CHAPTER V. CONCLUSIONS

V.1 Conclusions

The 8-hydroxyquinoline-based reagent TN 1911 has proved to be a powerful extractant for Pt-Pd from industrial chloride leach liquors. One of the difficulties addressed in an industrial scenario is the interfering impurity elements which may coextract as demonstrated by the semi-industrial solution tests *Experiments 1-2*. These interferences may cause complications such as strip liquor contamination and build-up in the organic phase. The study which was conducted, developed control strategies for the impurity elements Cu(II), Ni(II), Fe(III), Zn(II), Pb(II), Sn(IV), Ag(I), As(V), Sb(V), Bi(III), Se(IV) and Te(IV) expected to be present in typical PGM chloride leach solutions.

In order to develop these strategies it was desirable to gain an understanding of the distribution behaviour of all impurity elements, in the system HCI-TN 1911, by performing single metal extraction experiments. The findings of this part of the work, in conjunction with supporting information from the literature determined that the majority of the impurity elements are extracted as anionic chlorocomplexes via an ion-pair formation mechanism with the protonated extractant. With most elements, TN 1911 behaves as a weak basic extractant. Ni(II), As(V) and Se(IV) were the only elements which were found not to extract significantly in the investigated 1.3-4.0M HCl range.

Scrubbing/stripping tests were carried out on loaded organic phase on a single and multi-element basis to identify ways of controlling the deportment of impurity elements in the PGM strip liquors. These tests showed that Te(IV), Zn(II), Pb(II), Ag(I) and Bi(III) were the elements with the highest potential for contaminating the strip liquors.

Elements which tended to build-up in the organic and be difficult to strip in the acidic range were Sn(IV) and Sb(V). Scrubbing procedures developed consisted of an HCl solution (2.0M) which was capable of removing most of the coextracted elements followed by a 2.0M sulphuric acid solution mainly used for the removal of Bi(III). Another finding was that 1.0M NaOH scrubbing for long contact times (60 min) achieved complete removal of Sn(IV). The risk of emulsion formation could be avoided by water washing, for acid removal from the organic, prior to contact with alkali. For Sb(V), weak sodium potassium tartrate solution (0.1M) was successful only in removing half the amount in the organic, as was the 0.1M HCl+2.0M MgCl₂ solution for Ag(I).

All the accumulated data was used in the design of a tentative flowsheet in which some of the scrubbing procedures were incorporated. The flowsheet was designed keeping in mind that PGM losses were to be kept at a minimum while maximizing the transfer of the impurity elements into the aqueous scrub liquors. The flowsheet which was eventually tested included four scrubbing steps: two acid scrubs after extraction, consisting of 2.0M HCl followed by 2.0M H₂SO₄; a chloride scrub (0.1M HCl+2.0M MgCl₂) appearing after Pt stripping and a caustic scrub (1.0M NaOH) after Pd stripping. The Treybal counter-current simulation cascade technique was used to simulate the flowsheet in the laboratory and this consisted of a series of batch contacts. The results from the simulation test were very positive in terms of achieving high purity strip liquors, of the order of 99% + both for Pt and Pd. Also, the two acid scrubs were found to remove almost all the extracted elements efficiently. Sulphuric acid was found to be essential for Bi(III). The strong chloride scrub removed residual silver and the alkaline scrub pushed out all the tin. On the basis of the results, an improved flowsheet was suggested to offer better separation efficiency for Pt/Pd recovery.

V.2 Further Investigations

This work was successful in studying the basic extraction behaviour of a great number of impurity elements likely to be encountered in a possible solvent extractionbased refinery flowsheet applying an 8-hydroxyquinoline extractant. Any future work undertaken on this project should concentrate mainly in two areas: (1) to establish the fundamental solvent extraction chemistry in chloride liquors and (2) to optimize the scrubbing procedures designed in this work. After all, the great number of impurity elements which had to be investigated in the limited scope of a Master's thesis project did not allow for a complete and comprehensive study on all the aspects of the research. In particular, in further defining the flowsheet, future investigation should focus on the Pt stripping pH operating range (pH 0.7—2.0) by examining selectivity and recovery efficiency. This analysis should provide information as to whether bismuth truly reports in significant amounts to the strip solution and if pH control can keep it in the organic, and whether its removal can be effected after Pt stripping but before Pd stripping. Another possible area of research may be the total replacement of the sulphate-based scrub solution (primarily used for Bi(III) removal) with the strong chloride scrub which was originally designed for silver. From the single metal extraction tests, there is strong evidence that Bi(III) behaves very much like Ag(I) and can also be scrubbed with weak acid/strong chloride solution. Finally, the recovery of Pt/Pd from their respective strip liquors by precipitation should be investigated as well for evaluation of the selectivity of the whole separation flowsheet.

No.

APPENDIX A: FREE ACID DETERMINATION

A method for the free acid determination of diluted RC Mint feed was adopted by first comparing three different titration techniques. The first of these techniques was direct acid-base titration using diluted Royal Canadian Mint feed and 0.48M NaOH with three drops of phenolphthalein as indicator. Although the results were reproduced as demonstrated in Table A-1, they were not considered accurate as hydrolytic precipitation of cations was occurring at or just before the end point which was observed as a colourless-to-purple colour change.

A second method which was tried was based on the precipitation of Fe(OH)₁, a technique described by Moskowitz et al. The logic of this method lies in the formation of the FeF⁺⁺ ion which precipitates rapidly as ferric hydroxide in the presence of a stoichiometric amount of base. 0.05M solutions both of NH₄F and Fe₂(SO₄)₄ were prepared and added in equal proportions to diluted RC Mint feed solution. Using 0.1M NaOH solution, titration would result in an end point triggered off by the precipitation of brown Fe(OH)₃. This test was abandoned due to difficulty in the end point determination and poor reproducibility of the results.

The EDTA masking technique used by Kondos⁽⁷⁹⁾ was then tested. This method is based on the complexation of cations by the chelating ethylenediaminetetraacetate ion which is a common laboratory reagent. Relying on the complete assay of RC Mint-12-I, illustrated on Table III.1, 1:1 and 1:2 ratios of M_{aq}·EDTA were tested with diluted RCMint feed and 0.1M NaOH solution. A blank titration was also run on 0.049M EDTA solution to evaluate whether it would contribute significantly in acidity. The tabulated results on Table A-1 show good reproducibility for both 1:1 and 1:2 results without precipitation of cations. The 1:1 ratio was deemed to be sufficient for all intents and purposes, and this technique was considered best overall for free acid determination.

SOLUTION	DILUTION (mL/mL)	EDTA (mL)	NaOH (mol/L)	NaOH (mL)	Pttion.	Total [H ⁺] mol/L
1) ACID-BASE						
Mint-12-I	1.5/60	n/a	0.48	10.8	YES	3.45
Mint-12-II	1.5/60	n/a	0.48	11.0 9.0 9.0	YES YES YES	3.52 2.88 2.88
2) NH₄F- Fe(OH),						
0.036M HCl as olank	n/a	n/a	0.1	18.0 18.0	YES YES	0.036 0.036
Mint-12-I	0.5/50	n/a*	0.1	17.6 15.9	YES YES	3.52 3.18
Mint-12-II	0.5/50	n/a	0.1	15.5 18.3 16.5	YES YES YES	3.10 3.66 3.30
3) EDTA				16.4	YES	3.28
0.049M EDTA as blank	0.5/50	10.00	0.1	5.4 5.0 5.0	NO NO NO	0.054 0.050 0.050
1:1 Ratio Mint-12-I	0.5/50	3.00	0.1	18.0 17.4	NO NO	3.60 3.48
Mint-12-II	0.5/50	5.00	0.1	17.2 18.1 18.2 17.6	NO NO NO	3.40 3.62 3.64 3.52
1:2 Ratio Mint-12-I	0.5/50	6.00	0.1	18.7	NO	3.74
				18.4 18.4	NO NO	3.68 3.68
Mint-12-II	0.5/50	10.00	0.1	19.0 18.9 19.1	NO NO NO	3.80 3.78 3.82

Table A-1 Free acid determination experimental results.

1

^{*} $[NH_4F] = [Fe_2(SO_4)_1] = 0.05M$ added each as 5 mL. pH measurements were not taken.

APPENDIX B: THE SUPPRESSING EFFECT OF Sn(II) ON Pt(IV) EXTRACTION

During loading of TN 1911 in *Experiments 1*, the semi-synthetic feed was made up of Royal Canadian Mint solution spiked with a variety of impurity elements. It was found that Pt(IV) extraction was totally suppressed at 0.7M HCl.

It was thought that one of the impurity elements in the feed was responsible for this effect. Strongly loaded impurity elements such as Sb(III), Bi(III) and Sn(II/IV) were suspected of either totally "crowding" out Pt(IV) or transforming it into an inert species Preliminary tests involving 5v% TN 1911 and Royal Canadian Mint solution spiked individually with Bi(III), Sb(III) and Sn(II/IV) produced some clues on the interfering element. Table A-2 summarizes the findings which reveal that Sn(II/IV) may have a negative effect on Pt(IV) loading. These results were inconclusive due to the low concentrations (~400mg/L) of Pt(IV) in the feed, and further investigation was required.

Feed Solution	Pt(IV) mg/L	Impurity mg/L	Pt(IV) % Extraction
Mint ONLY	347	n/a	23.3
Mint+Bi(III)	347	430	42.5
Mint+Sb(III)	225	174	29.3
Mint+Sn(II/IV)	231	187	12.3

Table B-1 Effect of Sb(III), Bi(III) and Sn(II/IV) spiking on Pt(IV) extraction from RC Mint solutions (0.7M HCl) with 5v% TN 1911, A/O=1, 3 min.

Thus additional experiments were carried out in which the effect of Sn(II) and Sn(IV) on Pt(IV) extraction were examined more closely. Figures B-1 and B-2 show the results for single metal synthetic solutions of Pt(IV) prepared with Sn(II) and Sn(IV) individually added to the feed solutions, i.e., RC Mint solution was not used in this case. Figure B-1

shows that Sn(II) actually enhances Pt(IV) extraction at high Pt(IV):Sn(II) ratios. A literature review revealed that many investigators identified the exitence of Pt(II)-Sn(II) species. Ayres et al.^(80, 81) and Wittle et al.⁽⁸²⁾, all mention the observation of a red complex in solution upon addition of Sn(II) to Pt(IV) in HCl solutions. The investigators suggested that excess Sn(II) first reduces Pt(IV) to Pt(II):

$$Pt(IV) + Sn(II) \rightarrow Pt(II) + Sn(IV)$$
 (B-1)

A ligand exchange reaction with SnCl₃ follows then forming a dark red complex. This colour change was also observed in our case:

$$PtCl42- + SnCl3 \rightarrow PtCl3(SnCl3)2- + Cl-$$
(B-2)

As a result of the latter labilizing process, the extraction of Pt is enhanced as it has been reported with such extractants as TBP⁽⁸³⁾ and 2-mercaptobenzothiazole⁽⁸⁴⁾. Since we know that the Pt(IV) chloro-complex follows the anion-exchange route with TN 1911, we can suggest the following mechanism in single metal solution:

$$PtCl_3(SnCl_3)^{2-} + 2HL^+Cl^-_{(o)} \rightarrow PtCl_3(SnCl_3)^{2-}(H_2L)_2^+_{(o)} + 2Cl^-$$
 (B-3)

On the other hand Sn(IV) was found not to have any effect on Pt(IV) extraction as Figure B-2 shows.

As the results of Figure B-1 were exactly the opposite of what was observed with the RC Mint multi-element solution, it was decided that an additional test using this solution was to be performed. Thus, the results of Figure B-3 were obtained by adding successively increasing amounts of Sn(II) into RC Mint solution and performing metal extraction with TN 1911. As Figure B-3 shows, the observations at 0.7M HCl and greater than 1:1 molar ratio of Pt(IV) to Sn(II) can be summarized by the following equations:

$$Pt(IV) + Sn(II) \rightarrow Pt(II) + Sn(IV)$$
 (B-4)

and excess of Sn(II) produces a precipitate of Pt(0):

$$Pt(II) + Sn(II) \rightarrow Pt(0) + Sn(IV)$$
(B-5)

The presence of impurities in the feed solution or some colloidal suspensions may have had an important catalyzing contribution to promoting Pt(0) precipitation since this effect was not reproduced with the single metal synthetic solution (see Figure B-2).

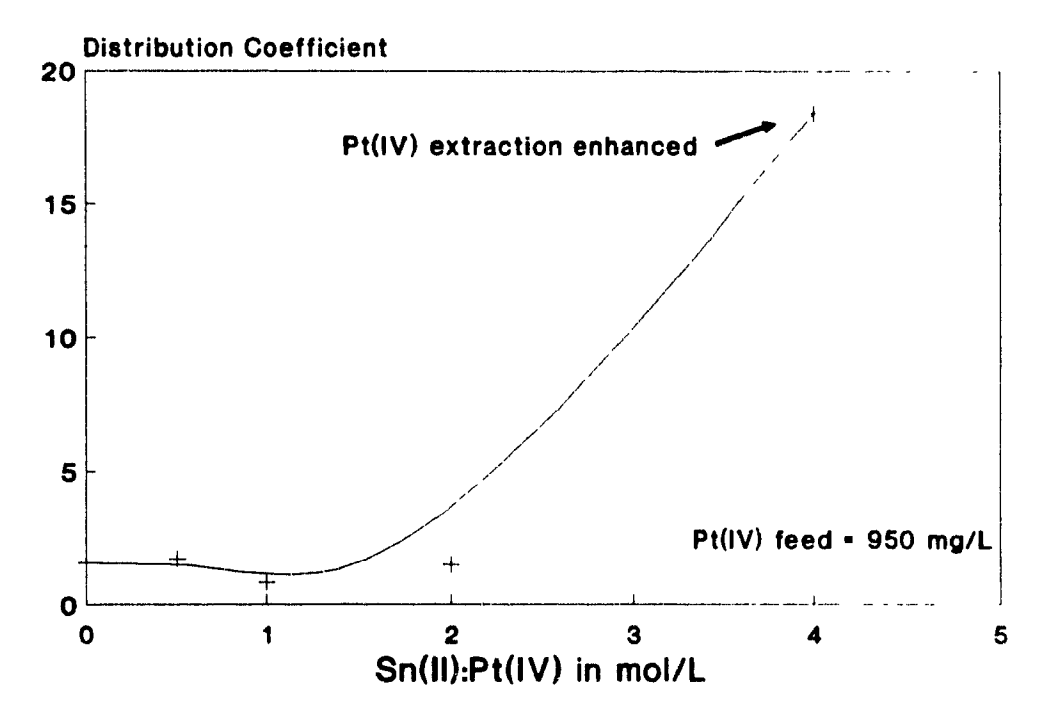


Figure B-1 The extraction of Pt(IV) in the presence of Sn(II) in single metal solution, 0.7M HCl, 5v% TN 1911, A/O=1, 3 min.

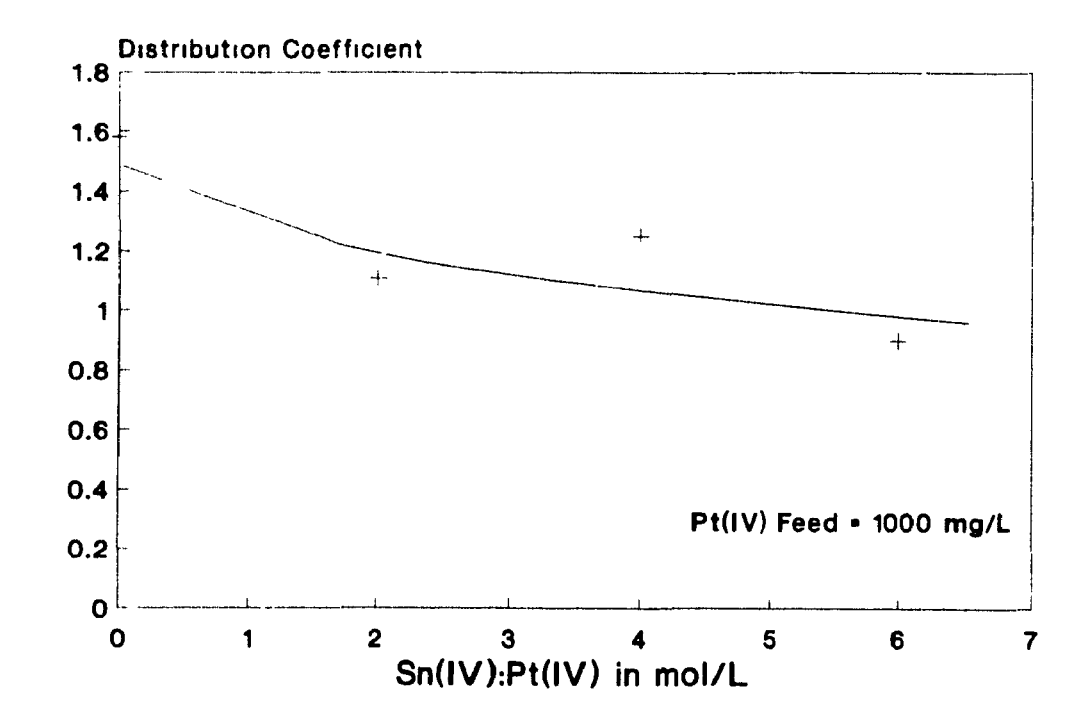


Figure B-2 The extraction of Pt(IV) in the presence of Sn(IV) in single metal solution, 0.7M HCl, 5v% TN 1911, A/O=1, 3 min.

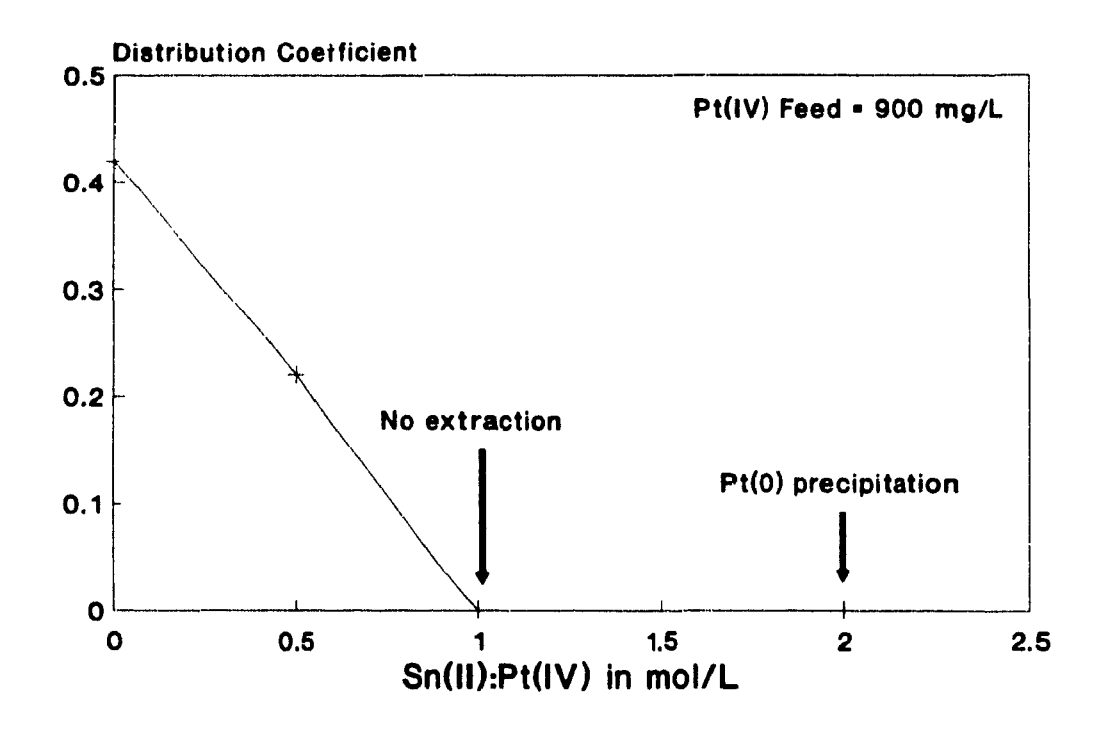


Figure B-3 The effect of Sn(II) on Pt(IV) in RC Mint solution and extraction with TN 1911. Conditions: 0.7M HCl, 5v% TN 1911, A/O=1, 3 min.

APPENDIX C: CALCULATIONS BASED ON THE DISTRIBUTION COEFFICIENT

The purpose of this section is to demonstrate how it is possible to calculate (i) the $S_{fM/P}$ value between an impurity element M_{aq} and Pt, and (ii) the theoretically expected final concentration in HCl scrub solution after 3 min. contacting with organic phase. The basis of the D_E values obtained from the single metal extraction tests is described in Section IV.3. It is clearly stated that all this theoretical analysis assumes metal transfer reactions to be reversible and the D values to refer to equilibrium calculations.

The following explanations are offered for the calculations presented on the following pages of Appendix C. Begining with 1,000 mg/L each of Pt and impurity element in aqueous solution at 2.7M HCl as feed, and based on the D_I for Pt and an impurity element M_{aq} , the element concentration in the organic phase (5v% TN 1911) was calculated for a 3 min., A/O=1 contact. The D_E for 1.5, 2.5 and 3.5M HCl were converted to D_S values using the following equation:

$$D_S = \frac{1}{D_E} \tag{C-1}$$

 $S_{fM/Pt}$ was then calculated for each of the HCl concentrations,

$$S_{f_{M/P}} = \frac{D_{S_M}}{D_{S_{P}}} \tag{C-2}$$

Mass balancing of the amounts of element distributed between organic and aqueous phase gives:

$$V_{aa} \times M_{aa,f} = [V_{org} \times M_{org,i}] - [V_{org} \times M_{org,f}]$$
 (C-3)

after assuming that

$$V_{aa} = V_{aa,i} = V_{aa,f}$$

and

4

$$V_{org} = V_{org,i} = V_{org,f}$$

where M_{aqf} and $M_{org,f}$ are the final concentrations of element in the aqueous and organic phases respectively and $M_{org,i}$ the initial concentration of element in the organic phase. V_{aq} and V_{org} are the volumes of aqueous and organic phases respectively.

Therefore if different A/O ratios are selected, say 1:2, 1:1, 2:1 and 3:1, it is possible to calculate the theoretical concentration of each element reporting to the scrub phase assuming that the same distribution coefficient applies in scrubbing and extraction (i.e, equilibrium is attained):

$$M_{aqf} = \frac{M_{org} \times V_{org}}{V_{aq} + \frac{V_{org}}{D_{S}}}$$
 (C-4)

The results appear in tabulated form and for each HCl concentration there are 4 columns. The first indicates the A/O ratio, the second the S_f value, and the rest of the columns indicate final Pt and element concentration in aqueous scrub medium. For 2.5M HCl, scrub calculations on a second contact with fresh scrub solution were effected for the elements Fe(III), Pb(II), Te(IV), Ag(I) and Zn(II). Tables IV.8 and IV.9 summarise the results for 1.5 and 2.5M HCl.

HCl ⇒	1.5M			2.5M			3 5M			
$D_{E, ext{Pt}} \ D_{F, ext{Pd}}$	62 90			100 25				115		
$egin{array}{c} D_{\mathcal{S},Pd} \ D_{\mathcal{S},Pd} \end{array}$	0.016 0.011			0.010 0.040			0.008 0 200			
SCRUBBING A/O	S _f	C _{Pt} mg/L	C _{Maq} scrub mg/L	S_f	C _{Pt} mg/L	C _{Maq} scrub mg/L	S,	C _{Pi} mg/L	C _{Maq} scrub mg/L	
1:2 1:1 2:1 3:1	0.7	16 16 15 15	10 10 10 10	4.0	10 10 10 10	36 36 36 34	25 0	9 9 8 8	168 154 132 115	

Table C-1 Expected Pt and Pd concentrations in HCl scrubbing solutions as a function of their extraction distribution coefficients (organic feed: 990 mg/L Pt and 923 mg/L Pd).

HCl ⇒	1.5M			2.5M			3 5M		
$D_{E,Pt} \ D_{E,Ag}$	62 4.3			100 4			115 2.3		
$D_{S,Pr} \ D_{S,Ag}$	0.016 0.233			0.010 0.250			0.009 0.434		
SCRUBBING A/O	S_f	C _{Pi} mg/L	C _{Maq} scrub mg/L	S _f	C _h mg/L	C _{May} scrub mg/L	S_f	C _{Pt} mg/L	C _{Meq} scrub mg/L
COwACT#1									
1:2 1:1 2:1 3:1	14.6	16 16 15 15	17 15 13	25.0	10 10 10 10	18 16 13	48.2	9 9 8 8	29 24 19 19
CONTACT#2									
1:2 1:1 2:1 3:1					10 10 10 9	16 13 9 7			

Table C-2 Expected Pt and Ag concentrations in the HCl scrubbing solutions as a function of their extraction distribution coefficients (organic feed: 990 mg/L Pt and 80 mg/L Ag).

HCl ⇒	1.5M			2.5M			3.5M			
$egin{array}{c} D_{\mathcal{E},\mathcal{P}_1} \ D_{\mathcal{E},\mathcal{O}_2} \end{array}$	62 0.16			100 0.035				115 0.01		
$D_{s,p_1} \ D_{s,c_0}$	0.016 6.25			0.010 28.57			0.009 100.0			
SCRUBBING A/O	S,	C _{Pt} mg/L	C _{Maq} scrub mg/L	S _f	C _{Pi} mg/L	C _{Maq} scrub mg/L	S _f	C _{Pt} mg/L	C _{Maq} scrub mg/L	
1:2 1:1 2:1 3:1	390	16 16 15 15	159 91 49 33	2857	10 10 10 10	196 101 52 35	1150 0	9 9 8 8	206 104 52 35	

Table C-3 Expected Pt and Cu concentrations in HCl scrubbing solutions as a function of their extraction distribution coefficients (organic feed: 990 mg/L Pt and 105 mg/L Cu).

HCl ⇒	1.5M			2.5M			3.5M		
$D_{F,Pt} \ D_{F,Fe}$	62 2.5			100 0.75			115 3.4		
$D_{S,Fe}$ $D_{S,Fe}$	0.016 0.400			0.010 1.333			0.009 0.294		
SCRUBBING A/O	S _f	C _{Pt} mg/L	C _{Meq} scrub mg/L	S_f	C _{Pt} mg/L	C _{Maq} scrub mg/L	S_f	C _{Pt} mg/L	C _{Meq} scrub mg/L
CONTACT#1									
1:2 1:1 2:1 3:1	25.0	16 16 15 15	77 66 51 42	133.3	10 10 10 10	185 132 84 62	32.7	9 9 8 8	59 52 43 36
CONTACT#2									
1:2 1:1 2:1 3:1					10 10 10 9	110 57 24 12			

Table C-4 Expected Pt and Fe concentrations in HCl scrubbing solutions as a function of extraction distribution coefficients (organic feed: 990 mg/L Pt and 231 mg/L Fe).

HCl ⇒	1.5M			2.5M			3.5M		
$egin{align*} D_{E, ext{Pt}} \ D_{E, ext{Zn}} \ \end{array}$	62 1.2			100 2.2			115 10		
D _{S,Pi} D _{S,Za}	0.016 0.833			0.010 0.454			0.009 0.100		
SCRUBBING A/O	S _f	C _{Pt} mg/L	C _{M=q} scrub mg/L	S_f	C _P mg/L	C _{Maq} scrub mg/L	Sj	C _{Pt} mg/L	C _{Maq} scrub mg/L
CONTACT#1									
1:2 1:1 2:1 3:1	52.1	16 16 15 15	410 367 218 166	45.5	10 10 10 10	258 218 166 134	11.1	9 9 8 8	183 162 132 111
CONTACT#2									
1:2 1:1 2:1 3:1					10 10 10 9	210 150 87 57			

Table C-5 Expected Pt and Zn concentrations in HCl scrubbing solutions as a function of extraction distribution coefficients (organic feed: 990 mg/L Pt and 697 mg/L Zn).

HCl ⇒	1.5M			2.5M			3.5M		
$D_{E,Pr}$ $D_{E,Sn}$	62 22			100 37			115 87		
$D_{S,Pt} \ D_{S,Su}$	0.016 0.045						0.009 0.015		
SCRUBBING A/O	S _f	C _{Pt} mg/L	C _{Meq} scrub mg/L	S _f	C _{Pt} mg/L	C _{Meq} scrub mg/L	S,	C _n mg/L	C _{Mmq} scrub mg/L
1:2 1:1 2:1 3:1	2.8	16 16 15 15	43 42 41 39	2.7	10 10 10 10	26 26 25 24	1.7	9 9 8 8	11 11 11 11

Table C-6 Expected Pt and Sn concentrations in HCl scrubbing solutions as a function of extraction distribution coefficients (organic feed: 990 mg/L Pt and 972 mg/L Sn).

HCl ⇒	1.5M			2.5M			3.5M		
$egin{array}{c} D_{E,Pc} \ D_{F,Pb} \end{array}$	62 0.25			100 1.25			115 10		
$D_{S,Ph} \ D_{S,Pb}$	0.016 4.000			0.010 0.833			0.009 0.714		
SCRUBBING A/O	S _f	C _{Pt} mg/L	C _{Meq} scrub mg/L	S _f	C _{Pt} mg/L	C _{Meq} scrub mg/L	S _f	C _n mg/L	C _{Meq} scrub mg/L
CONTACT#1									
1.2 1:1 2:1 3:1	250.0	16 16 15 15	753 452 251 174	83.3	10 10 10 10	332 257 177 135	79.3	9 9 8 8	297 235 166 128
CONTACT#2						-			
1:2 1:1 2:1 3:1					10 10 10 9	235 140 66 38			

Table C-7 Expected Pt and Pb concentrations in HCl scrubbing solutions as a function of extraction distribution coefficients (organic feed: 990 mg/L Pt and 565 mg/L Pb).

HCl ⇒	1.5 M			2.5M			3.5M			
$D_{E,Pt} \ D_{E,Ad}$	62 0.07			100 0.09				115 0.075		
D_{S,P_1} D_{S,A_0}	0.016 14.28			0.010 11.11			0.009 13.33			
SCRUBBING A/O	S _f	C _{Pt} mg/L	C _{Maq} scrub mg/L	S_f	C _{Pt} mg/L	C _{Meq} scrub mg/L	S _f	C _{Pt} mg/L	C _{Meq} scrub mg/L	
1:2 1:1 2:1 3:1	892.5	16 16 15 15	146 78 40 27	1111.1	10 10 10 10	141 76 40 27	1481.1	9 9 8 8	144 77 40 27	

Table C-8 Expected Pt and As concentrations in HCl scrubbing solutions as a function of extraction distribution coefficients (organic feed: 990 mg/L Pt and 83 mg/L As).

Z
1
ŝ
z
_

HCl ⇒	1.5 M			2.5M			3.5M			
$D_{\mathcal{E},Ph} \ D_{\mathcal{E},Sb}$	62 0.25			100 0.35			115 1			
$egin{array}{c} D_{S, ext{Pt}} \ D_{S, ext{Sb}} \end{array}$	0.016 4 000			0.010 2.857			0.009 1.000			
SCRUBBING A/O	S _f	C _{Pt} mg/L	C _{Maq} scrub mg/L	S _f	C _{Pt} mg/L	C _{Maq} scrub mg/L	S,	C _{Pt} mg/L	C _{Maq} scrub mg/L	
1:2 1:1 2:1 3:1	250	16 16 15 15	381 229 127 88	285.7	10 10 10 10	336 212 122 85	111.1	9 9 8 8	191 143 95 72	

Table C-9 Expected Pt and Sb concentrations in HCl scrubbing solutions as a function of extraction distribution coefficients (organic feed: 990 mg/L Pt and 286 mg/L Sb).

HCl ⇒	1.5M			2.5M			3.5M			
$D_{E, ext{Pt}} \ D_{E, ext{Bi}}$	62 800			100 53			115 47			
$D_{S,Pt} \ D_{S,Bt}$	0.016 0.001			0.010 0.019			0.009 0.021			
SCRUBBING A/O	S _f	C _{Pt} mg/L	C _{Meq} scrub mg/L	S_f	C _{Pt} mg/L	C _{Meq} scrub mg/L	S _f	C _{Pt} mg/L	C _{Meq} scrub mg/L	
1:2 1:1 2:1 3:1	0.1	16 16 15 15	1 1 1	1.9	10 10 10 10	18 18 18 18	2.3	9 9 8 8	21 20 20 20 20	

Table C-10 Expected Pt and Bi concentrations in HCl scrubbing solutions as a function of extraction distribution coefficients (organic feed: 990 mg/L Pt and 980 mg/L Bi).

HCl ⇒	1.5M			2.5M			3.5M			
$D_{E P}$ $D_{E Se}$	62 0.04			100 0.06			115 0.12			
$D_{S,Ph} \ D_{S,Se}$	0.016 25.00			0.010 16.67			0.009 8.33			
SCRUBBING A/O	s,	C _{Pi} mg/L	C _{Maq} scrub mg/L	S _f	C _n mg/L	C _{Maq} scrub mg/L	S _f	C _{Pt} mg/L	C _{Maq} scrub mg/L	
1:2 1:1 2:1 3:1	1562.5	16 16 15 15	111 58 29 20	1667.0	10 10 10 10	107 57 29 20	925.5	9 9 8 8	97 54 28 19	

Table C-11 Expected Pt and Se concentrations in HCl scrubbing solutions as a function of extraction distribution coefficients (organic feed: 990 mg/L Pt and 60 mg/L Se).

HCl ⇒	1.5M			2.5M			3.5M		
$D_{E,\mathrm{Pt}} \ D_{F,\mathrm{Tc}}$	62 0.8			100 2.2			115 10		
$D_{S,Pt} \ D_{S,Te}$	0.016 1.250			0.010 0.454			0.009 0.100		
SCRUBBING A/O	S _f	C _{Pt} mg/L	C _{Maq} scrub mg/L	S_f	C _n mg/L	C _{Meq} scrub mg/L	S _f	C _{Pt} mg/L	C _{Maq} scrub mg/L
CONTACT#1									
1:2 1:1 2:1 3:1	78.1	16 16 15 15	549 397 255 188	45.4	10 10 10 10	264 223 170 137	11.1	9 9 8 8	68 65 60 55
1:2 1:1 2:1 3:1					10 10 10 9	216 153 89 58			

Table C-12 Expected Pt and Te concentrations in HCl scrubbing solutions as a function of extraction distribution coefficients (organic feed: 990 mg/L and 714 mg/L Te).

APPENDIX D: AQUEOUS AND ORGANIC ASSAYS FOR SIMULATION TEST

No	Pt	Pd	Ag	Fe	Cu	Zn	Ni	የъ	Sn	A.	Sb	Bi	\c	Te
AF	1217	3243	84	391	3104	728	2722	653	407	101	500	456	118	441
r1	243	1947	39	295	2082	515	2722	624	28	304	500	104	383	чі
12	21	165	18	210	3087	170	2722	303	0	305	406	٠,	407	9¢
Ri	281	2010	55	281	3082	674	2722	623	28	794	יסי	190	496	129
R2	25	409	33	277	3000	252	2691	445	0	305	410	ıı	487	141
SI	128	68	12	6	29	110	11	85	0	o	,	30	*	114
•1	58	4	1	15	0	76	0	23	0	0	9	125] ,	23
a 2	67	1	0	7	3	9	1	7	0	ŋ	7	60	0	,
S2	63	3	1	20	0	44	1	15	0	0	,	110	;	15
S3	67	2	0	8	1	4	1	2	0	Q.	,	49	1	4
SPt	1020	0	1	0	0	6	0	0	0	0	1	0	1	1
S4	112	3	7	2	1	16	1	2 .	0	0	,] 2] 1	0
PSI	0	265	0	4	1	1	0	0	0	0	0	0	1	0
PSII	0	664	0	3	1	1	0	0	0	0	o	0	ı	o
PSIII	0	706	0	2	1	1	0	0	a	0	0	0	,	6
PSIV	0	1378	0	4	1	i	0	0	0	0	0	0	,	0
PSV	0	1903	0	4	1	1	0	0	0	0	0	0	,	0
PSVI	0	2136	0	4	1	1	0	0	0	0	e	0	1	0
\$5	0	403	0	3	1	0	1	0	44)7	o	15	0	1	0

Table D-1 Aqueous stream assays for simulation test (units in mg/L).

R/r= extraction raffinates, S/s= scrubbing raffinates, SPt= Pt strip liquor, PS= Pd strip liquors.

No	Pt	Pd	Ag	Fe	Cu	Zn	Ni	Pb	Sn	As	Sb	Bı	Se	Те
1	0	294	0	0	0	0	0	0	0	0	0	0	0	0
2	0	671	0	0	0	0	0	0	0	0	0	0	0	0
3	0	651	0	0	0	0	0	0	0	0	0	0	0	0
4	0	1067	0	0	0	0	0	0	0	0	0	0	0	0
5	0	1568	0	0	0	0	0	0	0	0	0	0	0	0
6	0	1467	0	0	0	0	0	0	0	0	0	0	0	0
7	0	1995	0	0	0	0	0	0	0	0	0	0	0	0
8	0	2160	0	0	0	0	0	0	0	0	0	0	0	0
02		1810	-	-	-	288		-	-		-	39	-	-
05	-	1780	-	-	-	<1	-	-	-		-	0		-
08	-	1710	-	-	-	<1	-	-	-	-	~	0	-	-
010	-	1150	-	-	-	<1	-	-	•	-	-	0	-	-
012	-	752	-	-		<1	-	_	-	-	-	0	-	-

Table D-2 Further aqueous stream assays and organic assays for simulation test (units in mg/L). Numbers= Pd strip liquor streams, O= organic streams in Pd stripping.

4REFERENCES

- 1. G. P. Demopoulos, *Journal of Metals* 36(6), 13 (1986).
- 2. G. P. Demopoulos, G. M. Ritcey and G. Pouskouleli, in *ISEC '86*, Vol. II, p. 581. Munich, F.R.G. (1986).
- 3. G. P. Pouskouleli, S. Kelebek and G. P. Demopoulos, in *Separation Processes in Hydrometallurgy* (edited by G. A. Davies), p. 174. Ellis Horwood Ltd., Chichester, U.K. (1987).
- 4. G. Demopoulos, N. Kuyucak, D. L. Gefvert and M. H. Richter, in *Precious Metals 1989* (edited by G. B. Harris), p. 201. IPMI, Montreal, Canada (1989).
- 5. G. P. Demopoulos, G. Pouskouleli and P. J. A. Prud'homme, U.S. Patent No. 4,654,145, (1987); Can. Patent No. 1,223,125, (1987).
- 6. G. B. Harris, S. Monette, J.-P. Barry and R. W. Stanley, U.S. Patent No. 5,045,290 (1991).
- 7. J. M. Ryder and K. Dymock, in *Recycling of Metalliferrous Materials*, p. 255. IMM, London, U.K. (1990).
- 8. D. Job, "PGMs: Overview and Outlook." Paper presented at "Refining and Recycling of Precious Metals: A Technology Update," Professional Development Seminar, McGill University, Montreal, Canada, April 19-May 1, 1991.
- 9. G. P. Demopoulos, "PGM Workshop." Paper presented at "Gold and Platinum Extraction Technology," Professional Development Seminar, McGill University, Montreal, Canada, June 8-10, 1989.
- 10. G. B. Harris, "The Refining of Gold and Precious Metals." Paper presented at "Refining and Recycling of Precious Metals: A Technology Update," Professional Development Seminar, McGill University, Montreal, Canada, April 29-May 1, 1991.
- 11. R. I. Edwards, Journal of Metals 28 (9), 4 (1976).

7

- 12. M. J. Cleare, R. A. Grant and P. Charlesworth, in *Extraction Metallurgy '81*, p. 38. IMM, London, U.K. (1981).
- 13. J. E. Barnes and J. D. Edwards, Chemistry and Industry 1982(5), 151 (1982).
- 14. G. P. Demopoulos, "The Separation Chemistry of Platinum Group Metals." Paper presented at "Refining And Recycling of Precious Metals: A Technology Update," Professional Development Seminar, McGill University, Montreal, Canada, April 29-May 1, 1991.
- 15. R. A. Grant, R. F. Burnham, S. Collard, "The High Efficiency Separation of Iridium from Rhodium by Solvent Extraction using a Mono N-Substituted Amide." Paper presented at "ISEC '90," Kyoto, Japan, July 16-21, 1990.
- 16. G. P. Demopoulos, *CIM Bulletin* **82**(923), 165 (1989).
- 17. W. M. Latimer, The Oxidation States of the Elements and Their Potentials in Aqueous Solutions, 2nd ed. Prentice-Hall Inc., New York, U.S.A. (1952).
- 18. D. R. Lide (editor), *CRC Handbook of Chemistry and Physics*, 72nd ed., p. 4-79. CRC Press, Boca Raton, U.S.A. (1991-92).
- 19. A. Bard, R. Parsons and J. Jordan (editors), Standard Potentials in Aqueous Solutions. IUPAC/Dekker, New York, U.S.A. (1985).
- 20. L. Meites, *Handbook of Analytical Chemistry*, p. 5-7. McGraw-Hill Co., New York, U.S.A. (1963).
- 21. R. A. Brown and E. H. Swift, *Journal of the American Chemical Society* 71, 2719 (1949).
- 22. W. M. Dutton and W. C. Cooper, Chemical Reviews 66, 657 (1966).
- 23. J. E. Hoffman, JOM 42(8), 51 (1990).
- 24. D. M. Muir and G. Senanayake, in *Extractive Metallurgy '85*, p. 65. IMM, London, U.K. (1985).
- 25. G. Senanayake and D. M. Muir, Metallurgical Transactions B 19B, 37 (1988).
- 26. M. A. Khan and M. J. Schwing-Weill, Inorganic Chemistry 15, 2203 (1976).

- 27. N. Fatouros, F. Rouelle and M. Chemla, *Journal de chimie physique* 75, 476 (1978).
- 28. G. G. Shitareva and V. A. Nazarenko, Russian Journal of Inorganic Chemistry 13, 941 (1968).
- 29. T. H. Lo, M. H. Baird and C. Hanson, *Handbook of Solvent Extraction*, p. 728. John Wiley and Sons, New York, U.S.A. (1983).
- 30. J. J. C. Jansz, "Calculation of Ionic Activities and Distribution Data for Chlorocomplexes." TMS paper A84-1 (1984).
- 31. J. J. C. Jansz, *Hydrometallurgy* 11, 13 (1983).
- 32. A. Warshawsky, Mineral Science and Engineering 5, 36 (1973).
- 33. M. W. Lister and P. Rosenblum, Canadian Journal of Chemistry 38, 1834 (1960).
- 34. B. R. Palmer, F. Nami and M. C. Fuerstenau, *Metallurgical Transactions B* 7B, 385 (1976).
- 35. Y. Marcus, Coordination Chemistry Reviews 2, 195 (1967).
- 36. L. Barcza and L. Gunnar Sillen, Acta Chemica Scandinavica 25, 1250 (1971).
- 37. R. Chiarizia and P. R. Danesi, Journal of Inorganic and Nuclear Chemistry 40, 1811 (1978).
- 38. Y. Xiawan, H. Aiping and Y. Sutian, in *ICHM* '88 (edited by Z. Yulian and Xu Jiazhong), p. 487. Inter. Academic Publishers/Pergamon Press, Beijing, China (1988).
- 39. H. M. Neumann, Journal of the American Chemical Society 76, 2611 (1954).
- 40. B. I. Nabivanets and E. E. Kapantsyan, Russian Journal of Inorganic Chemistry 13(7), 946 (1968).
- 41. "Fundamentals and Practice of Aqueous Electrometallurgy." Notes from a Professional Development Seminar and Short Course, CIM, Montreal, Canada, October 20-21, 1990.

- 42. P. G. Christie, V. I. Lakshmanan and G. J. Lawson, *Hydrometallurgy* 2, 105 (1976).
- 43. T. Sato, T. Shimomura, S. Murakami, T. Maeda and T. Nakamura, *Hydrometallurgy* 12, 245 (1984).
- 44. K. H. Soldenhoff, in *ISEC* '86, Vol. II, p. 123. Munich, F.R.G. (1986).
- 45. I. M. Ivanov, A. V. Nikolaev, L. M. Gindin, V. L. Kheifez and L. V. Volkov, *Hydrometallurgy* 4, 377 (1979).
- 46. T. Sato, T. Nakamura and M. Ikeno, Hydrometallurgy 15, 209 (1985).
- 47. D. Noriegua, J. M. Regife and P. M. Blythe, *Chemistry and Industry* 1980(2), 63 (1980).
- 48. D. Dyrssen and M. De Jesus Tavares, in *Solvent Extraction Chemistry (ISEC '67)* (edited by D. Dyrssen, J.-O. Liljenzin and J. Rydberg), p. 465. Gothenburg, Sweden (1967).
- 49. N. M. Rice and D. C. Smith, in *ISEC* '86, Vol. II, p. 633. Munich, F.R.G. (1986).
- 50. R. D. Groves and L. D. Redden, Hydrometallurgy 24, 271 (1990).
- 51. G. M. Ritcey and A. W. Ashbrook, Solvent Extraction: Principles and Applications to Process Metallurgy, p. 144. Elsevier Press, New York, U.S.A. (1984).
- 52. R. G. Holdich and G. J. Lawson, in *ISEC* '86, Vol. II, p. 19. Munich, F.R.G. (1986).
- 53. C. McDonald, M. H. Mahayni and M. Kanjo, Separation Science and Technology 13, 429 (1978).
- 54. M. Golinski, in ISEC '71, p. 603. The Hague, The Netherlands (1971).
- 55. T. Sato and S. Kikuchi, Hydrometallurgy 20, 97 (1988).
- 56. A. R. Selmer-Olsen, Acta Chemica Scandinavica 20, 1621 (1966).

- 57. D. Hay Liem and M. Zangen, in *ISEC '77* (CIM Special Vol.21), p. 107. Toronto, Canada (1977).
- 58. D. Sevdić, H. Meider and D. Pavkovic, Solvent Extraction and Ion Exchange 8, 643 (1990).
- 59. A. Baradel, R. Guerriero, L. Meregalli and I. Vittadini, *Journal of Metals* 38(2), 32 (1986).
- 60. A. Baradel, R. Guerriero, L. Meregalli and I. Vittadini, in *ISEC '86*, Vol. II, p. 401. Munich, F.R.G. (1986).
- 61. V. Bumbalek, K. Cermak and J. Haman, in *ISEC '80*, Paper 80-177. Liege, Belgium (1980).
- 62. T. Dhond and S. M. Khopkar, Separation Science and Technology 8, 379 (1973).
- 63. T. Sato and K. Sato, in *Solvent Extraction Symposium* '88, p. 121. Tokyo Institute of Technology, Tokyo, Japan (1988).
- 64. N. Jordanov and L. Futekov, *Talanta* 13, 163 (1966).
- 65. R. B. Heddur and S. M. Khopkar, in *ISEC* '86, Vol. II, p. 439. Munich, F.R.G. (1986).
- 66. T. Sekine, H. Iwaki, M. Sakairi and F. Shimada, Bulletin of the Chemical Society of Japan 41, 1 (1968).
- 67. G. Fischer, K. Gloe, P. Mühl and V. V. Bagreev, Journal of Inorganic and Nuclear Chemistry 40, 1793 (1978).
- 68. H. Mabuchi and I. Okada, Bulletin of the Chemical Society of Japan 38, 1478 (1965).
- 69. R. E. Treybal, Mass Transfer Operations, p. 519. McGraw-Hill Co., New York, U.S.A. (1980).
- 70. G. D. Christian, *Analytical Chemistry*, 3 ed., p. 324. John Wiley and Sons, New York, U.S.A. (1980).

- 1
- 71. G. P. Demopoulos and M. Brown, Unpublished Research Work, McGill University, Montreal, Canada, 1984.
- 72. C. F. Baes and R. E. Mesmer, *The Hydrolysis of Cations*, reprint ed., p. 353. Robert Krieger Pub. Co., Malabar, U.S.A. (1986).
- 73. G. Cotton and G. Wilkinson, *Advanced Inorganic Chemistry*, 4th ed., p. 394. John Wiley and Sons, New York, U.S.A. (1980).
- 74. C. H. R. Gentry and L. G. Sherrington, *The Analyst* 75, 17 (1950).
- 75. B. Côté, Ph.D. Research Work in Progress, McGill University, Montreal, Canada, 1991.
- 76. G. B. Harris, MITEC, Ottawa, Canada. Personal Communication, 1991.
- 77. F. Habashi, *Principles of Extractive Metallurgy*, 2nd ed., Vol. II, p. 331. Gordon and Breach Pub., New York, U.S.A. (1980).
- 78.. A. Moskowitz, J. Dasher and H. W. Jamison Jr., *Analytical Chemistry* 32, 1362 (1960).
- 79. P. Kondos, "Pressure Chloride Leaching of a Complex U/Ra/Ni/As Ore: Statistical Modelling and Solution Chemistry," p. 241. Ph.D. Thesis, McGill University, Montreal, Canada (1988).
- 80. G. H. Ayres and A. S. Meyer Jr., Analytical Chemistry 23, 299 (1951).
- 81. G. H. Ayres and A. S. Meyer Jr., Journal of the American Chemical Society 77, 2671 (1955).
- 82. J. K. Wittle and G. Urry, Inorganic Chemistry 7, 560 (1968).
- 83. M. Mojski, Talanta 27, 7 (1980).
- 84. A. Diamantatos, Analytica Chimica Acta 66, 147 (1973).

[&]quot;ISEC" stands for "International Solvent Extraction Conference".